# Analytical Probabilistic Models for Evaluating the Hydrologic Performance of Structural Low Impact Development Practices

By

**Shouhong Zhang**

B.Sc. (Agr.), M.Sc.

Faculty of Engineering
Department of Civil Engineering

A Thesis
Submitted to the School of Graduate Studies
In Partial Fulfillment of the Requirements
For the Degree

Doctor of Philosophy

McMaster University
Hamilton, Ontario, Canada
January 2014

DOCTOR OF PHILOSOPHY (2014) McMaster University
(Civil Engineering) Hamilton, Ontario

TITLE: Analytical Probabilistic Models for Evaluating the Hydrologic Performance of Structural Low Impact Development Practices

AUTHOR: Shouhong Zhang, B.Sc. (Agr.), M.Sc.

SUPERVISOR: Professor Yiping Guo, Ph.D., P. Eng.

NUMBER OF PAGES: 260 pages (I- XIV, 1-246)

# Abstract

Low Impact Development (LID) practices have been increasingly used to mitigate the adverse impacts of urbanization. Reliable methods are in need to provide hydrologic performance assessment of different types of LID practices. The purpose of this thesis is to develop a set of analytical models which can be used to assist the planning and design of commonly used structural LID practices such as green roofs, rain gardens, bioretention and permeable pavement systems.

The analytical LID models are derived on the basis of exponential probability density functions (PDF) of local rainfall characteristics and mathematical representations of the hydraulic and hydrologic processes occurring in association with the operation of LID practices. Exponential PDFs are found to provide good fits to the histograms of rainfall characteristics of five cities located in different climatic zones. The mathematical representations are all physically based and most of the input parameters used in these representations are the same as those required in commonly used numerical models.

The overall reliability of the analytical LID models are tested by comparing the results from these analytical models with results determined from long-term continuous simulations, in addition to that the accuracy of the analytical model for green roofs is also verified against observations from a real case study. The long-term rainfall data from the five cities and a variety

of LID practice design configurations are used in the comparisons. The relative differences between the results calculated using the analytical LID models and the results determined from corresponding SWMM simulations are all less than 10%.

The Howard's conservative assumption is adopted in the development of the analytical models for rain gardens and permeable pavement systems. This assumption results in conservative estimations of the stormwater management performances of these LID practices. Instead of adopting the Howard's conservative assumption, an approximate expected value of the surface depression water content of a bioretention system at the end of a random rainfall event [denoted as $E(S_{dw})$] is derived and used in the development of the analytical model for bioretention systems. The use of $E(S_{dw})$ is proven to be advantageous over the use of the Howard's conservative assumption.

The analytical LID models are comprised of closed-form mathematical expressions. The application of them can be easy and efficient as illustrated in the application examples. For a specific location of interest, with a goodness-of-fit examination of the exponential PDFs to local rainfall data and verification of the accuracy of the analytical LID models, these models can be used as a convenient planning, design, and management tool for LID practices.

# Acknowledgement

The completion of this thesis would not have been possible without the continuing support and encouragement of a number of fabulous people. I would like to begin by thanking my supervisor Dr. Y. Guo, for introducing me to this interesting area of research, for providing me with all the support I needed, and for his encouragement and tireless effort to make my work better. His continual patience and insightful guidance is greatly appreciated. A big thank you also goes to the other two supervisory committee members, Dr. P. Coulibaly and Dr. S. E. Dickson, for their thought-provoking questions and valuable comments.

For the sources of financial support granted to me throughout this degree from the China Scholarship Council, the School of Graduate Studies and the Department of Civil Engineering at McMaster Univ., as well as NSERC, and for the academic and studying services provided by the faculties and staff from McMaster Univ., I feel exceptionally fortunate and thankful. I wish to extend my thanks to my friends and my fellow graduate students.

My deepest gratitude goes to my parents for their continuous love and unwavering support. My very special thank you goes to my girlfriend Miss Y. Li, for believing in me and for supporting me in chasing my academic dreams. Without their support and understanding neither this thesis nor the opportunity to write it would have materialized. It is to them that I would like to dedicate this thesis.

# Publication List

This thesis consists of the following papers:

**Paper I**

Zhang, S., and Guo, Y. (2013). An analytical probabilistic model for evaluating the hydrologic performance of green roofs. The ASCE *Journal of Hydrologic Engineering*, 18(1), 19–28.

**Paper II**

Zhang, S., and Guo, Y. (2013). An explicit equation for estimating the stormwater capture efficiency of rain gardens. The ASCE *Journal of Hydrologic Engineering*, 18(12), 1739–1748.

**Paper III**

Zhang, S., and Guo, Y. (2014). Stormwater capture efficiency of bioretention systems. *Water Resources Management*, 28(1), 149–168.

**Paper IV**

Zhang, S., and Guo, Y. (2013). An analytical equation for evaluating the stormwater volume control performance of permeable pavement systems. Submitted to the ASCE *Journal of Irrigation and Drainage Engineering* in October, 2013, Reference Number: IRENG-6756.

**Thesis related Paper (Appendix A)**

Zhang, S., and Guo, Y. (2013). SWMM simulation of the stormwater volume control performance of permeable pavement systems. Submitted to the ASCE *Journal of Hydrologic Engineering* in September, 2013, Reference Number: HEENG-2003.

## Co-Authorship

This thesis was prepared in accordance with the regulations provided by the School of Graduate Studies, McMaster University for a sandwich thesis. The contribution of the co-authors for each publication that makes up this thesis is described below.

For all the four papers presented in Chapters 2 through 5, the literature review was conducted by S. Zhang, the mathematical derivation, continuous simulations, and comparison analysis were conducted by S. Zhang in consultation with Dr. Y. Guo, the papers were written by S. Zhang and edited by Dr. Y. Guo.

For Appendix A, the equivalent regular catchment method was proposed by Dr. Y. Guo, the continuous simulations and comparison analysis were conducted by S. Zhang, the paper was written by S. Zhang and edited by Dr. Y. Guo.

# Table of Contents

Abstract ..... III

Acknowledgement ..... V

Publication List ..... VII

Co-Authorship ..... IX

Table of Contents ..... XI

Chapter 1 Background and Objectives ..... 1

1.1 Urban Stormwater Management ..... 1

1.2 Low Impact Development Practices ..... 3

1.3 Hydrologic Performances of LID Practices ..... 6

1.4 Hydrologic Models of LID Practices ..... 10

1.5 The Analytical Probabilistic Approach ..... 13

1.6 Objectives and Organization ..... 21

References ..... 23

Chapter 2 An Analytical Probabilistic Model for Evaluating the Hydrologic Performance of Green Roofs ..... 35

2.1 Introduction ..... 36

2.2 Probabilistic Rainfall-Runoff Transformation of a Green Roof System 43

2.2.1 Probabilistic Models of Rainfall Event Characteristics ..... 43

2.2.2 Hydrologic and Hydraulic Processes Occurring on and inside a Green Roof System ..... 46

2.2.3 Estimation of the Runoff Reduction Rate of a Green Roof System 49

2.3 Verification of the Analytical Probabilistic Model ..... 56

2.3.1 Comparison with Continuous SWMM Simulation Results ..... 57
2.3.2 Comparison with Observations from a Real Case Study ..... 61
2.4 Application of the Analytical Model ..... 64
2.5 Summary, Discussion and Conclusions ..... 67
References ..... 71
Chapter 3 An Explicit Equation for Estimating the Stormwater Capture Efficiency of Rain Gardens ..... 79
3.1 Introduction ..... 85
3.2 Derivation of Analytical Equations ..... 85
3.2.1 Probabilistic Models of Rainfall Event Characteristics ..... 85
3.2.2 Hydrologic Processes Occurring on Rain Gardens ..... 91
3.2.3 Estimation of Average Annual Inflow Volume ..... 92
3.2.4 Estimation of Average Annual Overflow Volume ..... 94
3.2.5 Estimation of the Stormwater Capture Efficiency ..... 105
3.3 Comparison with Continuous Simulation Results ..... 106
3.4 Example Application of the Analytical Probabilistic Expression ..... 110
3.5 Summary and Conclusion ..... 113
References ..... 117
Chapter 4 Stormwater Capture Efficiency of Bioretention Systems ..... 125
4.1 Introduction ..... 127
4.2 Probabilistic Models of Rainfall ..... 132
4.3 Stormwater Capture Efficiency of Bioretention Systems ..... 136
4.3.1 Water Balance Equation and Stormwater Capture Efficiency ..... 136

4.3.2 Volume of Inflow ..... 137
4.3.3 Volume of Overflow ..... 138
4.4 Comparison with Continuous Simulations ..... 150
4.4.1 Development of Continuous Simulation Models ..... 150
4.4.2 Relationship between APE and SWMM Input Parameters ..... 153
4.4.3 Comparison of SWMM and APE Results ..... 156
4.5 Discussion ..... 160
4.6 Summary and Conclusions ..... 164
References ..... 166
Chapter 5 An Analytical Equation for Evaluating the Stormwater Volume Control Performance of Permeable Pavement Systems ..... 173
5.1 Introduction ..... 174
5.2 Derivation of the Analytical Equation ..... 180
5.2.1 Statistical Representation of Rainfall Data ..... 180
5.2.2 Hydrologic Processes Involved ..... 184
5.2.3 Water Balance Equation and Stormwater Capture Efficiency ..... 187
5.2.4 Expected Value of the Inflow Volume ..... 188
5.2.5 Expected Value of the Outflow Volume ..... 190
5.2.6 Long-term Average Stormwater Capture Efficiency ..... 195
5.3 Comparison with Continuous Simulation Results ..... 196
5.4 Summary and Conclusions ..... 202
References ..... 205
Chapter 6 Conclusions and Recommendations for Future Research ..... 213

6.1 Conclusions ..... 213
6.2 Recommendations for Future Research ..... 216
6.2.1 Further Validation of the Analytical LID Models ..... 216
6.2.2 Regional Distributions of Statistics of Rainfall Characteristics ..... 216
6.2.3 Initial Status of Stormwater Management Storage Facilities ..... 217
6.2.4 Stormwater Control Benefits of Impervious Surface Disconnection ..... 219
6.2.5 Hydrologic Modeling of LID Practices in a Watershed Scale ..... 220
References ..... 221
Appendix A SWMM Simulation of the Stormwater Volume Control Performance of Permeable Pavement Systems ..... 225
A.1 Introduction ..... 226
A.2 Methodology ..... 228
A.2.1 Hydrological Processes Involved ..... 228
A.2.2 Modeling Permeable Pavements Using the SWMM LID Module ..... 229
A.2.3 Modeling Permeable Pavements as Equivalent Subcatchments ..... 230
A.2.4 Simulation Runs ..... 234
A.3 Results and Analysis ..... 237
A.4 Recommendations ..... 242
References ..... 242

# Chapter 1

# Background and Objectives

## 1.1 Urban Stormwater Management

In urban areas, the increase of impervious surfaces (e.g., roads, driveways, parking lots and roof tops) may alter the natural hydrologic cycle of a watershed by reducing infiltration and on-site retention, and increasing stormwater runoff. Increased stormwater runoff aggravates the risk of flooding in urban areas. In order to prevent flooding, urban drainage systems consisting of catch basins and sewer pipes are constructed to efficiently collect and deliver stormwater runoff water to the nearest water bodies. The installation of drainage systems results in more rapid transmission of runoff and therefore a shorter time of concentration on urban catchments (USEPA 2000). Due to the increased volume of stormwater runoff and reduced time of concentration, the increase in discharge rates is usually an inevitable consequence of urban development. The increased volume and rate of discharge cause a variety of environmental impacts such as severe downstream flooding and stream channel erosion.

Human activities in urban areas generate various types of pollutants such as solids, nutrients, oxygen-demanding matters, microbiological pollutants,

toxic constituents and oil and grease (Adams and Papa 2000). These pollutants may be collected by stormwater runoff through erosion of pervious areas and washing off from impervious surfaces. The pollutants collected in urban stormwater runoff contribute greatly to the degradation of many surface waters (USEPA 2003).

Traditional methods of stormwater management sought to remove water from a site as quickly as possible and then store the larger volume at an off-site, downstream facility to control the peak discharge and improve the water quality. For instance, detention and retention ponds and other best management practices (BMPs) are commonly used to control discharge rates and improve water quality. To prevent stream bank erosion and provide more space for flood waters, some stream channels are enlarged and lined with concrete. These methods may be effective in solving the problems such as flooding, water quality and erosion. However, the problems related to increased runoff volume and decreased infiltration remain and the aquatic ecosystems in receiving water bodies are still severely damaged (USEPA 2000; Holman-Dodds et al. 2003).

In the last few decades, our understanding of the watershed ecosystems and the potential impacts of urbanization was improved further; a broad suite of issues related to stream channel stability, groundwater resources and aquatic and terrestrial ecosystems have been gradually recognized (USEPA 2000;

CVC and TRCA 2010). The recognition of these issues has inspired the development of innovative stormwater management approaches which emphasize not only the protection of human health and property, but also the preservation of ecosystems. One common core objective of these innovative stormwater management approaches is to allow for development of a site while maintaining as much of its natural hydrology as possible. Due to the differences in the focuses of them and the countries where they were first developed, these innovative approaches have different denominations, such as the Sustainable Urban Drainage Systems in United Kingdom (CIRIA 2000), the Water Sensitive Urban Design in Australia (Melbourne Water 2005), and the Low Impact Development Practices in North America (PGC 1999; CVC and TRCA 2010).

## 1.2 Low Impact Development Practices

Low Impact Development (LID) is an innovative stormwater management approach which seeks to maintain or replicate the natural (or predevelopment) hydrologic patterns of an urban site (USEPA 2000). The natural hydrologic functions of on-site retention, infiltration, and groundwater recharge, as well as the volume and frequency of discharges are maintained through the use of integrated and distributed micro-scale stormwater retention and detention areas, the reduction of impervious surfaces, and the lengthening

of flow paths and runoff time (Coffman, 2000). Pioneered in the early 1990s in Prince George's Country, Maryland, LID is gaining more and more popularity in recent years (PGC 1999; Dietz 2007; Ahiablame et al. 2012).

Different from traditional stormwater management approaches, LID has goals of stormwater volume control, aquatic ecosystem protection, and infiltration and groundwater recharge maintenance in addition to discharge rate control and water quality improvement. A number of key LID principles characterize these goals of LID (PGC 1999; Ahiablame et al., 2012): (1) integrating stormwater management strategies in the early stage of site planning and design; (2) managing stormwater close to the source with distributed micro-scale practices; (3) preserving the ecosystem's natural hydrological functions and cycles; (4) focusing on prevention rather than mitigation and remediation; (5) reducing impervious ground cover and building footprint; and so on. Adhering to these LID principles, LID practices such as rainwater harvesting systems, green roofs, bioretention systems (or rain gardens) and permeable pavements are now increasingly being used for the purpose of stormwater management.

Rainwater harvesting is the process of collecting, conveying and storing rainwater in rain barrels or cisterns for future use (CVC and TRCA 2010). The harvested rainwater is used to irrigate landscaped areas and can be either

evapotranspirated back to the atmosphere or infiltrated into the soil (Guo and Baetz 2007), thereby helping to maintain predevelopment water balance. Green roofs, also known as vegetated roofs, usually consist of a vegetation layer, a substrate or growing medium layer and a drainage layer over a series of waterproof and root repellent membranes. Reduction of runoff volume from building areas is the main stormwater management role that green roofs play (Berndtsson 2010).

A bioretention system, or a rain garden, is generally composed of a vegetated ponding area with a surface mulch layer underlaid by a fill media layer (Roy-Poirier et al. 2010). Bioretention systems capture the rainwater falling on their surfaces and the stormwater generated from their contributing areas, and retain the stormwater for evapotranspiration and infiltration. They can be efficiently used to control runoff volume and peak flow (Davis 2008; Hunt et al. 2008), to maintain evapotranspiration and groundwater recharge (Aravena and Dussaillant 2009; Li et al. 2009), and to reduce pollutants entering surface water bodies and groundwater (Dietz and Clausen 2006).

A permeable pavement system generally consists of a permeable pavement layer underlain by a stone reservoir (USEPA 1999; CVC and TRCA 2010). The surface pavement layer may be comprised of pervious concrete, porous asphalt, or other different types of porous structural pavers, which are usually highly permeable. Uniformly graded coarse aggregate is usually

recommended to form the stone reservoir (USEPA 1999). Similar bioretention systems, permeable pavement systems are also reported to be helpful in reducing surface runoff volumes as well as peak flows (Dreelin et al. 2006; Collins et al. 2008), in maintaining base flow and ground water recharge (USEPA 1999; Bean et al. 2007), and in improving stormwater quality (Rushton 2001; Fassman and Blackbourn 2011).

In addition to the aforementioned four LID practices, there are many others such as swale systems, infiltration trenches, and vegetated filter strips. More information about these LID practices can be found from USEPA (2000), CVC and TRCA (2010), and Ahiablame et al. (2012).

## 1.3 Hydrologic Performances of LID Practices

As the LID stormwater management approach gains its popularity, the beneficial uses of LID practices have been shown in numerous previous studies at both watershed and individual lot scales. From the perspective of hydrology, one of the significant differences between the LID practices and traditional stormwater management approaches is that the LID stormwater management approach also focuses on stormwater volume control (Ahiablame et al. 2012). Summarized below are the stormwater volume control performances of the aforementioned four LID practices.

At micro-scales (lot levels), stormwater volume management performances of individual LID practices have been demonstrated in numerous previous studies. For instance, using cisterns to collect rainwater for both indoor and outdoor uses was reported to be able to reduce total volume of runoff from roof tops by 89% at Guelph, Ontario (Farahbakhsh et al. 2009) and by 18%-43% at Toronto, Ontario (TRCA 2010). The runoff reduction rates of green roofs reported in previous studies are significantly different for different types of green roofs under different weather conditions. Mentens et al. (2006) reported that stormwater retention ranged from 85% for intensive green roofs to 27% for extensive green roofs. Getter et al. (2007) reported that the mean stormwater retention of green roofs changed from 94% for light rainfall events (smaller than 2 mm) to 63% for heavy rainfall events (more than 10 mm).

The stormwater volume control performance of a bioretention system (or a rain garden) is often expressed by its stormwater capture efficiency, which is defined as the long-term average fraction of stormwater volume captured by the surface depression of the system (instead of overflowing from the system). Stormwater capture efficiencies of bioretention systems reported in previous studies range from 67.9% to 99.2% (Dietz and Clausen 2005; Li et al. 2009; Trowsdale and Simcock 2011). Reduction of runoff volume is also one of the main stormwater management roles that permeable pavements play. Runoff

reduction rates of permeable pavements were reported to be 36%-64% at Kinston, North Carolina (Collins et al. 2008) and larger than 97% at Renton, Pennsylvania (Brattebo and Booth 2003).

At the watershed scale, a number of studies have also been conducted to evaluate the stormwater volume control benefits of LID practices. Selbig and Bannerman (2008) studied two residential basins (one was developed in a conventional way and the other was developed with LID) in Cross Plains, Wisconsin. The conventionally-developed basin consists of curbs, gutters, streets, and a fully connected stormwater-conveyance system. The LID basin consists of grassed swales, reduced impervious areas, street inlets draining to grass swales, a detention pond, and an infiltration basin. Total annual discharge volume measured from the conventional basin ranged from 1.3 to 9.2 times that of the LID basin. In a paired watershed study, the runoff volumes from a controlled, a traditional, and a LID watershed in Waterford, Connecticut were compared (Bedan and Clausen 2009). It was reported that the replacement of traditional curbs and gutters with bioretention swales and asphalt roads with pervious concrete-pavers could reduce 42% of the weekly storm flow depth.

Wang et al. (2010) used the curve number method to estimate stormwater volumes expected from storms with different return periods for the

pre-development conditions, a conventional design, and two LID designs of a 3-ha watershed near Coshocton, Ohio. It was reported that stormwater volumes from 2-, 10-, 25-, 50-, 100-year storms for the two LID designs were all smaller than those from the conventional design. For example, the stormwater volume from the conventional design increased by 55 % over that for the pre-development conditions for a 2-year storm, while the stormwater volumes from the two LID designs were only 26% and 17% greater than that for the pre-development conditions, respectively. Ahiablame et al. (2013) assessed the performance of rain barrel/cistern and porous pavement as retrofitting technologies in two urbanized watersheds of 70 and 40 $km^2$ near Indianapolis, Indiana. The various implementation levels of barrel/cistern and porous pavement were reported to be able to reduce 2-12% of the volume of runoff from the watersheds.

As summarized above, the reported stormwater volume management performances of LID practices vary significantly due to differences in design and climate conditions. The variation in reported stormwater volume control performances may cause problems in standardizing the hydrologic design of LID practices. To assist in the planning and design of LID practices, accurate and reliable tools are needed to evaluate their stormwater management performances.

## 1.4 Hydrologic Models of LID Practices

Hydrologic information (e.g., discharge volumes and rates, statistical performance measures, etc.) is needed in the planning and design of LID practices. Although the hydrologic performance of many LID practices has been evaluated and discussed in previous monitoring studies, due to the high costs and the required great efforts, monitoring studies are constrained to limited periods and conditions and therefore can hardly provide the hydrologic information of LID practices over all temporal and spatial scales and under all possible climatic conditions (Ahiablame et al. 2012). Hydrologic models, which are developed, calibrated and verified on the basis of monitoring information, can provide valuable insights into the hydrological operation of LID practices over different temporal (single-event and long-term) and spatial (lot level, watershed and regional) scales and can be employed to generate the required hydrologic information for the planning and design of LID practices.

Over the past several years, a number of hydrologic modeling techniques have been developed to simulate the hydrological processes associated with LID practices and to evaluate their stormwater management performances (e.g., Schluter and Jefferies 2002; Heasom et al. 2006; Palla et al. 2009; Engel and Ahiablame 2011). Based on their scopes of application, the hydrologic models for LID practices can be classified into two categories. The first category of LID models are developed for the purposes of testing the

configurations or evaluating the performances of a single type of LID practice at the micro-scale [e.g., the green roof model (She and Pang 2010), the bioretention model (He and Davis 2011)]. The second category of models can be used to model the hydrologic processes and to evaluate the hydrologic performance of a group of different types of LID practices implemented together in an urban catchment [e.g., the SUSTAIN model (USEPA 2009)].

Two different methods are usually used to represent LID practices in a hydrologic model. The first one is referred to as the aggregation method in which the hydrologic performance of LID practices are measured by combing all complex processes (e.g., evapotranspiration, infiltration, overflow) occurring in the practic in one parameter in the hydrologic model (Ahiablame et al. 2012). For example, the hydrologic effect of green roofs, permeable pavements, and rain barrels were represented with different curve number values in Carter and Jackson (2007) and Engel and Ahiablame (2011). The second LID modelling methods seek to model the detailed hydrologic processes occurring in the practic. For example, the HYDRUS-1D green roof model (Hilten et al. 2008) was developed based on the Van Genuchten–Mualem equations and the RECHARGE-2D rain garden model (Aravena and Dussaillant 2009) was developed using the Richard's equation and the finite-volume method.

The U. S. Environmental Protection Agency's Storm Water Management

Model or SWMM (Huber and Dickenson 1988) has been widely used to simulate the hydrologic performanc of various LID practices (e.g., Park et al. 2008; Alfredo et al. 2010; Abi Aad et al., 2010; Lee et al. 2013). A new module referred to as the LID module has recently been added to the SWMM to exclusively support simulations of LID practices (Rossman 2010). In the SWMM LID module, LID practices are represented by different combinations of a number of vertical layers including a surface layer, a soil layer, a storage layer and an underdrain layer (Rossman 2009). For example, a rain barrel may consist of a surface layer that receives rain water, a storage layer to retain stormwater, and an underdrain layer to control the discharge from the barrels. The hydrologic performanc of LID practices can be modeled by solving simple mass balance equations that express the change in water volume in each layer over time as the difference between the inflow and outflow water fluex (Rossman 2009).

Hydrologic models of LID practices provide quantitative tools to test the design configurations of individual LID practices and the watershed development scenarios incorporated with different LID strategies. Calibrated and verified properly, the LID models, specifically the ones seeking to model the detailed hydrologic processes occurring inside individual LID practices, can be used to generate a long-term time series of flow rates from, and water content levels of, the LID practices. These time series can then be used to

calculate the statistical performance measures of LID practices such as the long-term average runoff reduction rate of green roofs and stormwater capture efficiency of bioretention systems. However, data availability and processing requirements could be an issue for the long-term simulations using process-based hydrologic models. The analytical probabilistic approach (Eagleson 1972; Adams and Papa 2000), which has been used to derive the probability distributions of system performance variables (e.g., runoff from urban catchments and spill volumes from stormwater control facilities) from probability distributions of rainfall characteristics (e.g., Guo and Adams 1998a, 1999a), may be used as a computationally efficient alternative to continuous simulation for estimating the performance statistics of LID practices.

## 1.5 The Analytical Probabilistic Approach

The analytical probabilistic approach was developed on the basis of the derived probability distribution theory. The derived probability distribution theory can be simply expressed as the probability distribution of a dependent random variable being fundamentally related to, and may be derived from, those of the independent random variables using the functional relationship between the dependent and independent variables (Guo 1998). A more detailed explanation of the derived probability distribution theory can be found in Benjamin and Cornell (1970) and Adams and Papa (2000).

Initially introduced into the hydrologic practice by Eagleson (1972), the analytical probabilistic approach has been successfully used to develop probabilistic stormwater models for stormwater management planning and design purposes (e.g., Chan and Bras 1979; Adams and Papa 2000; Chen and Adams 2006). These probabilistic stormwater models are usually composed of closed-form analytical equations. The analytical equations can be used to directly calculate the values of not only runoff volumes and flood peaks (Hebson and Wood 1982; Diaz-Granados et al. 1984; Guo and Adams 1998a, 1998b) but also the performance index of storm water management facilities (Loganathan and Delleur 1984; Guo and Adams 1999a, 1999b； Li and Adams 2000; Balistrocchi et al. 2009).

Probability density functions (PDFs) of rainfall characteristics which represent the rainfall conditions of a location of interest are usually used as the foundation of the analytical probabilistic approach. These PDFs can be obtained by conducting a statistical analysis of rainfall events separated from a long-term rainfall record. A long-term continuous rainfall record is separated into individual rainfall events by applying two discretization thresholds: an interevent time definition (IETD) and a minimum volume (e.g., Balistrocchi et al. 2011; Guo et al. 2012). The histograms obtained from the statistical analysis of rainfall event-average intensities, event volumes, event durations and inter-event times at many locations can be best represented by exponential

PDFs (Eagleson 1972, 1978; Howard 1976; Adams et al. 1986; Adams and Papa 2000; Guo and Baetz 2007). The Weibull probability distribution was found to be more appropriate for rainfall event volumes in Italy (Bacchi et al. 2008; Balistrocchi et al. 2009).

In addition to the PDFs of rainfall characteristics, appropriate conceptualized rainfall-runoff or rainfall-runoff-overflow transformations representing the hydrological processes occurring on a catchment or in a stormwater management facility are also needed to derive the PDFs of the outputs of interest (e.g., runoff volumes and peak discharge rates from a catchment, overflow volumes from a stormwater management facility) using the analytical probabilistic approach. In the STORM model (USACE 1977), the runoff generation mechanism of a catchment is represented by the following rainfall-runoff model:

$$v_r = \begin{cases} 0, & v \le S_d \\ \phi\left(v - S_d\right), & v > S_d \end{cases} \tag{1.1}$$

where $v_r$ is the runoff volume, $v$ is the rainfall volume, $\phi$ is a dimensionless runoff coefficient of the catchment, and $S_d$ is the depression storage of the catchment. This rainfall-runoff relationship represents a lumped runoff generation mechanism which aggregates the pervious and impervious areas together and has been incorporated into many of the analytical probabilistic urban stormwater models developed at the University of Toronto (e.g., Smith 1980; Papa 1997; Adams and papa, 2000).

An extended form of the rainfall-runoff transformation was also used in many previous studies (e.g., Chen and Adams 2006) in which the entire catchment is divided into impervious and pervious areas and runoff generated from the impervious and pervious areas are considered separately. It is expressed as:

$$v_r = \begin{cases} 0, & v \le S_{di} \\ h\left(v - S_{di}\right), & S_{di} < v \le S_{dp} \\ \left[h + \phi_{dp}\left(1-h\right)\right]v - hS_{di} - \phi_{dp}S_{dp}\left(1-h\right), & v > S_{dp} \end{cases} \quad (1.2)$$

In Equation (1.2), $h$ is the fraction of the imperviousness of the catchment; $S_{di}$ is the impervious area depression storage; $S_{dp}$ is the pervious area depression storage; $\phi_{dp}$ is the pervious area runoff coefficient. In this rainfall-runoff transformation, pervious area infiltration losses were still accounted for by using a runoff coefficient (i.e., $\phi_{dp}$), thus neglecting the fact that infiltration losses are also affected by the infiltration capacity of the soil.

Incorporating the Horton infiltration model, a further extended form of rainfall-runoff transformation was proposed by Guo and Adams (1998a) as follows:

$$v_r = hv_{ri} + (1-h)v_{rp} = \begin{cases} 0 & , \quad v \le S_{di} \\ h(v - S_{di}) & , \quad S_{di} < v \le S_{il} + f_c t \\ v - S_d - f_c(1-h)t & , \quad v > S_{il} + f_c t \end{cases} \quad (1.3)$$

where $v_{ri}$ and $v_{rp}$ are the runoff volumes from impervious and pervious areas, respectively; $f_c$ is the ultimate infiltration capacity of the soil; $t$ is the duration of a random rainfall event; $S_{il}$ is the total pervious area initial losses, which includes the surface depression losses and the initial soil wetting infiltration losses during the initial period of a storm when infiltration capacity in higher than $f_c$; $S_d$ is the area-weighted depression storage of the impervious areas and the initial losses of the pervious areas. Equation (1.3) has largely extended the capabilities of the analytical probabilistic stormwater management models. On the basis of Equation (1.3), frequency distributions of runoff volumes and peak discharge rates from urban catchments were derived (Guo and Adams 1998a, 1998b). Also developed were analytical equations that can be used for flood and stormwater quality control analysis (Guo and Adams 1999a, 1999b; Guo et al. 2009).

One shortcoming of Equation (1.3) and of many other earlier representations of rainfall-runoff transformations (e.g., Eagleson 1972; Chan and Bras 1979; Loganathan and Delleur 1984) is that only the infiltration-excess runoff generation process is considered (Guo et al. 2012). Saturated overland flows can occur in an urban catchment especially when LID practices such as bio-retention systems and pervious pavements are implemented for urban stormwater management. Taking both infiltration and saturation excess runoff generation mechanisms into consideration, Guo et al.

(2012) proposed a more complete urban catchment rainfall-runoff transformation in which the maximum possible infiltration volume ($S_s$) of the soil layers was incorporated. With both the potential infiltration losses and $S_s$ considered, the analytical equations developed in Guo et al. (2012) may be used to evaluate the stormwater management effects of LID practices.

As represented by Equations (1.2) and (1.3), the impervious and pervious subareas are drained through two independent flow paths to the catchment outlet. The overall volume of runoff from the urban catchment is treated as the area-weighted combination of the volumes of runoff from the pervious and impervious subareas of the catchment. However, runoff from an urban catchment depends largely on not only the areas of impervious and pervious surfaces but also the connectivity of these surfaces to stormwater drainage systems (Lee and Heaney 2003). Routing stormwater runoff from impervious surfaces (e.g., rooftops) onto pervious surfaces (e.g., lawns) is one of the LID strategies that can help mitigate increases in stormwater volume resulting from urbanization (Mueller and Thompson 2009). The generation and routing processes of runoff from these disconnected impervious areas (i.e., impervious areas which are not directly connected to stormwater drainage systems) are not explicitly considered in any of the previous rainfall-runoff transformations incorporated by the analytical probabilistic models (e.g., Adams and papa, 2000; Chen and Adams 2006; Guo et al. 2012).

Joint PDFs of rainfall characteristics such as rainfall event volume, duration, average intensity, and/or inter-event dry period are usually required in the application of the derived probability distribution theory. In most of the previous studies (e.g., Eagelson 1972; Hebson and Wood 1982; Diaz-Granados et al. 1984; Li and Adams 2000; Chen and Adams 2006), the joint PDFs of rainfall characteristics were formulated as products of their marginal distributions by assuming statistical independence among these characteristics. Despite the remarkable results of these works, statistical dependences among these rainfall characteristics, especially among rainfall event volume, duration and intensity, are usually observed from sample statistics (Balistrocchi and Bacchi 2011). The potential limitations of using the assumption of independence among rainfall characteristics were noted. Seto (1984) and Adams and Papa (2000) compared analytical models derived on the basis of different representations of the joint PDFs of rainfall characteristics (both dependent and independent) to continuous simulations. Better performanc, however, obtained for the cases when the rainfall characteristics were treated as independent variables.

In applying the analytical probabilistic approach to assess the performance of stormwater management systems involving storage elements, it is necessary to specify the initial conditions (e.g., the initial water level or the initial moisture content) of the storage elements at the beginning of a

random rainfall event. Howard (1976) analyzed the problem of runoff diverted to a storage reservoir and assumed that the reservoir is full at the end of the rainfall event preceding the analyzed random rainfall event. Smith (1980) extended the Howard's model by solving the steady-state probability distribution of reservoir contents at the end of the rainfall event preceding the analyzed random rainfall event. This work alleviated the Howard's conservative assumption but also required a numerical solution in the analysis (Adams and Papa, 2000). The numerical solution required in the analysis makes it complicated and limits its practical application. For simplification, the Howard's conservative assumption was still employed in many studies (e.g., Loganathan and Delleur 1984; Guo and Baetz 2007) to study other types of stormwater management facilities. Another assumption about the initial conditions adopted in previous studies is that the storage elements are assumed to be completely empty at the beginning of the analyzed random rainfall event (e.g., Bacchi et al. 2008; Balistrocchi et al. 2009). Both of the above mentioned assumptions could result in systematic underestimation or overestimation of the performances of stormwater management systems.

Analytical probabilistic models have been compared to both continuous simulation results (e.g., Loganathan and Delleur 1984; Balistrocchi et al. 2009; Guo et al. 2012) and field measurements (e.g., Chan and Adams 2006) in many of the above mentioned studies. These comparisons have demonstrated

the satisfactory accuracy of analytical probabilistic models under a wide variety of hydrologic and climatic conditions. Given the satisfactory accuracy and its practical advantages as shown in these works, the application of the analytical probabilistic approach could be advantageous for an expedient evaluation of the performance of LID practices. Guo and Baetz (2007) derived analytical equations to evaluate the hydrologic performance of rain barrels, however, the analytical probabilistic approach has not been used for evaluation of the performance of other types of LID practices.

## 1.6 Objectives and Organization

The overall objective of this thesis is to develop a set of analytical probabilistic models which can be used to evaluate the hydrologic performance of structural LID practices such as green roofs, bioretention systems (rain gardens) and permeable pavements. These analytical models can be used as computationally efficient alternatives of, or together with, continuous simulations to assist in the planning and hydrologic design of structural LID practices. The accuracy of these analytical models will be demonstrated by comparing the analytical model results with field observations and/or with results determined from continuous simulations under different climatic conditions.

To achieve the overall objective of this thesis, four individual papers

have been completed. These four papers are presented in Chapters 2-5. Chapter 2 presents the development, verification and application of an analytical probabilistic model for green roofs. Analytical probabilistic models for rain gardens and bioretention systems are presented respectively in Chapters 3 and 4. Chapter 5 describes the development of an analytical equation for evaluating the stormwater volume control performance of permeable pavements. Following these four chapters, Chapter 6 summarizes the major conclusions of this study and lists some recommendations for future research. A technical note about simulating the stormwater volume control performance of permeable pavements using SWMM is also included in this thesis as supplemental findings.

## References

Abi Aad, M. P., Suidan, M. T., and Shuster, W. D. (2010). Modeling techniques of best management practices: rain barrels and rain gardens using EPA SWMM-5. *Journal of Hydrologic Engineering*, 15(6), 434–443.

Adams, B. J., and Papa, F. (2000). *Urban Stormwater Management Planning with Analytical Probabilistic Models*, John Wiley & Sons, Inc., New York, USA.

Adams, B. J., Fraser, H. G., Howard, C. D. D., and Hanafy, M. S. (1986). Meteorologic data analysis for drainage system design. *Journal of Environmental Engineering*, ASCE, 112(5), 827–848.

Ahiablame, L. M., Engel, B. A., and Chaubey, I. (2013). Effectiveness of low impact development practices in two urbanized watersheds: Retrofitting with rain barrel/cistern and porous pavement. *Journal of Environmental Management*, 119, 151-161.

Ahiablame, L., Engel, B., and Chaubey, I. (2012). Effectiveness of Low Impact Development practices: literature review and suggestions for future research. *Water, Air, and Soil Pollution*, 223(7), 4253-4273.

Alfredo, K., Montalto, F., and Goldstein, A. (2010). Observed and modeled performances of prototype green roof test plots subjected to simulated low- and high-intensity precipitations in a laboratory experiment. *Journal of Hydrologic Engineering*, 15(6), 444–457.

Aravena, J. E., and Dussaillant, A. (2009). Storm-water infiltration and focused recharge modeling with finite-volume two-dimensional Richards

Equation: application to an experimental rain garden. *Journal of Hydraulic Engineering*, 135(12), 1073–1080.

Bacchi, B., Balistrocchi, M., and Grossi, G. (2008). Proposal of a semiprobabilistic approach for storage facility design, *Urban Water Journal*, 5(3), 195–208.

Balistrocchi, M., and Bacchi, B. (2011). Modelling the statistical dependence of rainfall event variables by a trivariate copula function. *Hydrology and Earth System Sciences*, 15, 1959–1977.

Balistrocchi, M., Grossi, G., and Bacchi, B. (2009). An analytical probabilistic model of the quality efficiency of a sewer tank. *Water Resources Research*, 45, W12420, doi:10.1029/ 2009WR007822.

Bean, E. Z., Hunt, W. F., and Bidelspach, D. A. (2007). Field survey of permeable pavement surface infiltration rates. *Journal of Irrigation and Drainage Engineering*, 133(3), 247–255.

Bedan, E. S., and Clausen, J. C. (2009). Stormwater runoff quality and quantity from traditional and low impact development watersheds. *Journal of the American Water Resources Association*, 4, 998–1008.

Benjamin, J. R., and Cornell, C. A. (1970). *Probability, Statistics and Decision for* Civil Engineers, McGraw-Hill, New York, USA.

Berndtsson, J. C. (2010). Green roof performance towards management of runoff water quantity and quality: A review. *Ecological Engineering*, 36(4), 351–360.

Brattebo, B. O., and Booth, D. B. (2003). Long-term stormwater quantity and quality performance of permeable pavement systems. *Water Research*, 37(18), 4369–4376.

Carter, T. L., and Jackson, C. R. (2007). Vegetated roofs for storm water management at multiple spatial scales. *Landscape and Urban Planning*, 80 (1–2), 84–94.

Chan, S. O., and Bras, R. L. (1979). Urban storm water management: Distribution of flood volumes. *Water Resources Research*, 15(2), 371–382.

Chen, J., and Adams, B. J. (2006). A framework for urban storm water modeling and control analysis with analytical models. *Water Resources Research*, 42(6), W06419.

Coffman, Larry. (2000). *Low-Impact Development Design Strategies, An Integrated Design Approach*. EPA 841-B-00-003. Prince George's County, Maryland. Department of Environmental Resources, Programs and Planning Division.

Collins, K. A., Hunt, W. F., and Hathaway, J. M. (2008). Hydrologic comparison of four types of permeable pavement and standard asphalt in eastern North Carolina. *Journal of Hydrologic Engineering*, 13(12), 1146–1157.

Collins, K. A., Hunt, W. F., and Hathaway, J. M. (2008). Hydrologic comparison of four types of permeable pavement and standard asphalt in eastern North Carolina. *Journal of Hydrologic Engineering*, 13(12), 1146–1157.

Construction Industry Research and Information Association (CIRIA). (2000). *Sustainable Urban Drainage Systems: Design Manual for England and Wales*. Construction Industry Research and Information Association, Report C522. London, UK: Cromwell Press.

Credit Valley Conservation Authority and Toronto and Region Conservation Authority (CVC and TRCA), (2010). *Low impact development stormwater management planning and design guide*. CVC and TRCA, Downsview and Mississauga, ON, Canada.

Davis, A. P. (2008). Field performance of bioretention: Hydrology impact. *Journal of Hydrologic Engineering*, 13(2), 90–95.

Diaz-Granados, M. A., Valdes, J. B., and Bras, R. L. (1984). A physically based flood frequency distribution. *Water Resources Research*, 20(7), 995–1002.

Dietz, M. E. (2007). Low impact development practices: A review of current research and recommendations for future directions. *Water, Air, Soil Pollutant*, 186(1–4), 351–363.

Dietz, M. E., and Clausen, J. C. (2005). A field evaluation of rain garden flow and pollutant treatment. *Water, Air, Soil Pollutant*, 167(1–4), 123–138.

Dietz, M. E., and Clausen, J. C. (2006). Saturation to improve pollutant retention in a rain garden flow. *Environmental Science & Technology*, 40, 1335–1340.

Dreelin, E. A., Fowler, L., and Carroll, C. R. (2006). A test of porous pavement effectiveness on clay soils during natural storm events. *Water Research*, 40(4), 799–805.

Eagleson, P. S. (1978). Climate, soil, and vegetation, 2, the distribution of annual precipitation derived from observed storm sequences. *Water Resources Research*, 14(5), 713-721.

Eagleson, P. S. (1972). Dynamics of flood frequency, *Water Resources*

*Research*, 8(4), 878–898.

Engel, B., and, Ahiablame, L. M. (2011). L-THIA-LID long-term hydrologic impact assessment-low impact development model, sv_version1.1. Purdue University.

Farahbakhsh, K., Despins, C., and Leidl, C. (2009). Developing capacity for large-scale rainwater harvesting in Canada. *Water Quality Research Journal of Canada*. 44(1), 92-102.

Fassman, E. A., and Blackbourn, S. D. (2011). Road runoff water-quality mitigation by permeable modular concrete pavers. *Journal of Irrigation and Drainage Engineering*, 137 (11), 720–729.

Getter, K. L., Rowe, D. B., and Andresen, J. A. (2007). Quantifying the effect of slope on extensive green roof stormwater retention. *Ecological Engineering*, 31(4), 225–231.

Guo, Y. (1998). *Development of Analytical Probabilistic Urban Stormwater Models*, PhD thesis, Department of Civil Engineering, University of Toronto, Toronto, ON, Canada.

Guo, Y., and Adams, B. J. (1998a). Hydrologic analysis of urban catchments with event-based probabilistic models. Part I: Runoff volume, *Water Resources Research*, 34(12), 3421–3431.

Guo, Y., and Adams, B. J. (1998b). Hydrologic analysis of urban catchments with event-based probabilistic models. Part II: Peak discharge rate, *Water Resources Research*, 34(12), 3433–3443.

Guo, Y., and Adams, B. J. (1999a). Analysis of detention ponds for storm water quality control, *Water Resources Research*, 35(8), 2447–2456.

Guo, Y., and Adams, B. J. (1999b). An analytical probabilistic approach to sizing flood control detention facilities, *Water Resources Research*, 35(8), 2457–2468.

Guo, Y., and Baetz, B. W. (2007). Sizing of rainwater storage units for green building applications. *Journal of Hydrological Engineering*, 12(2), 197–205.

Guo, Y., Hansen, D., and Li, C. (2009). Probabilistic approach to estimating the effects of channel reaches on flood frequencies, *Water Resources Research*, 45, W08404, doi: 10.1029/2008WR007387.

Guo, Y., Liu, S., and Baetz, B. W. (2012). Probabilistic rainfall-runoff transformation considering both infiltration and saturation excess runoff generation processes, *Water Resources Research*, 48, W06513, doi:10.1029/2011WR011613.

He, Z., and Davis, A. P. (2011). Process modeling of storm-water flow in a bioretention cell, *Journal of Irrigation and Drainage Engineering*, 137(3), 121–131.

Heasom, W., Traver, R., and Welker, A. (2006). Hydrologic modeling of a bioinfiltration best management practice. *Journal of the American Water Resources Association*, 42(5), 1329–1347.

Hebson, C., and Wood, E. F. (1982). A derived flood frequency distribution. *Water Resources Research*, 18(5), 325–340.

Hilten, R. N., Lawrence, T. M., and Tollner, E. W. (2008). Modeling storm water runoff from green roofs with HYDRUS-1D. *Journal of Hydrology*, 358 (3–4), 288–293.

Holman-Dodds, J. K., Bradley, A. A., and Potter, K. W. (2003). Evaluation of hydrologic benefits of infiltration based urban storm water management. *Journal of the American Water Resources Association*, 39 (1), 205–215.

Howard, C. D. D. (1976). Theory of storage and treatment plant overflows, *Journal of Environmental Engineering Division,* ASCE, 102(EE4), 709–722.

Huber, W. C., and Dickinson, R. E. (1988). *Storm Water Management Model, version 4, user's manual*. EPA 600/388/001a (NTIS PB88-236641/AS). USEPA, Athens, GA.

Hunt, W. F., Smith, J. T., Jadlocki, S. J., Hathaway, J. M., and Eubanks, P. R. (2008). Pollutant removal and peak flow mitigation by a bioretention cell in urban Charlotte, NC. *Journal of Environmental Engineering*, 134(5), 403–408.

Lee, J. G., and Heaney, J. P. (2003). Estimation of urban imperviousness and its impacts on storm water systems. *Journal of Water Resourources Planning and Management*, 129(5), 419–426.

Lee, J., Hyun, K., and Choi, J. (2013). Analysis of the impact of low impact development on runoff from a new district in Korea. *Water Science and Technology*, 68(6), 1315-1321.

Li, H., Sharkey, L. J., Hunt, W. F., and Davis, A. P. (2009). Mitigation of impervious surface hydrology using bioretention in North Carolina and Maryland. *Journal of Hydrologic Engineering*, 14(4), 407–415.

Li, J. Y., and Adams B. J. (2000). Probabilistic models for analysis of urban runoff control systems. *Journal of Environmental Engineering*, 126(3),

217–224.

Loganathan, G. V., and Delleur, J. W. (1984). Effects of urbanization on frequencies of overflows and pollutant loadings from storm sewer overflows: A derived distribution approach. *Water Resources Research*, 20(7), 857–865.

Melbourne Water. (2005). *WSUD Engineering Procedures: Stormwater*. CSIRO Publishing, Melbourne, Australia.

Mentens, J., Raes, D., and Hermy, M. (2006). Green roofs as a tool for solving the rainwater runoff problem in the urbanised 21st century. *Landscape and Urban Planning*, 77(3), 217–226.

Mueller, G. D., and Thompson, A. M. (2009). The ability of urban residential lawns to disconnect impervious area from municipal sewer systems. *Journal of American Water Resources Association*, 45 (5), 1116–1126.

Palla, A., Gnecco, I., and Lanza, L. G. (2009). Unsaturated 2D modelling of subsurface water flow in the coarse-grained porous matrix of a green roof. *Journal of Hydrology*, 379(1-2), 193–204.

Papa, F. (1997). *Analytical probabilistic models for urban stormwater planning*, M.A.Sc thesis, Department of Civil Engineering, University of Toronto, Toronto, ON, Canada.

Park, J., Yoo, Y., Park, Y., Yoon, H., Kim, J., Park, Y., Jeon, J., and Lim, K. J. (2008). Analysis of runoff reduction with LID adoption using the SWMM. *Journal of Korean Society of Water Quality*, 24(6), 805–815.

Pennsylvania Department of Environmental Protection (PDEP) (2006).

*Pennsylvania stormwater best management practices manual*. PA DEP, Rep. No. 363-0300-002, Harrisburg, PA, USA.

Prince George's County (PGC), Maryland, Department of Environmental Resource, Programs and Planning Division, (1999). "*Low Impact Development Design Strategies: An Integrated Approach*".

Rossman, L. A. (2009). *Modeling Low Impact Development Alternatives with SWMM*. Presented at Stormwater and Urban Water Systems Modeling, Toronto, ON, Canada, February 19 – 20.

Rossman, L. A. (2010). *Storm Water Management Model User's Manual, Version 5.0*, EPA/600/R-05/040, U.S. Environmental Protection Agency, Cincinnati, OH, USA .

Roy-Poirier, A., Champagne, P., and Filion, Y. (2010). Review of bioretention system research and design: past, present, and future. *Journal of Environmental Engineering*, 136(9), 878–889.

Rushton, B. T. (2001). Low-impact parking lot design reduces runoff and pollutant loads. *Journal of Water Resourources Planning and Management*, ASCE, 127(3), 172–179.

Schluter, W., and Jefferies, C. (2002). Modelling the outflow from a porous pavement. *Urban WaterJournal*, 4(3), 245-253.

Selbig, W. R., and Bannerman, R.T. (2008). *A comparison of runoff quantity and quality from two small basins undergoing implementation of conventional- and low-impactdevelopment (LID) strategies: Cross Plains, Wisconsin, water years 1999–2005*. U.S. Geological Survey Scientific Investigations Report, 2008–5008, p. 57.

Seto, M. Y. K. (1984). *Comparison of alternative derived probability distribution models for urban stormwater management*, M.A.Sc thesis, Department of Civil Engineering, University of Toronto, Toronto, ON, Canada.

She, N., and Pang, J. (2010). Physically based green roof model. *Journal of Hydrologic Engineering*, 15(6), 458–464.

Smith, D. I. (1980). *Probability of storage overflow for stormwater management*, M.A.Sc thesis, Department of Civil Engineering, University of Toronto, Toronto, ON, Canada.

Toronto and Region Conservation Authority (TRCA). (2010). *Performance Evaluation of Rainwater Harvesting Systems*. Final Draft Report. Sustainable Technologies Evaluation Program (STEP), Toronto, ON, Canada.

Trowsdale, S. A., and Simcock, R. (2011). Urban stormwater treatment using bioretention. *Journal of Hydrology*, 397, 167–174.

U. S. Environmental Protection Agency (USEPA). (1999). *Storm Water Technology Fact Sheet: Porous Pavement*. EPA 832-F-99-023.

U. S. Environmental Protection Agency (USEPA). (2000). *Low impact development (LID), A literature review*. Washington, D.C: Office of Water. EPA-841-B-00-005.

U. S. Environmental Protection Agency (USEPA). (2003). *Bacterial water quality standards for recreational waters (freshwater and marine waters) status report*. *Rep. No. EPA-823-R-03–008*, USEPA, Washington, D.C., USA.

U. S. Environmental Protection Agency (USEPA). (2009). *SUSTAIN, A framework for placement of best management practices in urban watersheds to protect water quality*. Office of Research and Development National Risk Management Research Laboratory-Water Supply and Water Resources Division. EPA-600-R-09-095.

U.S. Army Corps of Engineers (USACE) (1977), *Storage, treatment, overflow, runoff model (STORM)*, Gen. Comput. Prog. 723– S8–L7520, Hydrol. Eng. Cent., Davis, CA, USA.

Wang, X., Shuster, W., Pal, C., Buchberger, S., Bonta, J., and Avadhanula, K. (2010). Low impact development design integrating suitability analysis and site planning for reduction of post-development stormwater quantity. *Sustainability*, 2(8), 2467–2482.

# Chapter 2

# An Analytical Probabilistic Model for Evaluating the Hydrologic Performance of Green Roofs

**Shouhong Zhang and Yiping Guo**

**Abstract：** An easy-to-use and physically-based analytical probabilistic model is developed to evaluate the long-term average hydrologic performance of green roofs. The probabilistic models of local rainfall characteristics are introduced first, the hydrologic and hydraulic processes occurring on and inside a green roof system are then described mathematically, and the closed-form mathematical expressions depicting the stormwater management performance of a green roof system are finally obtained by using the derived probability distribution theory. Simplifying assumptions are made to mathematically describe the hydrologic and hydraulic processes. The validity of these assumptions and the overall probabilistic approach is demonstrated by comparing its outcomes with results from a series of continuous simulations using long-term rainfall data from Detroit, Michigan and observations from a real case study in Portland, Oregon.

**Key Words:** Green roof, Stormwater management, Runoff reduction rate, Probabilistic methods

## 2.1 Introduction

Urban habitats are constantly expanding in terms of space and density (Berndtsson 2010). The percentage of the population living in urban settings will exceed 80% by 2030 (United Nations 2002; Antrop 2004). The expansion of urban areas results in significant changes in land surfaces. One of these changes is the increase of impermeable areas. Farmland, grassland and forests are replaced by the impervious surfaces of rooftops, roads and parking lots. These impervious surfaces greatly decrease infiltration and increase surface runoff, which in turn increase the stress on existing stormwater infrastructure and the risk of urban and downstream flooding.

Tools for increasing on-site retention of runoff include storage reservoirs (i.e., detention/retention ponds) where water can be temporarily stored and green areas where water can infiltrate and be evapotranspirated (Mentens et al. 2006). In urban areas, application of these stormwater management practices is always constrained by space availabilities. There are, however, a lot of "unused" roof areas, about 40 - 50% of the impermeable surfaces in urban areas (Dunnett and Kingsbury 2004; Palla et al. 2009). Turning these roof areas green by covering them with a vegetation-soil system is beneficial in several ways (Oberndorfer et al. 2007), including energy conservation (Wong et al. 2003, 2007; Fang 2008), urban habitat provision (Brenneisen 2006; Gedge and Kadas 2005), and stormwater management (Bengtsson et al. 2005;

Carter and Rasmussen 2006; Mentens et al. 2006). It was estimated that covering 6% of all buildings in Toronto, Ontario, Canada with green roofs would result in the same stormwater retention effect as building a $60 million storage tunnel (Peck 2005); and changing 20% of building tops in Washington DC into green roofs would add over 71 million liters to the city's stormwater storage capacity and store approximately 958 million liters of rainwater during an average year (Deutsch et al. 2005). Therefore, green roofs have been considered a promising stormwater management practice.

A green roof system generally consists of a vegetation layer, a growing medium or substrate layer (where vegetation is planted and rain water is retained), a drainage layer (to drain out excess water), as well as a waterproof and root repellent layer (to protect the roof structure). Some green roofs are designed with an additional water storage layer which is combined with the drainage layer, in order to increase the rain water storage capacity of the green roof system, as well as to hold more water to satisfy the water requirement of the vegetation layer. The composition (Table 2.1) and depth of the growing medium vary greatly between green roofs designed by different professionals. Based on the depth of the growing medium, green roofs are typically divided into two main engineering categories: intensive and extensive (Mentens et al. 2006; Berndtsson 2010). Extensive green roofs are established with thin growing media layers having depths of 50 - 150 mm (Kosareo and Ries 2007).

**Table 2.1 The composition and hydraulic properties of different types of growing media**

| Composition | Porosity | Field Capacity | Wilting Point | Hydraulic Conductivity | Reference |
|---|---|---|---|---|---|
| 43% crushed roof tiles 8–12 mm, 37% sand, 10% organic material, 5% crushed limestone 8–12 mm, and 5% clay | 0.65 | 0.45 | 0.15 | N/A* | Bengtsson et al. ( 2005)； Villarreal and Bengtsson (2005) |
| 55 % Stalite expanded slate, 30% United States Golf Association sand, and 15 % organic matter | 0.51 | N/A* | N/A* | N/A* | Carter and Rasmussen (2006); Carter and Jackson (2007) |
| 91.2% sand, 5.6% silt, and 3.2% clay | 0.41 | N/A* | N/A* | N/A* | Getter et al.( 2007 ) |
| 80% expanded slate, 20% organic matter (100% sand was actually used in the model) | 0.43 | 0.11 | 0.08 | 120.4 mm/h | Hilten et al. (2008) |
| 84% volcanic material and 16% organic matter | 0.65 | N/A* | N/A* | 288 mm/h | Palla et al. (2009) |
| 28% sandy loam, 22% coarse perlite, 20% fiber, and 10% compost** | 0.41 | 0.35 | N/A* | 69.9-80.3 mm/h | She and Pang (2010) |
| 80% pumice and 20% composed bark fines | 0.59 | 0.47 | N/A* | N/A* | Voyde et al. 2010a |
| 50% pumice, 30% zeolite and 20% composed bark fines | 0.66 | 0.50 | N/A* | N/A* | |

* Not available;

** The summation is 80%, less than 100%, as reported in the literature.

Intensive green roofs have growing medium layers exceeding 110 - 150 mm in depth (Berndtsson 2010). The vast majority of green roofs installed for the purpose of stormwater management are often designed as the extensive type (She and Pang 2010). The focus of this study is therefore extensive green roofs having growing medium depths from 50 to 150 mm.

In terms of stormwater management, one of the main performance indicators of a green roof system is its reduction of runoff volume. A green roof system captures part of the precipitation (which would simply runoff over a regular roof) and eventually depletes the captured precipitation through evapotranspiration from vegetation and the growing medium (Palla et al. 2009). The runoff reduction rate of green roofs may vary widely under different weather conditions depending on the characteristics of rainfall events, the length of dry periods, etc. (Villarreal and Bengtsson 2005; Carter and Rasmussen 2006; Mentens et al. 2006; Simmons et al. 2008; Berndtsson 2010). The characteristics (number of layers, type of growing medium, depth of growing medium, type and density of vegetation, etc.) of green roofs also affect their runoff reduction rates (Monterusso et al. 2004; Bengtsson et al. 2005; Getter et al. 2007; Wolf and Lundholm 2008; Alfredo et al. 2010; Berghage et al. 2007; DiGiovanni et al. 2010). The stormwater management performance of green roof systems varies widely due to differences in design and operating conditions.

Several models have been developed to simulate the hydrologic and hydraulic processes occurring on and inside a green roof system and to assess its stormwater management performance. For instance, with the assumption that water flux from each sub-layer of the growing medium is proportional to the amount of water stored in the sub-layer and the antecedent water content of the growing medium equals its field capacity, Zimmer and Geiger (1997) developed a linear-storage green roof model solved by the Fourier transform method. For the non-linear behavior of fluxes, however, the equations need to be solved by more complex numerical methods which were not presented in detail in that study. Based on an empirical rainfall-runoff relationship of a green roof system obtained from observed data of 31 storm events, Carter and Jackson (2007) developed a Curve Number (CN)-based green roof model. That empirical model avoids the complexities of the physically-based model and eliminates the need for the use of many site-specific parameter values (Chau et al. 2005). However, in order to apply this model for another green roof system with different physical characteristics, a number of rainfall-runoff observations may have to be made first in order to estimate the CN of the green roof.

The HYDRUS-1D green roof model (Hilten et al. 2008) and the SWMS-2D green roof model (Palla et al. 2009) were developed based on Richards' law and the Van Genuchten–Mualem functions to simulate the

unsaturated flow within a green roof system. She and Pang (2010) developed another physically-based green roof model based on the Green-Ampt infiltration equations. In that model, both the field capacity of the growing medium and the gravity drainage of rain water through the voids of the growing medium under unsaturated conditions are taken into consideration (She and Pang 2010).

The U. S. EPA Storm Water Management Model (SWMM) is a dynamic rainfall-runoff simulation model used for single event or continuous simulation of runoff quantity and quality from primarily urban areas (Rossman 2010). Alfredo et al. (2010) employed the SWMM model to simulate the hydrologic performance of green roofs. It was found that the SWMM model tends to underpredict the volume and rate of discharge from green roofs and therefore caution should be exercised in applying the SWMM model, especially when the model is not validated with experimental data (Alfredo et al. 2010). The newly added Low Impact Development (LID) module of SWMM is expected to have the capability of simulating the stormwater management performance of various types of LID practices, including green roofs, rain barrels, porous pavements, and vegetative swales. For the continuous rainfall-runoff simulation of green roofs, SWMM may use the Horton Model, the Green-Ampt Model or the Curve Number procedure to calculate the infiltration of rain water through the growing medium.

Most of the above-mentioned green roof models have been reasonably tested and were shown to be able to capture approximately the long-term average stormwater management performance of green roofs if they are run under continuous simulation mode. However, the parameters required for the simulation of the detailed seepage processes in some of the physically-based models are difficult to obtain. Given the small scale of most green roof applications, the use of computer simulation with detailed data input as required in these models may be too time-consuming for the majority of design projects. Many European countries and the United States have started providing incentive programs such as exemptions from stormwater management taxes to encourage building owners to install green roof systems (She and Pang 2010). To guarantee that appropriate amount of incentives are awarded and that optimum green roof systems are designed and constructed, reliable and easy-to-use methods are needed to evaluate the stormwater management performance of green roof systems.

Green roofs' stormwater management performance is manifested in three aspects: (1) reduction of the total runoff volume; (2) delay in the initiation of runoff; and (3) distribution of runoff over a longer time period through a relatively slow release of the excess water that is temporarily stored in the pores of the substrate (Mentens et al. 2006). The main objective of this study is to develop a physically-based analytical probabilistic model to

quantitatively evaluate the runoff volume reduction performance of green roof systems. The hydraulic and hydrologic processes occurring on and inside a green roof system is analyzed first, followed by the derivation of closed-form mathematical expressions depicting the stormwater management performance of a green roof system. This derivation is based on the probabilistic models of the local rainfall characteristics. The validity of this probabilistic approach is demonstrated by comparing its outcomes with the results of a series of continuous simulations using long-term rainfall data from Detroit, Michigan and observations from a real case study in Portland, Oregon.

## 2.2 Probabilistic Rainfall-Runoff Transformation of a Green Roof System

### 2.2.1 Probabilistic Models of Rainfall Event Characteristics

The foundation of the probabilistic approach is the frequency distribution of local rainfall characteristics. Frequency distribution models for local rainfall characteristics may be obtained by conducting statistical analysis on the rainfall record of a gauge station. As a first step of this statistical analysis, a minimum period without rainfall, referred to as the inter-event time definition (IETD), is selected to isolate individual storms from a continuous rainfall time series. Whether a selected IETD is suitable or not

depends on the location (Guo et al. 2009) and the type of application. It was found that 6 to 12 hours are suitable for many locations and applications (Guo and Baetz 2007).

To obtain the suitable IETD for a specific location, the statistical test method described in detail in Guo and Baetz (2007) may be employed. That statistical test is based on the theory that the occurrence of storm events can be approximated as a Poisson process when the dry periods between storms (inter-event times) are exponentially distributed (Restrepo-Posada and Eagleson 1982). The likelihood of correlation between a series of events is greatly reduced when the series is accepted as a Poisson process (Ashkar and Rousselle 1987). Different IETD values will result in different number of rainfall events every year. Choosing one IETD value, the annual number of events ($n$) can be obtained for every year in the rainfall record; the variance Var[$n$] and the mean E[$n$] of $n$ can be calculated, the ratio $r$ between Var[$n$] and E[$n$] can also be calculated. Since the mean and variance of a Poisson distribution are equal (Cunnane 1979; Cruise and Arora 1990), the ratio $r$ should approach unity as the IETD is increased if the occurrence of storm events does follow a Poison process. Therefore, a statistical test may be devised for $r$ based on the approximation that the factor $(N\text{-}1)r$ is $\chi^2$ distributed with $(N\text{-}1)$ degrees of freedom (Cunnane 1979), here $N$ is the number of years of record. The critical values of $r$ can thus be determined for selected levels

of significance (Cruise and Arora 1990).

Once a suitable IETD is selected, statistical analysis on the isolated rainfall event volumes and inter-event times can be performed. For many locations, exponential probability density functions (PDFs) have been found to provide good fits to the histograms obtained from frequency analysis of the rainfall event volumes and inter-event times (Adams and Papa 2000). These exponential distributions may be expressed as

$$f_V(v) = \zeta e^{-\zeta v}, \quad v \geq 0 \tag{2.1}$$

$$f_B(b) = \psi e^{(-\psi b)}, \quad b \geq 0 \tag{2.2}$$

where $V$ is the rainfall event volume regarded as a random variable, $v$ is a specific value of $V$ (mm); $B$ is the inter-event time regarded as a random variable, $b$ is a specific value of $B$ (h); $\zeta$ is the distribution parameter for rainfall event volume, which can be estimated as the inverse of the mean of rainfall event volumes ($mm^{-1}$); $\psi$ is the distribution parameter for inter-event time, which can be estimated as the inverse of the mean of inter-event times ($h^{-1}$).

The goodness-of-fit of the exponential distribution models has been evaluated by many researchers (Eagleson 1972, 1978; Howard 1976; Adams et al. 1986; Guo and Adams 1998; Guo, 2001; Guo and Baetz 2007). For

locations throughout Canada and the USA, the values of these parameters ($\zeta$ and $\psi$) are available from Adams and Papa (2000) and Guo and Baetz (2007), respectively.

For illustration purposes, Detroit, Michigan was selected as the test location in this study. The rainfall data is from the Metro International Airport Station in Detroit (42.231˚N, 83.331˚W) and covers the years from 1960 to 2006. For each year, the non-winter period rainfall data from April 1st through October 31st were analyzed. An IETD of 8 h was found to give an *r* value 0.896 for the rainfall at the Metro International Airport Station in Detroit. It is within the range of the critical values of *r* (0.744 - 1.276) at 0.10 significance level. Using the selected IETD of 8 hours, the continuous non-winter rainfall record from 1960 to 2006 was isolated into 2203 individual rainfall events and the histograms of the rainfall event's *v* and *b* are shown in Figure 2.1. Exponential distributions fit both histograms very well as shown visually in Figure 2.1. The means used to estimate the distribution parameters are: $\bar{v} = 14.35$ mm, $\bar{b} =$ 97.95 h.

### 2.2.2 Hydrologic and Hydraulic Processes Occurring on and inside a Green Roof System

As rain falls onto a green roof, a portion of the rain water is intercepted by vegetation or trapped by small depressions on the surface and eventually

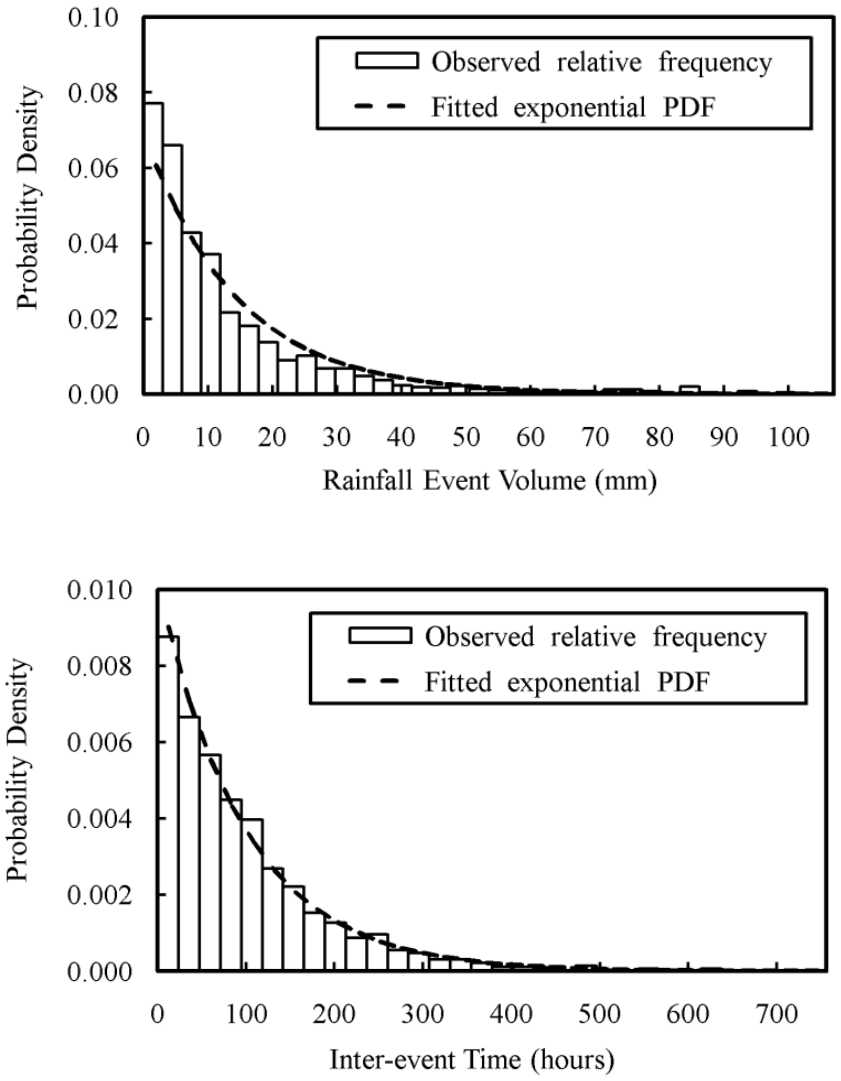


**Figure 2.1 Frequency distributions of rainfall event volume and inter-event time at Detroit, Michigan**

evaporates back to the atmosphere. The rest of the rain water moves downward through the surface of the growing medium (with a depth of *h*, mm) and replenishes the growing medium moisture, this process is known as infiltration. As more rain water infiltrates into the growing medium, the moisture of the medium increases, and the capillary suction in the growing

medium decreases. Bengtsson et al. (2005) observed that runoff from the growing medium does not occur until the medium is at its field capacity, denoted as $\theta_f$. Field capacity, expressed as a fraction of the total volume of the medium, corresponds to the maximum amount of water that a growing medium can hold within its structure against the pull of gravity.

When the field capacity of the medium is exceeded, some water will move through the bottom of the growing medium and will be drained out by the drainage system. Such movement of water is believed to be due to the fact that the upward capillary force of water in the larger voids of the growing medium is exceeded by gravity while the capillary force of water in smaller voids still can resist the pull of gravity (She and Pang 2010). The infiltrated rain water used to fill the growing medium to its field capacity will be retained in the green roof system. This retained water will be depleted through evapotranspiration, which is the mechanism by which the rainfall retention capacity of the green roof system is recovered between storm events (Voyde et al. 2010b). It is the evaporated and transpired water which enables green roofs to reduce runoff volume.

Some green roofs are designed with a storage layer, which can hold a certain amount of rain water to keep the roots of plants moist longer after rainfall. For this kind of green roof, the seepage water from the bottom of the

growing medium flows into the storage layer first. After the storage capacity of the storage layer (denoted as $S_c$, mm) is filled, runoff from the green roof begins. Due to the high hydraulic conductivity (Table 2.1) of most growing media, surface runoff seldom occurs on the top of green roofs. Only during extremely heavy rainfall events, ponding of water on the surface of green roofs may occur and the ponded water would be drained away through the spillway and drainage systems of the roof.

### 2.2.3 Estimation of the Runoff Reduction Rate of a Green Roof System

Probabilistic models of local rainfall characteristics will be used to analyze the average stormwater management performance of a green roof system. The analysis focuses on a rainfall event cycle starting from the beginning of a *b*-hour dry period, followed by a rainfall event with a volume of *v* mm. For each rainfall event cycle, the time of the dry period and the volume of the rainfall event are treated as random variables following their respective probability distributions. The expected value of a dependent random variable resulting from the rainfall event cycle, for instance, the volume of runoff generated from a green roof system per rainfall event, may be derived by using the functional relationships between the related variables and incorporating the PDFs listed in Equations (2.1) and (2.2). The derived probability distribution theory is employed to obtain the probability

distribution and the expected value of the dependent random variable. Details about the derived probability distribution theory can be found in Benjamin and Cornell (1970).

The volume of runoff generated from a green roof system during a rainfall event cycle is controlled by the volume of the rainfall event occurred in the rainfall event cycle and the retention capacity of the green roof system at the beginning of the rainfall event. The retention capacity of the green roof system could be expressed as

$$R_c = S_l + S_c + (\theta_f - \theta_i)h \qquad (2.3)$$

where $S_l$ is the summation of the volumes of rain water that may be intercepted by vegetation and trapped by small depressions (mm); $S_c$ is the storage capacity of the storage layer (mm, for a green roof system without storage layer, $S_c = 0$); $\theta_f$ is the field capacity of the growing medium (dimensionless fraction); $\theta_i$ is the initial moisture content of the growing medium at the beginning of the rainfall event (dimensionless fraction); $h$ is the depth of the growing medium (mm).

As shown in Equation (2.3), the retention capacity of a green roof system is partly determined by the initial moisture content of the growing medium. The minimum moisture content that a growing medium holds

against drainage and evapotranspiration is defined as the residual moisture content. In order to keep the green roof plants from wilting, appropriate irrigation is recommended during dry periods to maintain the moisture content of the growing medium at or above the wilting point soil moisture content (denoted as $\theta_w$, dimensionless fraction). As a result, the value of $\theta_i$ of a green roof system would not usually be less than $\theta_w$. Therefore, the maximum retention capacity of a green roof system at the beginning of a rainfall event could be represented as

$$R_{c\max} = S_l + S_c + (\theta_f - \theta_w)h \tag{2.4}$$

The initial moisture content of the growing medium at the beginning of a rainfall event (hereafter referred to as the current rainfall event) is controlled by the evapotranspiration rate during the dry periods and the evapotranspirable water content (denoted as $W_i$ and expressed as mm of water over the roof area) of the green roof system at the beginning of the dry period preceding the current rainfall event. $W_i$, which includes the water stored in the storage layer, could be at its maximum ($W_{i\max} = R_{c\max}$), its minimum ($W_{i\min} = 0$) or some values between the two, depending mainly on the magnitude of the last rainfall event and weather conditions preceding the last rainfall event.

Denoting the average evapotranspiration rate from a green roof system

as $E_a$, in mm/hour, the initial moisture content of the growing medium at the beginning of the current rainfall event could be calculated using the following equation:

$$\theta_i = \begin{cases} \frac{W_i - E_a b}{h} + \theta_w, & b \le \frac{W_i}{E_a} \\ \theta_w, & b > \frac{W_i}{E_a} \end{cases} \quad (2.5)$$

Equation (2.5) is valid assuming that $W_i$ can always be completely evapotranspirated if the dry period *b* is long enough. This assumption should be acceptable given the shallow depth of the green roof. Substitution of Equation (2.5) into Equation (2.3) gives the retention capacity of a green roof system at the beginning of the current rainfall event:

$$R_c = \begin{cases} R_{c\max} + E_a b - W_i, & b \le \frac{W_i}{E_a} \\ R_{c\max}, & b > \frac{W_i}{E_a} \end{cases} \quad (2.6)$$

The volume of runoff (denoted as $v_{rg}$ , mm) generated from the green roof system as a result of the current rainfall event is

$$v_{rg} = \begin{cases} 0, & \left[ v \le R_{\text{cmax}} \text{ and } b > \dfrac{W_i}{E_a} \right] \\ & \text{or } \left[ v \le R_{\text{cmax}} - W_i + E_a b \text{ and } b \le \dfrac{W_i}{E_a} \right] \\ v + W_i - R_{\text{cmax}} - E_a b, & \left[ v > R_{\text{cmax}} - W_i + E_a b \text{ and } b \le \dfrac{W_i}{E_a} \right] \\ v - R_{\text{cmax}}, & \left[ v > R_{\text{cmax}} \text{ and } b > \dfrac{W_i}{E_a} \right] \end{cases} \tag{2.7}$$

Equation (2.7) is based on the assumption that the infiltration capacity of the growing medium is always greater than rainfall intensity. This assumption is reasonable since the majority of the engineered growing media common to extensive green roofs are primarily comprised of non-cohesive aggregates which achieve very high permeability (Table 2.1).

The PDF of runoff volume generated from a green roof system per rainfall event may be obtained by determining the cumulative distribution function (CDF) of $v_{rg}$ first. Given the marginal PDFs of rainfall event volume ($v$) and inter-event time ($b$) of a rainfall event cycle, the CDF of $v_{rg}$ can be obtained using the derived probability distribution theory. According to Equation (2.7), there is an impulse probability that no runoff will be generated. This impulse probability is given by:

$$
\begin{aligned}
\mathrm{P}_{V_{rg}}(0) &= \mathrm{Prob.}\left( v \le R_{cmax} \text{ and } b > \frac{W_i}{E_a} \right) + \mathrm{Prob.}\left( v \le R_{\mathrm{cmax}} - W_i + E_a b \text{ and } b \le \frac{W_i}{E_a} \right) \\
&= \int_{\frac{W_i}{E_a}}^{\infty} \int_0^{R_{cmax}} \zeta \mathrm{e}^{-\zeta v} \psi \mathrm{e}^{-\psi b} dv db + \int_0^{\frac{W_i}{E_a}} \int_0^{R_{cmax} - W_i + bE_a} \zeta \mathrm{e}^{-\zeta v} \psi \mathrm{e}^{-\psi b} dv db \\
&= 1 - \frac{\mathrm{e}^{-\zeta R_{cmax}}}{\psi + \zeta E_a} \left( \psi \mathrm{e}^{\zeta W_i} + \zeta E_a \mathrm{e}^{-\frac{\psi W_i}{E_a}} \right)
\end{aligned}
\tag{2.8}
$$

The CDF of $v_{rg}$, $F_{V_{rg}}(v_{rg})$, can be derived as follows:

$$
\begin{aligned}
F_{V_{rg}}(v_{rg} > 0) &= \mathrm{Prob.}\left( R_{cmax} - W_i + bE_a < v \le R_{cmax} - W_i + bE_a + v_{rg} \text{ and } b \le \frac{W_i}{E_a} \right) \\
&\quad + \mathrm{Prob.}\left( R_{cmax} < v \le R_{cmax} + v_{rg} \text{ and } b > \frac{W_i}{E_a} \right) + P_{V_{rg}}(0) \\
&= \int_0^{\frac{W_i}{E_a}} \int_{R_{cmax} - W_i + bE_a}^{R_{cmax} - W_i + bE_a + v_{rg}} \zeta \mathrm{e}^{-\zeta v} \psi \mathrm{e}^{-\psi b} dv db \\
&\quad + \int_{\frac{W_i}{E_a}}^{\infty} \int_{R_{cmax}}^{R_{cmax} + v_{rg}} \zeta \mathrm{e}^{-\zeta v} \psi \mathrm{e}^{-\psi b} dv db + \mathrm{P}_{V_{rg}}(0) \\
&= 1 - \frac{\mathrm{e}^{-\zeta(v_{rg} + R_{cmax})}}{\psi + \zeta E_a} \left( \psi \mathrm{e}^{\zeta W_i} + \zeta E_a \mathrm{e}^{-\frac{\psi W_i}{E_a}} \right)
\end{aligned}
\tag{2.9}
$$

The PDF of $v_{rg}$, $f_{V_{rg}}(v_{rg})$, may be obtained as the first order derivative of $F_{V_{rg}}(v_{rg})$ with respect to $v_{rg}$:

$$
f_{V_{rg}}\left(v_{rg}\right) = \frac{d}{dv_{rg}} \left[ F_{V_{rg}}\left(v_{rg} > 0\right) \right] = \frac{\zeta \mathrm{e}^{-\zeta(v_{rg} + R_{cmax})}}{\psi + \zeta E_a} \left( \psi e^{\zeta W_i} + \zeta E_a e^{-\frac{\psi W_i}{E_a}} \right) \tag{2.10}
$$

The expected value of the runoff volume generated from a green roof system per rainfall event, $\mathrm{E}(v_{rg})$, is given as:

$$\begin{aligned} \mathrm{E}(v_{rg}) &= 0\mathrm{P}_{v_{rg}}(0) + \int_{v_{rg}=0}^{\infty} v_{rg} \frac{\zeta \mathrm{e}^{-\zeta(v_{rg}+R_{cmax})}}{\psi+\zeta E_a} \left( \psi e^{\zeta W_i} + \zeta E_a e^{-\frac{\psi W_i}{E_a}} \right) dv_{rg} \\ &= \frac{\mathrm{e}^{-\zeta R_{cmax}}}{\zeta(\psi+\zeta E_a)} \left( \psi e^{\zeta W_i} + \zeta E_a e^{-\frac{\psi W_i}{E_a}} \right) \end{aligned} \tag{2.11}$$

Using the same approach, the expected value of runoff volume generated from a regular roof per rainfall event, $\mathrm{E}(v_r)$, could also be derived. Depending on the design and construction of roofs, some regular roofs may convert 100% of rainfall to runoff, while some others may convert a fraction of rainfall to runoff (Guo and Baetz 2007). As a general case, a runoff coefficient $\phi$ may be applied to transform volume of rainfall to volume of runoff for regular roofs. The expected value of the volume of runoff generated from a regular roof per rainfall event was determined as (Guo and Baetz 2007):

$$\mathrm{E}(v_r) = \int_0^{\infty} v_r \frac{\zeta}{\phi} \mathrm{e}^{-\frac{\zeta}{\phi} v_r} dv_r = \frac{\phi}{\zeta} \tag{2.12}$$

The runoff volume reduction rate of a green roof system, $R_r$, as compared to a regular roof of the same area, could be calculated as:

$$R_r = \frac{\mathrm{E}(v_r) - \mathrm{E}(v_{rg})}{\mathrm{E}(v_r)} = 1 - \frac{\mathrm{e}^{-\zeta R_{cmax}}}{\phi(\psi+\zeta E_a)} \left( \psi e^{\zeta W_i} + \zeta E_a e^{-\frac{\psi W_i}{E_a}} \right) \tag{2.13}$$

For a particular green roof system at a specific location, the only

unknown in Equation (2.13) is $W_i$ , i.e., the evapotranspirable water content of the green roof system at the beginning of the dry period preceding the current rainfall event. Using Equation (2.13) and let $W_i = W_{i\max}$ , the most conservative estimate of the runoff reduction rate, denoted as $R_{r\min}$ , could be obtained; and let $W_i = W_{i\min}$ , the most overestimated value of the runoff reduction rate, denote as $R_{r\max}$ , could be calculated. As mentioned earlier, $W_i$ is dependent on the antecedent moisture condition of the growing medium preceding the last rainfall event and the magnitude of the last rainfall event. For the estimation of the average stormwater management performance of a green roof system, the mean value of $R_{r\max}$ and $R_{r\min}$ may be used to describe the long-term average runoff reduction rate of green roofs. That is

$$R_{r\text{ave}} = \frac{R_{r\max} + R_{r\min}}{2} \tag{2.14}$$

Equations (2.11) through (2.14) are collectively referred to as the analytical probabilistic green roof hydrologic performance models. Using these equations, the average volume of runoff per rainfall event and the long-term average runoff reduction rate of a green roof system can be analytically determined.

## 2.3 Verification of the Analytical Probabilistic Model

The closed-form mathematical expressions derived in the previous

section provide a flexible and convenient tool to evaluate the average runoff volume and the runoff reduction rate of green roofs. To validate the assumptions made in the development of these equations, a set of continuous SWMM simulations using the LID module were performed for green roofs with different depths and various growing medium types. Results from SWMM simulations were compared to those from the analytical probabilistic model. Observations from a real case study in Portland, Oregon were used to further verify the analytical probabilistic model.

### 2.3.1 Comparison with Continuous SWMM Simulation Results

The 47-year hourly rainfall record of the Metro International Airport in Detroit was used as the rainfall input to the continuous SWMM (with the LID module) simulations. Green roofs with an area of 100 $m^2$ were simulated. Two soil types, sand and loam, were evaluated under different growing medium depths (from 50 mm to 150 mm). It should be noted that sand and loam are only used as surrogates for different types of growing media. The majority of real growing media are mixed non-cohesive aggregates with almost no capillary suction but very high permeability. The properties of sand as used here are representative of average growing medium, while the properties of loam are used to represent extreme cases.

**Table 2.2: Input parameter values in SWMM and the analytical probabilistic model**

| Soil Type | Loam | | Sand | |
|---|---|---|---|---|
| | SWMM | Analytical | SWMM | Analytical |
| $\phi$ (unitless) | 0.95 | 0.95 | 0.95 | 0.95 |
| $E_a$ (mm/h) | 0.11 | 0.11 | 0.11 | 0.11 |
| $S_l$ (mm) | 2 | 2 | 2 | 2 |
| $S_c$ (mm) | 0 | 0 | 0 | 0 |
| *h* (mm) | 50-150 | 50-150 | 50-150 | 50-150 |
| $\theta_f$ (fraction) | 0.232 | 0.232 | 0.062 | 0.062 |
| $\theta_w$ (fraction) | 0.116 | 0.116 | 0.024 | 0.024 |
| *P* (fraction) | 0.463 | N/N* | 0.437 | N/N* |
| *K* (mm/h) | 3.40 | N/N* | 120.40 | N/N* |
| *CS* (unitless) | 8.0 | N/N* | 5.0 | N/N* |
| *SH* (mm) | 88.90 | N/N* | 49.02 | N/N* |
| S (percentage) | 0 | N/N* | 0 | N/N* |

**Notes:**

*P* is the porosity of the growing medium;

*K* is the saturated hydraulic conductivity of the growing medium;

*CS* is the slope of the curve of log(conductivity) versus soil moisture content of the growing medium;

*SH* is the suction head of the growing medium;

*S* is the slope of the rooftop.

N/N* Not needed when using the analytical model.

Values of $\theta_f$, $\theta_w$, *P*, *K*, *SH* are from Rawls et al. (1983).

The values of the major hydrologic and hydraulic parameters of green roofs used in the analytical model and the SWMM simulations are listed in Table 2.2. The Green-Ampt infiltration model was selected to describe the rain water movement within the growing medium in the continuous SWMM simulations. Table 2.3 presents the total volumes of rainfall and runoff from

the continuous SWMM simulations for years from 1960 through 2006. Using the total volumes of rainfall and runoff from the results of the continuous SWMM simulations, the average runoff reduction rates can be calculated as

$$R_{rSWMM} = \frac{\phi V_{rain} - V_{runoff}}{\phi V_{rain}} \tag{2.15}$$

where $R_{rSWMM}$ is the runoff reduction rate of a green roof system calculated from the results of the continuous SWMM simulations; $V_{rain}$ is the total volume of rainfall (mm); $V_{runoff}$ is the total volume of runoff (mm). In using Equation (2.15), the runoff coefficient $\phi$ is applied to transform volume of rainfall to volume of runoff over regular roofs. This runoff coefficient should be the same as the one used in Equation (2.13). The calculated runoff reduction rates are presented in Table 2.3.

The analytically calculated and SWMM simulated runoff reduction rates of green roofs are compared in Figures 2.2 and 2.3 for growing medium types of loam and sand, respectively. These two figures show that close agreement between the analytical and continuous simulation results are obtained for both types of growing medium and all possible medium depths. For green roofs with loam as the growing medium, the differences between the analytically calculated and SWMM simulated runoff reduction rates are all less than 0.03

with the depth of growing medium changing from 50 mm to 150 mm (Figure 2.2). While for green roofs with sand as the growing medium, the differences are slightly larger (0.04 – 0.02) when the depth of growing medium is shallower than 80 mm (Figure 2.3); for medium depth between 80 and 150 mm, the differences are less than 0.02.

**Table 2.3 Results of continuous SWMM simulations**

| Growing Medium Depth (mm) | Rainfall (mm) | Loam | | Sand | |
|---|---|---|---|---|---|
| | | Runoff (mm) | $R_{r\,SWMM}$ | Runoff (mm) | $R_{r\,SWMM}$ |
| 50 | 32758 | 20504 | 0.341 | 26558 | 0.147 |
| 60 | 32758 | 19295 | 0.380 | 25799 | 0.171 |
| 70 | 32758 | 18074 | 0.419 | 25093 | 0.194 |
| 80 | 32758 | 17171 | 0.448 | 24438 | 0.215 |
| 90 | 32758 | 16386 | 0.473 | 23790 | 0.236 |
| 100 | 32758 | 15686 | 0.496 | 23218 | 0.254 |
| 110 | 32758 | 15074 | 0.516 | 22648 | 0.272 |
| 120 | 32758 | 14544 | 0.533 | 22115 | 0.289 |
| 130 | 32758 | 14105 | 0.547 | 21614 | 0.305 |
| 140 | 32758 | 13637 | 0.562 | 21141 | 0.321 |
| 150 | 32758 | 13259 | 0.574 | 20695 | 0.335 |

The close resemblance between the analytically determined and SWMM simulated runoff reduction rate curves in Figures 2.2 and 2.3 indicates that the analytical model derived from the simplified, event-based rainfall-runoff transformation of green roofs can generate results comparable to those from continuous SWMM simulations whereby the infiltration process is modeled in

detail on a time step-by-time step basis. It also indicates that the fitted exponential distribution models of rainfall event characteristics for Detroit are acceptable.

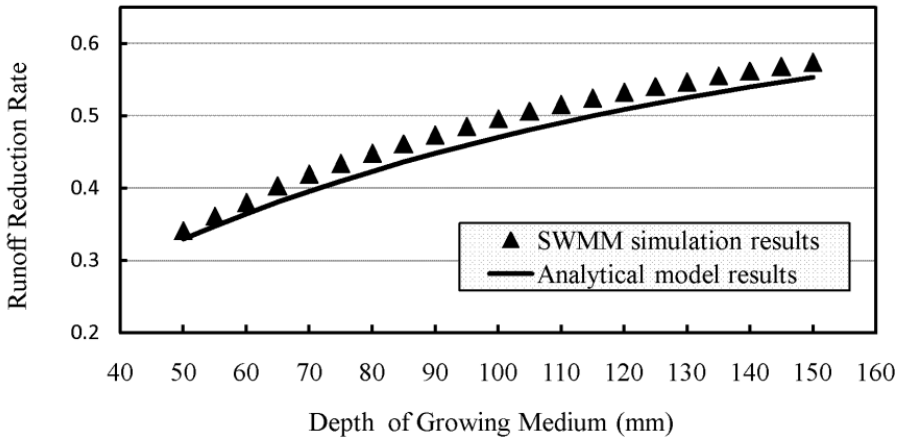


**Figure 2.2 Comparison of analytical and SWMM simulation results (loam soil)**

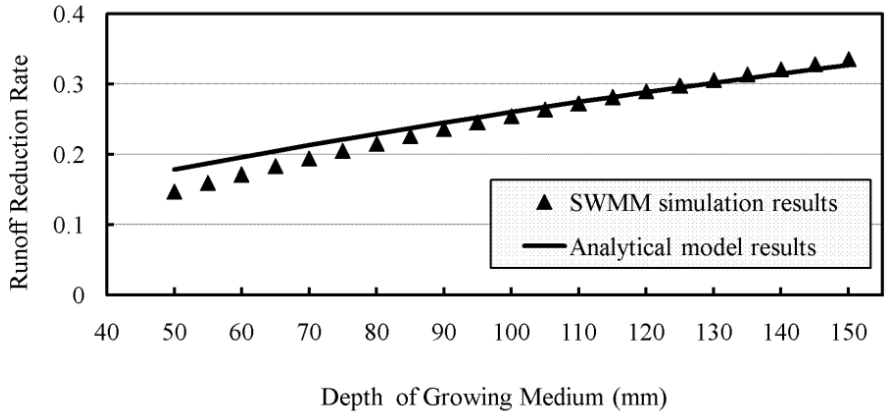


**Figure 2.3 Comparison of analytical and SWMM simulation results (sand soil)**

### 2.3.2 Comparison with Observations from a Real Case Study

Observed data from a green roof located in Portland, Oregon was used as the real case study in this paper to further verify the reliability of the

closed-form mathematical expressions. As described in Hutchinson et al. (2003) and She and Pang (2010), the West Wing's green roof of the Hamilton Building in the city of Portland is planted with sedum. The 102 mm deep growing medium of the green roof consists of 20% digested fiber, 10% compost, 22% coarse perlite, and 28% sandy loam. The field capacity and porosity of the medium were reported to be 0.35 and 0.41, respectively (She and Pang 2010). Based on the rainfall and runoff observation of the green roof system from January 2002 to April 2003, the runoff reduction rate was calculated to be 69% (Hutchinson et al. 2003).

To apply the closed-form mathematical expressions of the analytical model in estimating the runoff reduction rate of this real case, in addition to the field capacity ($\theta_f = 0.35$), the depth of the growing medium ($h$ =102 mm) and the storage capacity of the storage layer ($S_c = 0$ mm), the other two parameters of the green roof system ($\theta_w$ and $S_l$) and three parameters related to the local climate ($\bar{v}$, $\bar{b}$ and $E_a$) are required. As shown in Table 2.1, the wilting point ($\theta_w$) of growing medium may change from 0.08 to 0.15 (Bengtsson et al. 2005; Hilten et al. 2008). Since no $\theta_w$ was given for the specific growing medium, the average value of 0.12 was used for the West Wing green roof. As sedum was planted on a relatively flat green roof, $S_l$ of 4 mm could be a reasonable estimate of the summation of rainfall volume that may be intercepted by vegetation and trapped in depression storages of the

green roof. Pan evaporation data of Portland was obtained online (http://www.wrcc.dri.edu/htmlfiles/westevap.final.html ) as 1051.6 mm per year. A pan coefficient of 0.6 was selected. Therefore, the average evapotranspiration rate of the green roof system could be estimated as 0.072 mm / h. This estimate is within the range of ET estimates obtained by other means in earlier studies [e.g., using the empirical equations presented in Berghage et al. (2007), with a dry period of 64.6 h, the average ET of the green roofs planted with D. Nubigenum and S. Sexangulare could be calculated as 0.088 mm/h and 0.042 mm/h, respectively]. The runoff reduction rate in Hutchinson et al. (2003) was calculated by using the difference between the observed rainfall and runoff volumes, which implies that the corresponding regular roof converts 100% of rainfall to runoff, thus the equivalent $\phi$ in the analytical model should be 100%.

The meteorological station at the Portland International Airport (45.590˚N, 122.600˚W) was found to be very close to the West Wing of the Hamilton Building. Precipitation data of this station obtained from the National Climatic Data Center (NCDC) was analyzed to get the representative parameters (i.e. $\bar{v}$ and $\bar{b}$) of the local rainfall events. Using the rainfall statistical analysis method described previously, the continuous precipitation data from January 2002 to April 2003 was isolated into 140 individual rainfall events and the means used to estimate the distribution parameters of rainfall

event volumes and inter-event times are 8.91 mm for $\bar{v}$ and 64.60 h for $\bar{b}$.

With the parameter values for the West Wing green roof of the Hamilton Building as described in the previous paragraphs, the runoff reduction rate calculated using the closed-form mathematical expressions is 0.65. Since no specific values were given for $\theta_w$ and $S_l$ of the green roof system, the sensitivity of reduction rate with respect to $\theta_w$ and $S_l$ were analyzed further. When $\theta_w$ equals to 0.12 and $S_l$ changes from 2 mm to 6 mm, the runoff reduction rate calculated using the closed-form mathematical expressions changes from 0.64 to 0.65. When $S_l$ equals to 4 mm and $\theta_w$ changes from 0.08 to 0.15, the calculated runoff reduction rate changes from 0.64 to 0.66. Compared to the observed value of 0.69, these results indicate again that the analytical model may provide reasonably accurate estimates of a green roof's runoff reduction rate.

## 2.4 Application of the Analytical Model

The analytical model developed in this paper can be used in the evaluation of the stormwater management performance (i.e. the runoff reduction rate) of green roof systems and in the optimization of the design of green roof systems. The climatic characteristics ($\bar{v}$, $\bar{b}$ and $E_a$) of a locality can be calculated statistically, whereas the hydraulic and hydrologic properties ($\theta_f$, $\theta_w$, $S_l$, $S_c$ and $h$) of a green roof system can be measured or

estimated based on the design of the system.

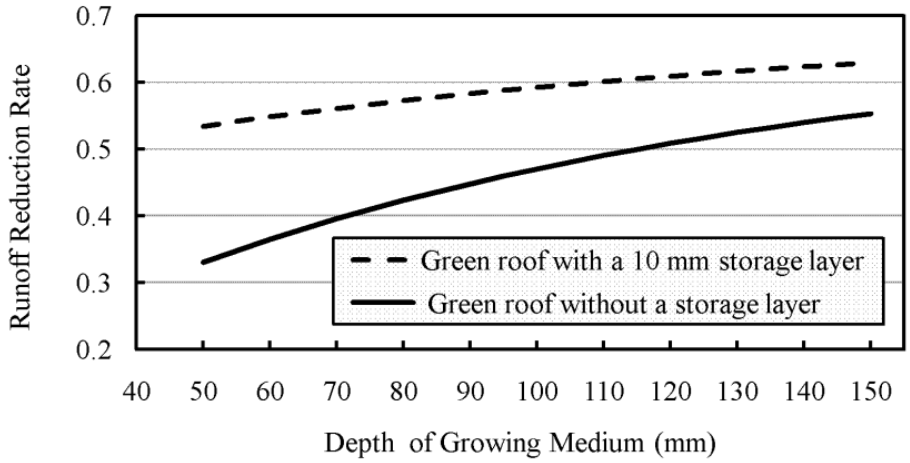


**Figure 2.4 Runoff reduction rates of green roofs changing with the depths of growing medium and storage layer**

Using Equation (2.14), the runoff reduction rate of a green roof system located in Detroit with loam as its growing medium having 2 mm surface depression and interception losses were obtained as a function of the depth of growing medium (Figure 2.4). To illustrate the effect of storage layers of green roof systems, the storage capacities ($S_c$) of 0 and 10 mm were calculated in this example. In Figure 2.4, both curves show that the runoff reduction rates of green roofs increase with the depth of growing medium. However, the difference between the slopes of the two curves demonstrates that increases in the depth of growing medium translate to smaller increases in runoff reduction rate for a green roof system with a storage layer, as compared to a green roof system without a storage layer. The higher runoff reduction

rates of the green roof system with a 10 mm storage layer indicate that a storage layer in the green roof system can significantly enhance its runoff reduction performance.

The analytical model can also be useful in the optimization of green roof design. Comparison of Figures 2.2 and 2.3 indicates that, under a specific climate condition, the stormwater management performance of a green roof system is determined not only by the depth of the growing medium, but also by the type or the water retention capacity ($\theta_f$ - $\theta_w$) of the growing medium. Therefore, to achieve a specific stormwater management objective, one needs to take into consideration both the depth and the water retention capacity of a growing medium when designing a green roof system.

Again using Equation (2.14), the runoff reduction rate curves of green roofs in Detroit were obtained as a function of the two design variables, i.e., the depth and the water retention capacity of the growing medium (Figure 2.5). For each selected runoff reduction rate, there is a specific curve in Figure 2.5 corresponding to it. From the curve for a selected runoff reduction rate, a series of paired values of the two design variables could be obtained. Designed with any one of these paired values, a green roof system can meet the specific runoff reduction requirement. In practice, the optimal pair of values can be identified according to the cost of increasing the depth of

growing medium, the cost of improving its water retention capacity, the moisture requirements of the plants, and the cost of increasing the supporting capacity of the roof structure.

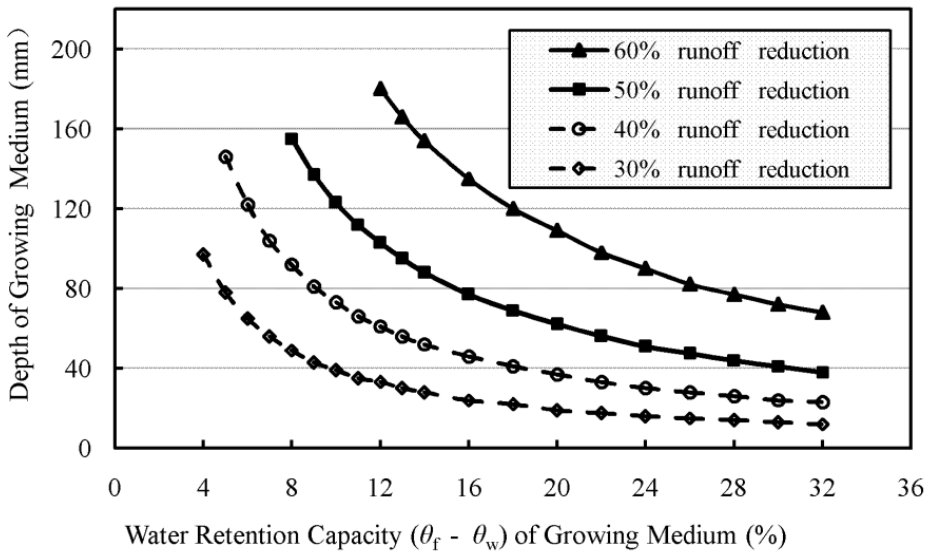


**Figure 2.5 Runoff reduction rates of green roofs changing with both the depth and water retention capacity of growing medium**

## 2.5 Summary, Discussion and Conclusions

In this study, an analytical probabilistic model for the hydrologic performance of green roofs was developed based on a probabilistic description of local rainfall characteristics and a simplified representation of the hydrologic and hydraulic processes occurring on and inside a green roof system. The analytical probabilistic model is comprised of Equations (2.11) through (2.14). In the derivation of these equations, the following assumptions were made:

i. Exponential probability density functions provide good fits to the histograms obtained from the frequency analysis of rainfall event volumes and inter-event times.

ii. The maximum amount of rain water that the growing medium of a green roof system can retain is equal to the field capacity ($\theta_f$) of the growing medium.

iii. The infiltration capacity of the growing medium is always greater than the intensity of the incoming rainfall.

iv. The water content of the growing medium in a green roof system is expected to be no less than the wilting point water content ($\theta_w$).

All these simplifying assumptions required for the development of the analytical probabilistic model are shown to be acceptable based on previous research or are justifiable given the specific operating conditions of extensive green roof systems. To verify the accuracy of the analytical model, continuous SWMM simulations that do not require similar simplifying assumptions were conducted. The small differences between the analytical model and SWMM simulation results show that the accuracy of the analytical model is acceptable for practical purposes. The observed data from a real case in Portland, Oregon further verify the accuracy of the analytical model.

The growing media of green roofs are often specially-mixed engineered

aggregates and their compositions, hydraulic and hydrologic properties vary greatly. Although many observations have been made and quite a few models have been developed in order to assess the hydrologic performance of green roofs (Palla et al. 2009), a set of representative values of the hydraulic and hydrologic parameters of the growing media could not be found since the focus of the researchers, the composition of the growing media and the parameter requirements of the models are different in various earlier studies (e.g., Zimmer and Geiger 1997; Carter and Jackson 2007; Hilten et al. 2008; Palla et al. 2009; She and Pang 2010; Alfredo et al. 2010). That is why sand and loam were used as the surrogates for growing media in our verification studies to cover a wide range of possible hydraulic and hydrologic parameter values. In applying the analytical probabilistic model, the same level of care as would be required in using other modeling approaches should be given to the proper estimation of growing medium's hydraulic and hydrologic properties.

The reliability of a modeling technique should not be solely verified based on results in the literature (Wu et al. 2009) or simply by comparison against results from another modeling technique. Comparison against more long-term observed data is desirable to further verify our analytical model. However, although green roofs were developed to achieve aesthetic benefits in the Nordic countries centuries ago (Berndtsson 2010), experiments to examine

their stormwater management performance only started in the last decade (e.g., Bengtsson et al. 2005; Mentens et al. 2006; Carter and Rasmussen 2006; Getter et al. 2007; Simmons et al. 2008; She and Pang 2010; Berghage et al. 2007; DiGiovanni et al. 2010; Voyde et al. 2010). As more data become available, the analytical model can be more thoroughly verified.

As in the application of any other models, it would be better if the model developed here could first be calibrated using observed data for multiple objectives (Chen et al. 2002). As longer-term observed data become available, part of the data may be used for calibration purposes while the other part may be used for verification and validation purposes. With more testing using observed data, the modeling methodologies employed in the newly developed LID modules of SWMM may be improved in the future, the improved modeling methodologies may be used as basis to further refine the analytical probabilistic approach proposed in this study.

**ACKNOWLEDGEMENTS:** This work has been supported by the Natural Sciences and Engineering Research Council of Canada and the China Scholarship Council.

## References

Adams, B. J. and Papa, F. (2000). *Urban Stormwater Management Planning with Analytical Probabilistic Models*, John Wiley & Sons, Inc., New York, USA.

Adams, B. J., Fraser, H. G., Howard, C. D. D., and Hanafy, M. S. (1986). Meteorologic data analysis for drainage system design. *Journal of Environmental Engineering*, ASCE, 112(5), 827–848.

Alfredo, K., Montalto, F., and Goldstein, A. (2010). Observed and modeled performances of prototype green roof test plots subjected to simulated low- and high-intensity precipitations in a laboratory experiment. *Journal of Hydrologic Engineering*, 15(6), 444–457.

Antrop, M. (2004). Landscape change and the urbanization process in Europe. *Landscape and Urban Planning*, 67(1–4), 9–26.

Ashkar, F., and Rousselle, J. (1987). Partial duration series modeling under the assumption of a Poissonian Flood Count. *Journal of Hydrology*, 90(1-2), 135–144.

Bengtsson, L., Grahn, L., and Olsson, J. (2005). Hydrological function of a thin extensive green roof in southern Sweden. *Nordic Hydrology*, 36(3), 259–268.

Benjamin, J. R., and Cornell, C. A. (1970). *Probability, Statistics and Decision for Civil Engineers*, McGraw-Hill, New York, USA.

Berghage, R. D., Jarrett, A. R., Beattie, D. J., Kelley, K., Husain, S., Rezaei, F.,

et al. (2007). *Quantifying Evaporation and Transpirational Water Losses from Green Roofs and Green Roof Media Capacity for Neutralizing Acid Rain*, National Decentralized Water Resources Capacity Development Project. Pennsylvania State University, University Park, Pennsylvania.

Berndtsson, J. C. (2010). Green roof performance towards management of runoff water quantity and quality: A review. *Ecological Engineering*, 36(4), 351–360.

Brenneisen, S. (2006). Space for urban wildlife: Designing green roofs as habitats in Switzerland. *Urban Habitats*, 4(1), 27–36.

Carter, T. L., and Jackson, C. R. (2007). Vegetated roofs for storm water management at multiple spatial scales. *Landscape and Urban Planning*, 80 (1–2), 84–94.

Carter, T. L., and Rasmussen, T. C. (2006). Hydrologic behavior of vegetated roofs. *Journal of the American Water Resources Association*, 42 (5), 1261–1274.

Chau, K. W., Wu, C. L., and Li, Y. S. (2005). Comparison of several flood forecasting models in Yangtze River. *Journal of Hydrologic Engineering*, 10(6), 485–491.

Cheng, C. T., Ou, C. P., and Chau, K. W. (2002). Combining a fuzzy optimal model with a genetic algorithm to solve multiobjective rainfall-runoff model calibration. *Journal of Hydrology*, 268(1–4), 72–86.

Cruise, J. F., and Arora, K. (1990). A hydroclimatic application strategy for the Poisson partial duration model. *Water Resources Bulletin*, American Water

Resources Association, 26(3), 431–442.

Cunnane, C. (1979). A note on the Poisson assumption in partial duration series models. *Water Resources Research*, 15(2), 489–494.

Deutsch, B., Whitlow, H., Sullivan, M., and Savineau, A. (2005). Re-greening Washington, DC. A green roof vision based on environmental benefits for air quality and storm water management. *In: Proceedings of the 3rd North American: Green Roof Conference on Greening Rooftops for Sustainable Communities*, Washington, DC, May 4–6. The Cardinal Group,Toronto, pp. 379–384.

DiGiovanni, K., Gaffin, S., and Montalto, F. (2010). Green Roof Hydrology: Results from a Small-Scale Lysimeter Setup (Bronx, NY). *Paper presented at the Low Impact Development 2010: Redefining Water in the City*, San Francisco, CA.

Dunnett, N., and Kingsbury, N. (2004). *Planting Green Roofs and Living Walls*. Timber Press, Portland.

Eagleson, P. S. (1978). Climate, soil, and vegetation, 2, the distribution of annual precipitation derived from observed storm sequences. *Water Resources Research,* 14(5), 713–721.

Eagleson, P. S. (1972). Dynamics of flood frequency. *Water Resources Research,* 8(4), 878–898.

Fang, C. (2008). Evaluating the thermal reduction effect of plant layers on rooftops. *Energy and Buildings*, 40(6), 1048–1052.

Gedge, D., and Kadas, G. (2005). Green roofs and biodiversity. *Biologist*, 52

(3), 161–169.

Getter, K. L., Rowe, D. B., and Andresen, J. A. (2007). Quantifying the effect of slope on extensive green roof stormwater retention. *Ecological Engineering*, 31(4), 225–231.

Guo, Y. (2001). Hydrologic design of urban flood control detention ponds. *Journal of Hydrologic Engineering*, 6(6), 472–479.

Guo, Y., and Adams, B. J. (1998). Hydrologic analysis of urban catchments with event-based probabilistic models. Part I: Runoff volume. *Water Resources Research*, 34(12), 3421–3431.

Guo, Y., and Baetz, B. W. (2007). Sizing of rainwater storage units for green building applications. *Journal of Hydrologic Engineering*, 12(2), 197–205.

Guo, Y., Hansen, D., and Li, C. (2009). Probabilistic approach to estimating the effects of channel reaches on flood frequencies. *Water Resources Research*, 45, W08404, doi:10.1029/2008WR007387.

Hilten, R. N., Lawrence, T. M., and Tollner, E. W. (2008). Modeling storm water runoff from green roofs with HYDRUS-1D. *Journal of Hydrology*, 358 (3–4), 288–293.

Howard, C. D. D. (1976). Theory of storage and treatment plant overflows. *Journal of the Environmental Engineering Division*, ASCE, 102(EE4), 709–722.

Hutchinson, D., Abrams, P., Retzlaff, R., and Liptan, T. (2003). Stormwater monitoring two ecoroofs in Portland, Oregon, USA. Proc., *Greening Rooftops for Sustainable Communities*.

Kosareo, L., and Ries, R. (2007). Comparative environmental life cycle assessment of green roofs. *Building and Environment*, 42(7), 2606–2613.

Mentens, J., Raes, D., and Hermy, M. (2006). Green roofs as a tool for solving the rainwater runoff problem in the urbanised 21st century. *Landscape and Urban Planning*, 77(3), 217–226.

Oberndorfer, E., Lundholm, J., Bass, B., Coffman, R. R., Doshi, H., Dunnett, N. Gaffin, S., Kohler, M., Liu, K. K. Y., and Rowe, B. (2007). Green Roofs as Urban Ecosystems: Ecological Structures, Functions, and Services. *BioScience*, 57 (10), 823–833.

Palla, A., Gnecco, I., and Lanza, L. G. (2009). Unsaturated 2D modelling of subsurface water flow in the coarse-grained porous matrix of a green roof. *Journal of Hydrology*, 379(1–2), 193–204.

Peck, S. W. (2005). *Toronto: A Model for North American Infrastructure Development. In: EarthPledge. Green Roofs: Ecological Design and Construction*. Schiffer Books, Atglen, PA, pp. 127–129.

Rawls, W. J., Brakensiek, D. L., and Miller, N. (1983). Green-Ampt infiltration parameters from soils data. *Journal of Hydraulic Engineering*, 109(1), 62–70.

Restrepo-Posada, P. J., and Eagleson, P. S. (1982). Identification of independent rainstorms. *Journal of Hydrology,* 55(1982), 303–319.

Rossman, L. A. (2010). *Storm Water Management Model User's Manual, Version 5.0,* EPA/600/R-05/040, U.S. Environmental Protection Agency, Cincinnati, OH, USA.

She, N. and Pang, J. (2010). Physically based green roof model. *Journal of Hydrologic Engineering*, 15(6), 458–464.

Simmons, M. T., Gardiner, B., Windhager, S., and Tinsley, J. (2008). Green roofs are not created equal: the hydrologic and thermal performance of six different extensive green roofs and reflective and non-reflective roofs in a sub-tropical climate. *Urban Ecosystem*, 11(4), 339–348.

United Nations (2002).*World Urbanization Prospects: The 2001 Revision*. United Nations, New York.

Villarreal, E. L. and Bengtsson, L. (2005). Response of a sedum green-roof to individual rain events. *Ecological Engineering*, 25(1), 1–7.

Voyde, E., Fassman, E., and Simcock, R. (2010a). Hydrology of an extensive living roof under sub-tropical climate conditions in Auckland, New Zealand. *Journal of Hydrology*, 394, 384–395.

Voyde, E., Fassman, E., Simcock, R., and Wells, J. (2010b). Quantifying evapotranspiration rates for New Zealand green roofs. *Journal of Hydrologic Engineering*, 15(6), 395–403.

Wolf, D., and Lundholm, J. T. (2008). Water uptake in green roof microcosms: effects of plant species and water availability. *Ecological Engineering*, 33(2), 179–186.

Wong, N. H., Chen, Y., Ong, C. L., and Sia, A. (2003). Investigation of thermal benefits of rooftop garden in the tropical environment. *Building and Environment*, 38(2), 261–270.

Wong, N. H., Tan, P. Y., and Chen, Y. (2007). Study of thermal performance of

extensive rooftop greenery systems in the tropical climate. *Building and Environment*, 42(1), 25–54.

Wu, C. L., Chau, K. W. and Li, Y. S. (2009). Predicting monthly streamflow using data-driven models coupled with data-preprocessing techniques. *Water Resources Research*, 45, W08432, doi:10.1029/2007WR006737.

Zimmer, U., and Geiger, W. F. (1997). Model for the design of multi-layered infiltration systems. *Water Science and Technology*, 36 (8–9), 301–306.

# Chapter 3

# An Explicit Equation for Estimating the Stormwater Capture Efficiency of Rain Gardens

**Shouhong Zhang and Yiping Guo**

**Abstract:** Rain gardens have increasingly been used to control the adverse effects of urbanization on stormwater quantity and quality. The ratio or percentage of stormwater generated from the contributing area of a rain garden that is captured by the surface depression of the rain garden is known as its stormwater capture efficiency. This capture efficiency is an important indicator of a rain garden's performance for stormwater management. Based on the probability distributions of local rainfall event characteristics and the hydrologic operation of rain gardens, an explicit analytical equation is derived for estimating the long-term average stormwater capture efficiency of a rain garden. The validity of the analytical equation is demonstrated by comparing its outcomes with results from a series of continuous simulations. Example applications of this equation are made for two locations.

**Key Words:** Rain garden, BMP/LID, Stormwater management, Stormwater capture efficiency, Probabilistic methods.

## 3.1 Introduction

Urbanization is a worldwide process, with well-known adverse hydrologic effects (Klein 1979). To reduce these adverse effects, many best management practices (BMPs) and low impact development (LID) practices have been developed and implemented (Heasom et al. 2006; Davis 2008; Li et al. 2009; Jenkins et al. 2010). Rain gardens are one type of stormwater BMP and also an integral part of LID practices. Recently, the use of rain gardens have increased significantly throughout the United States and many other parts of the world (Hager 2003; Hunt et al. 2008; Davis 2008; Davis et al. 2009; DeBusk et al. 2011). Previous studies indicate that rain gardens have the potential to reduce runoff volumes (Davis 2008; Yang et al. 2009; Davis et al. 2012), minimize peak flows (Dietz and Clausen 2005; Hunt et al. 2008; James and Dymond 2012), recharge ground water (Dussaillant et al. 2004; Aravena and Dussaillant 2009), increase evapotranspiration (Sharkey 2006; Li et al. 2009), and reduce the mass of pollutants entering surface and ground waters (Davis et al. 2003; Kim et al. 2003; Hsieh and Davis 2005; Dietz and Clausen 2006; Hunt et al. 2008).

A rain garden is a vegetated depression with a surface mulch layer and a fill media layer that receives stormwater runoff from a much larger impervious area such as a roof or a parking lot (PGC DEP 1993; PDEP 2006; Davis et al.

2009; Aravena and Dussaillant 2009). It is designed to capture a significant amount of stormwater runoff from each storm with the excess volume from larger storms bypassed as overflows (Heasom et al. 2006). The stormwater capture efficiency of a rain garden is defined as the fraction of stormwater volume captured by the surface depression of the rain garden (instead of overflowing from the rain garden) over its lifetime of operation. It not only demonstrates the hydrologic performance of a rain garden but also is an important indicator of its water quality improvement performance. The stormwater capture efficiency of rain gardens may vary widely under different weather conditions (Emerson and Traver 2008; Muthanna et al. 2008). The ratio between the contributing drainage area and the rain garden surface area (hereafter simply referred to as the area ratio), the depth of the surface depression, the infiltration capacity of the fill media layer, and the type and density of vegetation of rain gardens all affect their stormwater capture efficiencies. Rain garden stormwater capture efficiencies reported in previous studies range from 67.9% to 99.2% (Dietz and Clausen 2005; Li et al. 2009; Trowsdale and Simcock 2011).

The design of a rain garden can vary in complexity. To achieve different stormwater quantity and quality management objectives, rain gardens are designed with area ratios changing from 45:1 to 5:1 (PDEP 2006; Davis et al. 2009), surface depression depths (allowing the pooling of stormwater

runoff) changing from 150 to 520 mm (Clar and Green 1993; MDE 2000; DNREC 2005; Davis et al. 2012), and depths of the fill media layer changing from 0.5 to1.2 m (Clar and Green 1993; Li et al. 2009). The fill media layer of rain gardens typically has a high sand content so that water in the surface depression can be infiltrated within 48 to 96 h (Clar and Green 1993; Davis et al. 2001; Davis et al. 2009) under the design rainfall event. Engineered soils [e.g., soil mixes consisting of 86% sand, 10% fines, and 4% organic materials (Hunt and Loard 2006)] and natural soils with high permeability [e.g., sand and sandy loam (Clar and Green 1993)] are commonly used fill media.

The unreasonable design of rain gardens for individual buildings or parking lots resulting from the use of inaccurate design approaches may not cause significant economic or environmental losses; however, the cumulative losses may become significant as the number of applications increases over a watershed or jurisdiction. Therefore, although small in its spatial scale, the design of rain gardens should still be treated as a full-scale hydrologic engineering design problem. Reliable and easy-to-use approaches are needed to assess the stormwater management performance of rain gardens.

Many monitoring studies have been conducted to assess the stormwater management performance of rain gardens. Monitoring studies observe the performance of rain gardens under a sufficient number and variety of storm

events over a long period of time. Significant efforts are required in monitoring studies, and unavoidable uncertainty is still contained in the final assessment of the long-term average performance (Asleson et al. 2009). Hydrological models have also been developed and employed in recent years for evaluating the performance of rain gardens. For instance, three deterministic and physically-based rain garden models, namely the RECHARGE-1D model (Dussaillant et al. 2004), the RECHARGE-2D model (Aravena and Dussaillant 2009), and the 2-D variable saturated flow model (He and Davis 2011), were developed based on the Richards equation. Two of the most-widely used deterministic continuous-simulation hydrologic models, i.e., the U. S. Army Corp of Engineers' HEC-HMS model and the U. S. Environmental Protection Agency's SWMM model, have also been employed to model rain gardens. Using the HEC-HMS model, Heasom et al. (2006) developed a technique that could successfully model the hydrologic behavior of a rain garden. Abi Aad et al. (2010) employed the Version 5 of the SWMM model to quantify the stormwater management performance of a rain garden.

All of the above-described models have been tested and were shown to be able to quantify the long-term average stormwater management performance of rain gardens if they are run under continuous simulation mode. However, the parameters used to simulate the detailed infiltration/seepage

processes in the three Richards equation-based models are difficult to obtain. The extensive data and computation requirements limit the practical application of the other two deterministic continuous simulation models. Moreover, given the small spatial scale of most rain gardens, the use of computer simulation with extensive data input and output may not be justified for the majority of design cases.

A more appealing approach may be the use of analytical equations that consider the basic hydrologic operation of a rain garden and also account for the influence of local climate conditions. The analytical probabilistic approach (Eagleson 1972, 1978; Adams and Papa 2000) has been successfully applied to develop event-based probabilistic stormwater models for stormwater management planning and design purposes (Guo and Adams 1998a, b; 1999a, b; Bacchi et al. 2008; Balistrocchi et al. 2009; Guo et al. 2009). Using a similar analytical probabilistic approach, Guo and Baetz (2007) and Zhang and Guo (2012) derived analytical equations to, respectively, size rain barrels and evaluate the hydrologic performance of green roofs used for stormwater management purposes.

In this paper, the analytical probabilistic approach is applied to study the hydrologic operation of rain gardens. The aim is to develop analytical equations that can be used at different locations for designing the critical

dimensions of rain gardens in order to provide the desired stormwater capture efficiencies. The probabilistic models of rainfall event characteristics are presented and the hydrologic processes involved in the operation of rain gardens are analyzed first. Analytical equations which can be used as design tools are then derived based on the probabilistic models of rainfall event characteristics and the mathematical description of the hydrologic processes. The validity of the analytical equations is demonstrated by comparing their outcomes with results from a series of continuous simulations using long-term rainfall data from Atlanta, Georgia. The application of these equations at different locations for designing the critical dimensions of rain gardens is also illustrated.

## 3.2 Derivation of Analytical Equations

### 3.2.1 Probabilistic Models of Rainfall Event Characteristics

Probabilistic models of rainfall event characteristics may be obtained by conducting statistical analysis on the historical rainfall record of a gauging station. In this analysis, the historical rainfall time series is first divided into discrete rainfall events. The criterion used to separate discrete rainfall events from the continuous rainfall time series is a minimum period without rainfall, referred to as the inter-event time definition (IETD). The choice of IETD is usually dependent on the location and the type of application (Guo and Baetz

2007; Bacchi et al. 2008; Guo et al. 2009).

To obtain the suitable IETD for a specific location, the statistical test method described in Guo and Baetz (2007) may be employed. That statistical test is based on the theory that the occurrence of storm events can be approximated as a Poisson process when the dry periods between storms are exponentially distributed (Restrepo-Posada and Eagleson 1982). The likelihood of correlation between a series of events is greatly reduced when the series is accepted as a Poisson process (Ashkar and Rousselle 1987). Different IETD values will result in different number of rainfall events every year. Choosing one IETD value, the annual number of events ($n$) can be obtained for every year in the rainfall record; the variance Var[$n$] and the mean E[$n$] of $n$ can be calculated, the ratio (denoted as $r_{ve}$) between Var[$n$] and E[$n$] can also be calculated. Since the mean and variance of a Poisson distribution are equal (Cunnane 1979; Cruise and Arora 1990), the ratio $r_{ve}$ should approach unity as the IETD is increased if the occurrence of storm events does follow a Poison process. Therefore, a statistical test may be devised for $r_{ve}$ based on the approximation that the factor $(N-1)r_{ve}$ is $\chi^2$ distributed with ($N$-1) degrees of freedom (Cunnane 1979), here $N$ is the number of years of record. The critical values of $r_{ve}$ can thus be determined for selected levels of significance (Cruise and Arora 1990).

Once a suitable IETD is selected, the historical rainfall time series can be separated into individual rainfall events. Each rainfall event is characterized by its rainfall volume *v*, rainfall duration *t*, and inter-event time *b*. The volumes and durations of the isolated rainfall events, as well as the inter-event times are then statistically analyzed. Although for some locations, the Weibull probability distribution was found to be more appropriate for rainfall event volume (Bacchi et al. 2008; Balistrocchi et al. 2009), for many other locations, exponential probability density functions (PDFs) were found to provide good fits to the histograms obtained from the frequency analysis of rainfall event volumes, durations and inter-event times (Eagleson 1972, 1978; Howard 1976; Adams et al. 1986; Guo and Adams 1998a; Adams and Papa 2000; Guo 2001; Guo and Baetz 2007). These exponential distributions may be expressed as

$$f_V(v) = \zeta e^{-\zeta v}, \quad v \geq 0 \tag{3.1}$$

$$f_T(t) = \lambda e^{-\lambda t}, \quad t \geq 0 \tag{3.2}$$

$$f_B(b) = \psi e^{(-\psi b)}, \quad b \geq 0 \tag{3.3}$$

where $V$ is the rainfall event volume regarded as a random variable, $v$ is a specific value of $V$ (mm); $T$ is the rainfall event duration regarded as a random variable, $t$ is a specific value of $T$ (h); $B$ is the inter-event time

regarded as a random variable, $b$ is a specific value of $B$ (h). The terms $\zeta$, $\lambda$ and $\psi$ are the distribution parameters for rainfall event volume, duration and inter-event time, respectively; their values can be estimated as the inverse of the mean of rainfall event volumes ($mm^{-1}$), the inverse of the mean of rainfall event durations ($h^{-1}$), and the inverse of the mean of inter-event times ($h^{-1}$), respectively. The annual average number of rainfall events ($\theta$) can also be obtained.

For illustration purposes, Atlanta, Georgia and Flagstaff, Arizona were selected as the test locations in this study. The Atlanta and Flagstaff rainfall data are respectively from the Atlanta Hartsfield Airport (33.63° N, 84.44° W) and the Flagstaff Pulliam Airport (35.14° N, 111.67° W). The two rainfall data sets are from the National Climatic Data Center (NCDC) of the USA and cover the years of 1945-2005 and 1947-2005, respectively. An IETD of 8 h was found to give a $r_{ve}$ value of 1.07 for the rainfall data of Atlanta, and an IETD of 12 h was found to give a $r_{ve}$ value of 1.168 for the rainfall data of Flagstaff. Both of the $r_{ve}$ values are within the range of the critical values at a significance level of 0.10. Using these selected IETDs, the rainfall records of Atlanta and Flagstaff were isolated into 4786 and 2750 individual rainfall events, respectively. The histograms of the rainfall events' $v$, $t$ and $b$ of Atlanta and Flagstaff are shown in Figure 3.1 and Figure 3.2, respectively. As shown visually in the figures, the exponential distributions fit all the

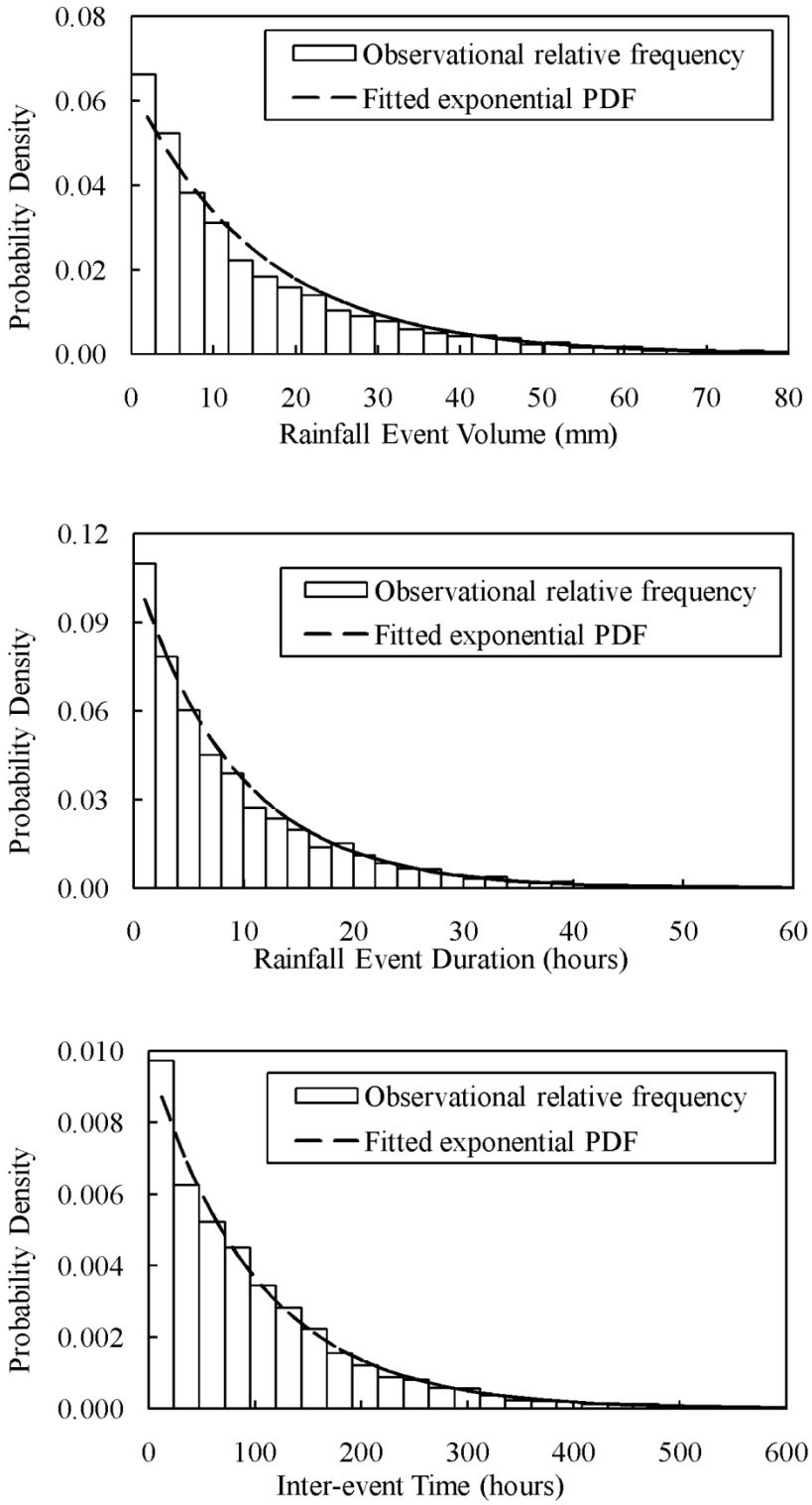


**Figure 3.1 Frequency distributions of the rainfall event volume, duration and inter-event time at Atlanta, Georgia (IETD = 8 hours)**

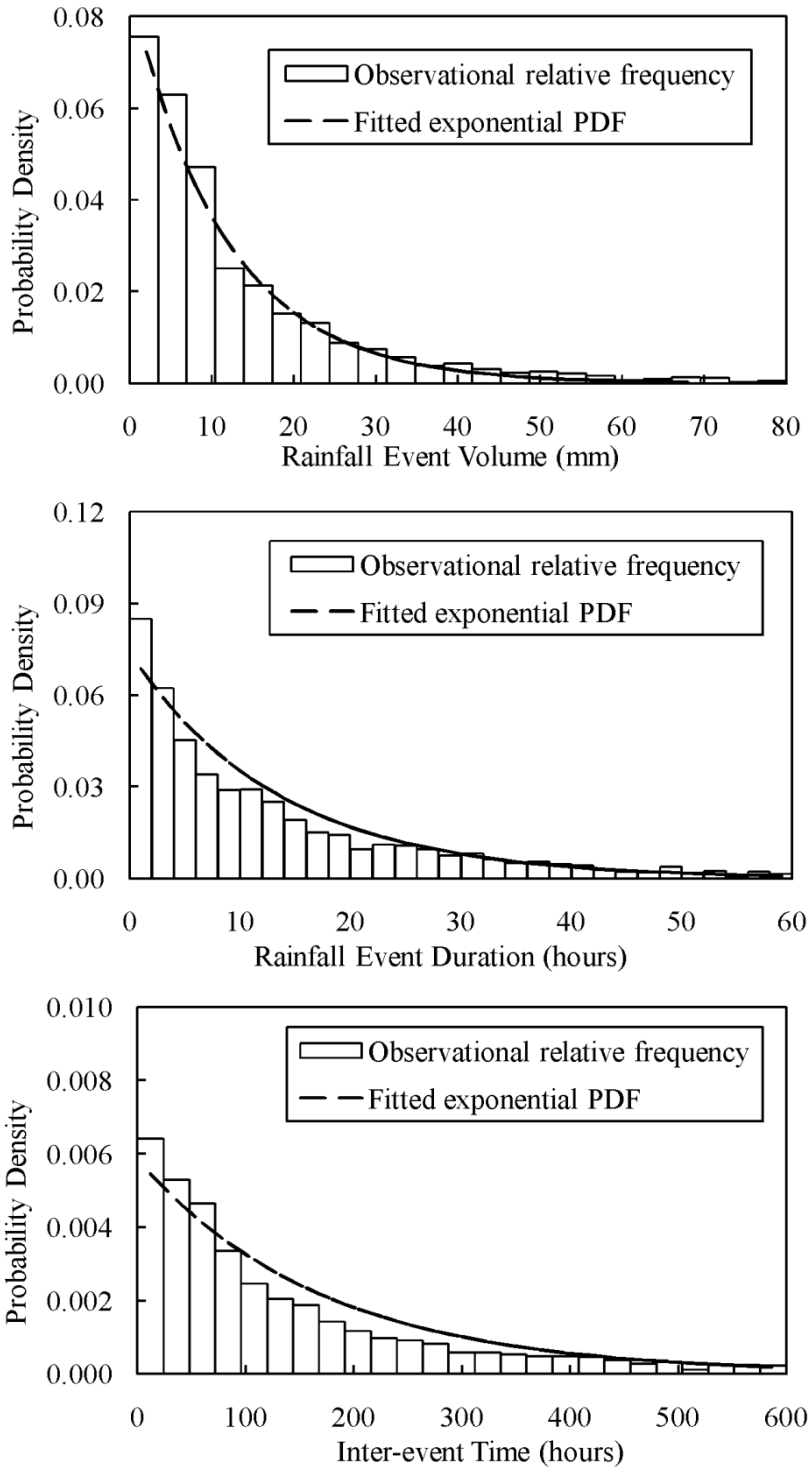


**Figure 3.2 Frequency distributions of the rainfall event volume, duration and inter-event time at Flagstaff, Arizona (IETD = 12 hours)**

histograms well. The means used to estimate the distribution parameters and the average annual number of rainfall events of the two test locations are presented in Table 3.1.

**Table 3.1 Statistical analysis results of the rainfall records of the two test locations**

| Station | IETD (h) | $\theta$ | $\bar{v}$ (mm) | $\bar{t}$ (h) | $\bar{b}$ (h) |
|---|---|---|---|---|---|
| Atlanta | 8 | 78 | 15.68 | 9.18 | 101.84 |
| Flagstaff | 12 | 45 | 11.63 | 13.54 | 170.75 |

### 3.2.2 Hydrologic Processes Occurring on Rain Gardens

As rain falls onto the contributing impervious area (e.g., a parking lot or a roof) of a rain garden, a portion of the rain water becomes surface runoff and is directed to the rain garden. The surface runoff from the contributing impervious area together with the rain water directly falling onto the rain garden surface is considered as the inflow into the rain garden. The inflow begins to infiltrate through the fill media layer of the rain garden immediately after it is received. When the inflow rate exceeds the infiltration capacity of the fill media layer, ponding occurs in the surface depression of the rain garden. During a large and intense storm, the surface depression could be filled completely by ponded water, with excess bypassed as overflows. When a rainfall event ceases, the ponded water is depleted through infiltration and evapotranspiration. Complete depletion of ponded water usually takes

about 48 to 96 hours without additional rainfall (Clar and Green 1993; Davis et al. 2001; Davis et al. 2009).

Infiltration occurs during the entire time there is inflow into or ponded water in the rain garden. Proper siting of rain gardens ensures that impermeable soil layers or high seasonal ground water tables do not interfere with rain gardens' infiltration process (Heasom et al. 2006). Underdrains need to be installed to avoid overly long standing of water on the surface and saturated conditions in the root zone when a rain garden is located at places where the natural soil's infiltration capacity is insufficient (Davis et al. 2009; Roy-Poirier et al. 2010). Therefore, with a properly designed rain garden, the infiltrating water through the fill media layer could either recharge ground water or be drained away through the underdrain. In other words, there should be no layer of material impeding the percolation of infiltrated water.

### 3.2.3 Estimation of Average Annual Inflow Volume

As described in the previous section, the inflow entering a rain garden includes two parts: the surface runoff from the contributing impervious area and the rain water directly falling on the rain garden surface. When a rainfall event with a volume of $v$ mm falls onto the contributing impervious area, a portion of the rain water is trapped by the small depressions on the surface of the impervious area and the remainder of the rain water flows into the rain

garden as surface runoff. The typical values of depression storage for impervious areas are very small, usually changing from 1.27 mm to 2.54 mm (Tholin and Kiefer 1960; ASCE 2012). For simplification, it is assumed that the contributing impervious areas of rain gardens convert 100% of rainfall to surface runoff. Based on the reported small values of depression storage for impervious areas, this assumption is expected to have minimal impact on the estimation of the inflow volume. Taking the area ratio ($r$, dimensionless) between the contributing impervious area and the rain garden surface area into consideration, the volume of inflow into a rain garden can be expressed as

$$v_i = (r+1)v \tag{3.4}$$

where $v_i$ is the volume of inflow into a rain garden during a random rainfall event, expressed in the unit of mm of water over the rain garden surface area. Here, $v_i$ is considered as one realization of the random variable $V_i$ since it is a function of $v$ which is one realization of random variable $V$.

Based on the functional relationship between $v_i$ and $v$ expressed in Equation (3.4), as well as the PDF of $V$ [i.e., Equation (3.1)], the expected value of $V_i$ per rainfall event can be determined as

$$\mathrm{E}(V_i) = \int_0^\infty (r+1)v\zeta e^{-\zeta v} dv = \frac{r+1}{\zeta} \tag{3.5}$$

The average annual volume of inflow into the rain garden is

$$I_a = \theta\left(\frac{r+1}{\zeta}\right) \tag{3.6}$$

where $I_a$ is expressed in the unit of mm of water over the rain garden surface area; and $\theta$ is the average number of rainfall events per year when the rain garden is in operation.

### 3.2.4 Estimation of Average Annual Overflow Volume

The following analysis focuses on a random dry period-rainfall event cycle (hereafter referred to as the current cycle and the rainfall event is referred to as the current rainfall event) starting from the beginning of a *b*-hour dry period, followed by a *t*-hour rainfall event with a volume of *v* mm. For each cycle, the dry period duration, the rainfall duration and the volume of the rainfall event are assumed as independent random variables following their respective probability distributions. The joint PDFs of the three random variables are the product of their marginal PDFs. A more complete discussion of this independent assumption could be found in Adams et al. (1986) and Adams and Papa (2000).

To test this independence assumption for the two stations studied in this paper, the correlation coefficients between rainfall event volume and duration

**Table 3.2 Correlation coefficients between the rainfall event characteristics**

| Station | $r_{VT}$ | $r_{VB}$ | $r_{TB}$ |
|---|---|---|---|
| Atlanta | 0.624 ($p < 0.01$) | 0.005 ($p = 0.69$) | 0.003 ($p = 0.80$) |
| Flagstaff | 0.653 ($p < 0.01$) | 0.006 ($p = 0.78$) | 0.002 ($p = 0.93$) |

Note: Here $p$ stands for the $p$-values with the null hypothesis that the two random variables are linearly uncorrelated. Although a formal statistical test was not conducted, $p$-values less than commonly selected significance levels may indicate that the null hypothesis should be rejected.

(denoted as $r_{VT}$), the correlation coefficients between rainfall event volume and inter-event time (denoted as $r_{VB}$), as well as the correlation coefficients between rainfall event duration and inter-event time (denoted as $r_{TB}$) were all calculated. As shown in Table 3.2, the small values of $r_{VB}$ and $r_{BT}$ for both Atlanta and Flagstaff demonstrate the independence between rainfall event volume and inter-event time, as well as the independence between rainfall event duration and inter-event time. The $r_{VT}$ for both Atlanta and Flagstaff are relatively high (0.62 and 0.65, respectively) and the linear correlations between rainfall event volumes and durations for both stations are statistically significant (with $p$-values < 0.01 under the null hypothesis that there is no correlation between rainfall event volume and duration). However, the wide spreading of the scatter diagrams (Figure 3.3) of the rainfall event volume and duration illustrate that little loss of accuracy may result when rainfall event volume and duration are treated as linearly independent. This

is demonstrated later on by comparing analytical and continuous simulation results. Therefore, for derivation purposes, it is assumed that the inter-event time, the duration and volume of rainfall events are independent random variables.

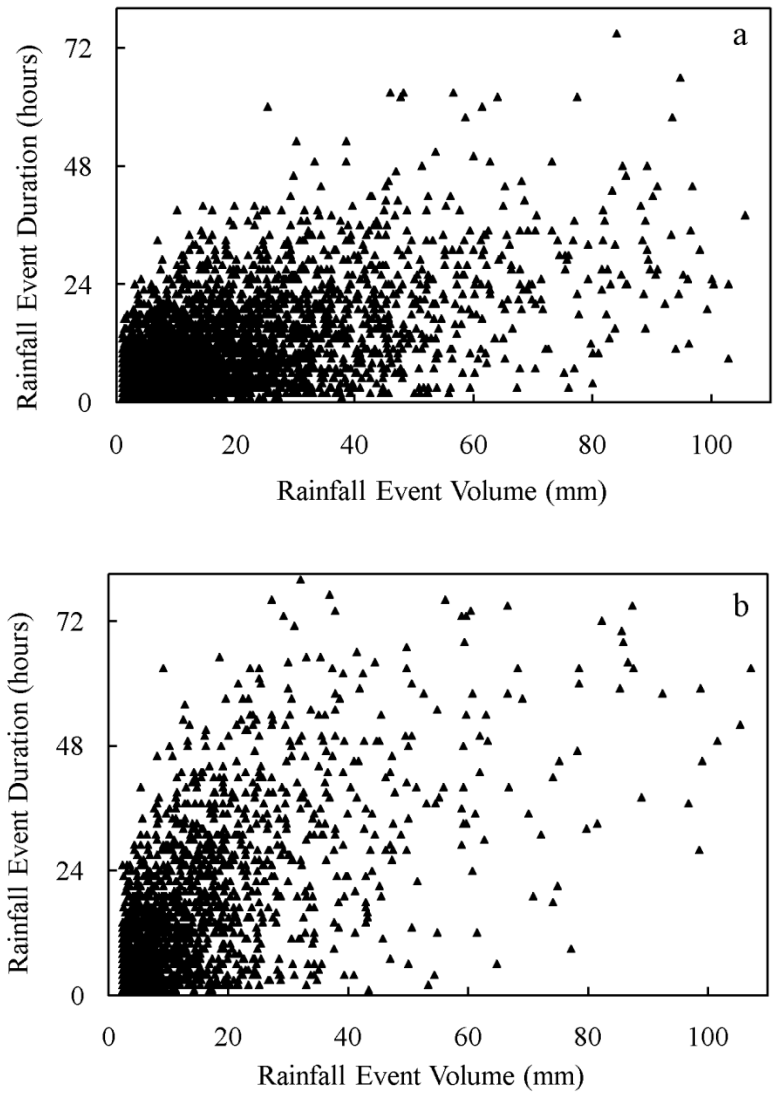


**Figure 3.3 Scatter diagrams of the rainfall event volumes and durations at Atlanta (a) and Flagstaff (b)**

The water balance of the surface depressions of a rain garden over the current cycle can be expressed as

$$v_o = v_i - R_c - F_t \tag{3.7}$$

where $R_c$ is the available retention capacity of the surface depressions of the rain garden at the beginning of the current rainfall event; $F_t$ is the volume of infiltration through the fill media layer of the rain garden during the current rainfall event; and $v_o$ is the volume of overflow bypassing the rain garden during the current rainfall event. All the terms in Equation (3.7) are treated as realizations of their corresponding random variables and expressed in units of mm of water over the rain garden surface area.

As shown in Equation (3.7), $v_o$ is controlled by $v_i$, $R_c$, and $F_t$. Equation (3.4) can be used to calculate $v_i$. The term $R_c$ is determined by the depth of water (denoted as $D_{sd}$) held in the surface depression of the rain garden at the end of the previous rainfall event (or the beginning of the current cycle) and the evapotranspiration and infiltration rates during the *b*-hour dry period of the current cycle. The term $F_t$ depends on the infiltration capacity of the fill media of the rain garden, the duration of the current rainfall event, and the availability of rain water for infiltration.

The value of $D_{sd}$ is required in order to estimate $R_c$. $D_{sd}$ is a random

variable and varies depending on many factors (e.g., the characteristics of previous rainfall event and the infiltration rate of the rain garden). As a result, the surface depression of a rain garden may be nearly full, partly full, or empty at the start of the current cycle. Theoretically, the expected value of $D_{sd}$ should be used in estimating the average $R_c$ and this expected value should exist. However, it has been found that such an expected value cannot be derived analytically (Smith 1980; Adams and Papa 2000). For simplification, it is conservatively assumed that the surface depression of the rain garden is completely full at the start of the current cycle, or at the end of a random rainfall event preceding the current cycle. This assumption will result in an overestimation of the overflow volume and therefore a conservative estimation of the stormwater capture efficiency of rain gardens. Similar conservative assumptions were adopted by Howard (1976), Loganathan and Delleur (1984), Adams and Papa (2000), and Guo and Baetz (2007) in studying other urban stormwater management problems.

During the dry period after the previous rainfall event, water held in the surface depression is depleted through evapotranspiration and infiltration. It is assumed that infiltration takes place at a constant rate $K$ when there is water held in, or inflow into, the surface depression. The initially higher infiltration rates at the beginning of a rainfall event due to drier fill media conditions are therefore not considered. This assumption is expected to have

a minimal impact on the estimation of the expected value of the overflow volume, since most of the fill media are required to be highly permeable and the initially higher infiltration rate is relatively close to the constant infiltration rate. Given that the surface depression is completely filled at the beginning of the current cycle, the time needed ($t_d$, in h) to drain out the surface depression can be calculated as

$$t_d = \frac{S_d}{E_a + K} \tag{3.8}$$

where $S_d$ is the storage capacity of the surface depression, in mm of water over the rain garden surface area; $E_a$ is the average evapotranspiration rate of the rain garden in mm/h; and $K$ is the constant infiltration rate or the saturated hydraulic conductivity of the fill media in mm/h.

Depending on the magnitude of $t_d$ and $b$, the available retention capacity ($R_c$) of the surface depression at the beginning of the current rainfall event can be expressed as:

$$R_c = \begin{cases} (E_a + K)b, & b \le t_d \\ S_d, & b > t_d \end{cases} \tag{3.9}$$

Knowing the infiltration rate $K$ and the duration of the current rainfall event $t$, the volume of potential infiltration through the fill media during the current rainfall event ($F_t$) can be calculated as

$$F_t = Kt \tag{3.10}$$

Depending on the magnitude of $t_d$ and $b$, and the difference between $K$ and the average rate of inflow into the rain garden (denoted as $r_i$, $r_i = v_i / t$, in mm/h), the operational history of the rain garden within the current cycle can be generalized as being one of the four cases depicted in Figures 3.4 through 3.7. Figure 3.4 illustrates the case where the surface depression of the rain garden still has water remaining when the current rainfall event starts (i.e., $b \le t_d$) and the depth of water held in the surface depression keeps decreasing (or stays at a constant level) during the current rainfall event (i.e., $K \ge r_i$). Figure 3.5 illustrates the case where the surface depression of the rain garden is empty before the current rainfall event starts (i.e., $b > t_d$) and remains empty during the current rainfall event (i.e., $K \ge r_i$). Figure 3.6 represents the case where the surface depression of the rain garden still has water remaining when the current rainfall event starts (i.e., $b \le t_d$) and the depth of water held in the surface depression keeps increasing until the surface depression is completely filled and overflow occurs (i.e., $K < r_i$). Figure 3.7 represents the case where the surface depression of the rain garden is empty when the current rainfall event starts (i.e., $b > t_d$) and the depth of water held in the surface depression keeps increasing until the surface depression is completely filled and overflow occurs (i.e., $K < r_i$).

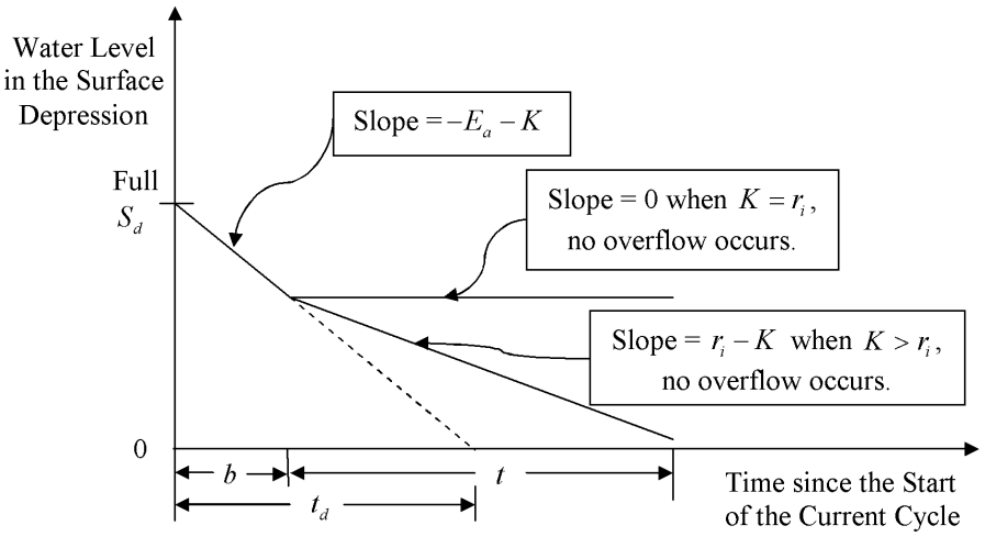


**Figure 3.4 The operational history of rain gardens within the current cycle**

**when** $b \le t_d$ **and** $K \ge r_i$

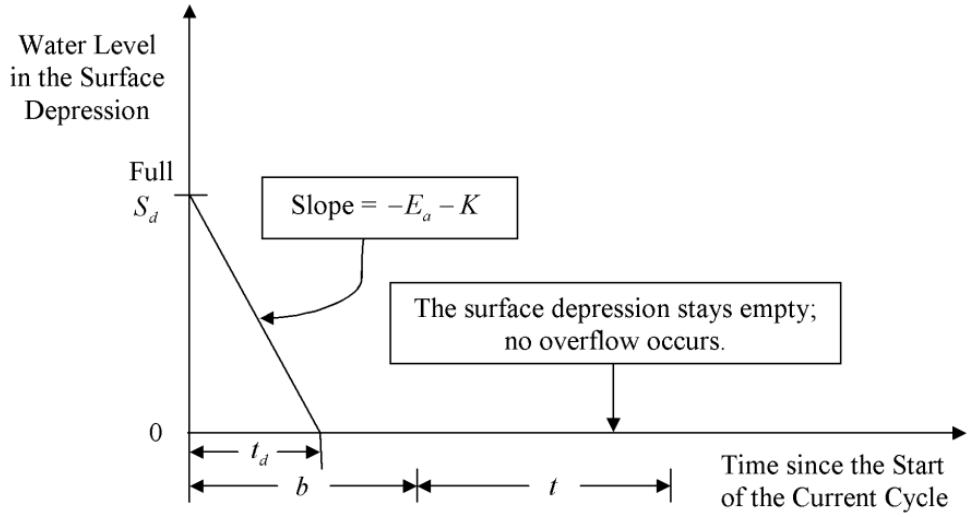


**Figure 3.5 The operational history of rain gardens within the current cycle**

**when** $b > t_d$ **and** $K \ge r_i$

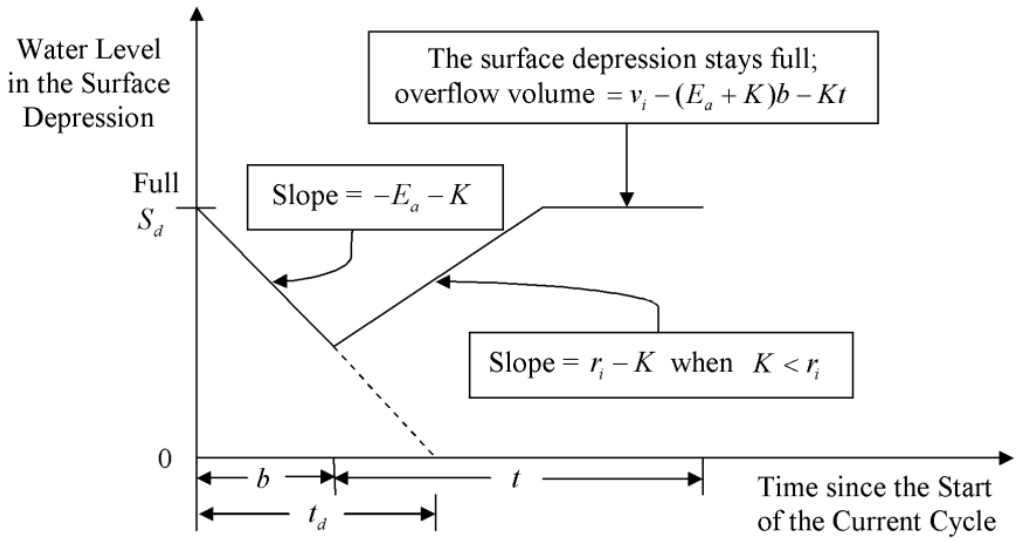


**Figure 3.6 The operational history of rain gardens within the current cycle**

**when** $b \le t_d$ **and** $K < r_i$

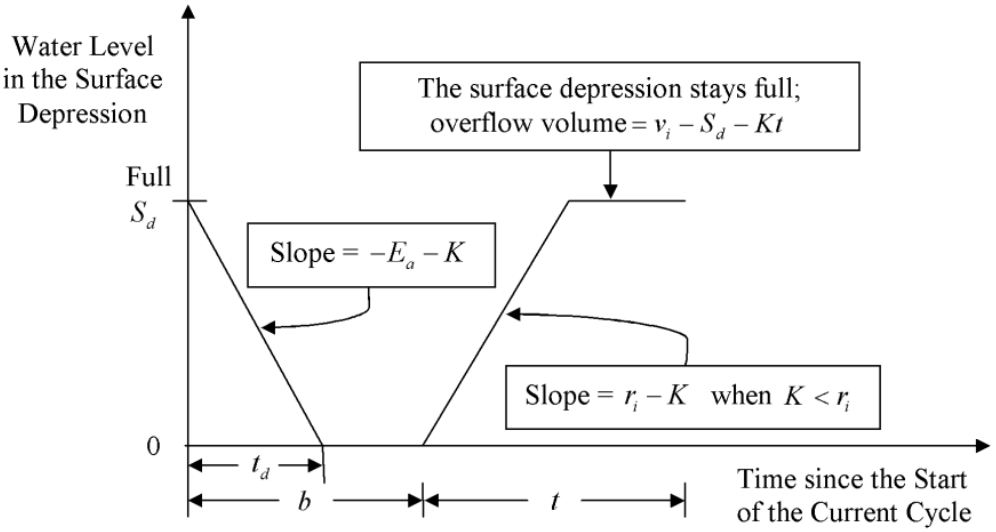


**Figure 3.7 The operational history of rain gardens within the current cycle**

**when** $b > t_d$ **and** $K < r_i$

The volume of overflow $v_o$ can be estimated by substituting Equations (3.4), (3.9) and (3.10) into Equation (3.7). As illustrated in Figures 3.4

through 3.7, the result for $v_o$ is different for each case. For all the four cases, the results can be summarized as follows:

$$v_o = \begin{cases} 0, & \left\{ b \le t_d \text{ and } v \le \frac{1}{r+1}\left[(E_a + K)b + Kt\right] \right\} \\ & \text{or } \left\{ b > t_d \text{ and } v \le \frac{1}{r+1}(S_d + Kt) \right\} \\ (r+1)v - (E_a + K)b - Kt, & \left\{ b \le t_d \text{ and } v > \frac{1}{r+1}\left[(E_a + K)b + Kt\right] \right\} \\ (r+1)v - S_d - Kt, & \left\{ b > t_d \text{ and } v > \frac{1}{r+1}(S_d + Kt) \right\} \end{cases} \tag{3.11}$$

In Equation (3.11), $v_o$ can be viewed as a realization of its corresponding random variable $V_o$ which depends on random variables *V*, *T*, and *B*. This relationship is the basis for deriving the probability distribution of $V_o$ through the use of the derived probability distribution theory. Details about the derived probability distribution theory can be found in Benjamin and Cornell (1970).

As shown in Equation (3.11), there are two cases when no overflow occurs. The probability that no overflow occurs can be derived by carrying out the integration of the joint PDF of *V*, *T*, and *B* over the regions of the *V*, *T*, and *B* values that enclose the two cases:

$$\mathrm{P}_{V_o}(V_o = 0) = \int_0^{\infty}\int_0^{t_d}\int_0^{\frac{1}{r+1}[(E_a+K)b+Kt]} \zeta \mathrm{e}^{-\zeta v}\psi \mathrm{e}^{-\psi b}\lambda \mathrm{e}^{-\lambda t} dvdbdt +$$
$$\int_0^{\infty}\int_{t_d}^{\infty}\int_0^{\frac{1}{r+1}(S_d+Kt)} \zeta \mathrm{e}^{-\zeta v}\psi \mathrm{e}^{-\psi b}\lambda \mathrm{e}^{-\lambda t} dvdbdt \qquad (3.12)$$
$$= 1 - \frac{\lambda(r+1)}{\lambda(r+1)+\zeta K}\left[ e^{-\frac{\psi(r+1)+\zeta(E_a+K)}{(r+1)(E_a+K)}S_d} + \frac{\psi(r+1)(1-e^{-\frac{\psi(r+1)+\zeta(E_a+K)}{(r+1)(E_a+K)}S_d})}{\psi(r+1)+\zeta(E_a+K)}\right]$$

There are another two cases, as shown in Equation (3.11), when overflows occur. The two cases are mutually exclusive; therefore, the probability that overflow is greater than zero but less than $v_o$ can be derived as follows:

$$\mathrm{P}_{V_o}(0 < V_o < v_o) = \int_0^{\infty}\int_0^{t_d}\int_{\frac{1}{r+1}[(E_a+K)b+Kt]}^{\frac{1}{r+1}[(E_a+K)b+Kt+v_o]} \zeta \mathrm{e}^{-\zeta v}\psi \mathrm{e}^{-\psi b}\lambda \mathrm{e}^{-\lambda t} dvdbdt +$$
$$\int_0^{\infty}\int_{t_d}^{\infty}\int_{\frac{1}{r+1}(S_d+Kt)}^{\frac{1}{r+1}(S_d+Kt+v_o)} \zeta \mathrm{e}^{-\zeta v}\psi \mathrm{e}^{-\psi b}\lambda \mathrm{e}^{-\lambda t} dvdbdt \qquad (3.13)$$
$$= \frac{\lambda(r+1)}{\lambda(r+1)+\zeta K}(1-e^{-\frac{\zeta v_o}{r+1}})\left[ e^{-\frac{\psi(r+1)+\zeta(E_a+K)}{(r+1)(E_a+K)}S_d} + \frac{\psi(r+1)(1-e^{-\frac{\psi(r+1)+\zeta(E_a+K)}{(r+1)(E_a+K)}S_d})}{\psi(r+1)+\zeta(E_a+K)}\right]$$

The integration upper limit for $v$ for each case is determined based on the requirement that overflow is less than a given value $v_o$. The cumulative distribution function (CDF) of $V_o$, $F_{V_o}(v_o)$, can be calculated as:

$$\mathrm{F}_{V_o}(v_o) = \mathrm{P}_{V_o}(V_o = 0) + \mathrm{P}_{V_o}(0 < V_o < v_o)$$
$$= 1 - \frac{\lambda(r+1)}{\lambda(r+1)+\zeta K} e^{-\frac{\zeta v_o}{r+1}}\left[ e^{-\frac{\psi(r+1)+\zeta(E_a+K)}{(r+1)(E_a+K)}S_d} + \frac{\psi(r+1)(1-e^{-\frac{\psi(r+1)+\zeta(E_a+K)}{(r+1)(E_a+K)}S_d})}{\psi(r+1)+\zeta(E_a+K)}\right] \qquad (3.14)$$

The PDF of $V_0$ is denoted as $f_{V_o}(v_o)$ and can be obtained as the first order derivative of $F_{V_o}(v_o)$ with respect to $v_o$:

$$f_{V_o}(v_o) = \frac{\lambda\zeta}{\lambda(r+1)+\zeta K} e^{-\frac{\zeta v_o}{r+1}} \left[ e^{-\frac{\psi(r+1)+\zeta(E_a+K)}{(r+1)(E_a+K)}S_d} + \frac{\psi(r+1)(1-e^{-\frac{\psi(r+1)+\zeta(E_a+K)}{(r+1)(E_a+K)}S_d})}{\psi(r+1)+\zeta(E_a+K)} \right] \tag{3.15}$$

The expected value of $V_0$ per cycle can be determined as:

$$\begin{aligned} \mathrm{E}(V_o) &= \int_0^\infty v_o f_{V_o}(v_o) dv_o \\ &= \frac{\lambda(r+1)^2}{\zeta\lambda(r+1)+K\zeta^2} \left[ e^{-\frac{\psi(r+1)+\zeta(E_a+K)}{(r+1)(E_a+K)}S_d} + \frac{\psi(r+1)(1-e^{-\frac{\psi(r+1)+\zeta(E_a+K)}{(r+1)(E_a+K)}S_d})}{\psi(r+1)+\zeta(E_a+K)} \right] \end{aligned} \tag{3.16}$$

The average annual volume of overflow ($O_a$) bypassing the rain garden is $\mathrm{E}(V_o)$ multiplied by the average annual number of rainfall events:

$$O_a = \frac{\theta\lambda(r+1)^2}{\zeta\lambda(r+1)+K\zeta^2} \left[ e^{-\frac{\psi(r+1)+\zeta(E_a+K)}{(r+1)(E_a+K)}S_d} + \frac{\psi(r+1)(1-e^{-\frac{\psi(r+1)+\zeta(E_a+K)}{(r+1)(E_a+K)}S_d})}{\psi(r+1)+\zeta(E_a+K)} \right] \tag{3.17}$$

### 3.2.5 Estimation of the Stormwater Capture Efficiency

The average annual volume of stormwater captured by a rain garden is the average annual volume of inflow entering minus the average annual volume of overflow bypassing the rain garden, i.e., $I_a - O_a$. The long-term

average stormwater capture efficiency ( $C_e$ ) of the rain garden can be calculated as the ratio between the average annual volume of stormwater captured and the average annual volume of inflow, i.e.,

$$C_e = \frac{I_a - O_a}{I_a} \tag{3.18}$$

Substituting Equations (3.6) and (3.17) into Equation (3.18) gives

$$C_e = 1 - \frac{\lambda(r+1)}{\lambda(r+1)+K\zeta}\left[ e^{-\frac{\psi(r+1)+\zeta(E_a+K)}{(r+1)(E_a+K)}S_d} + \frac{\psi(r+1)(1-e^{-\frac{\psi(r+1)+\zeta(E_a+K)}{(r+1)(E_a+K)}S_d})}{\psi(r+1)+\zeta(E_a+K)} \right] \tag{3.19}$$

## 3.3 Comparison with Continuous Simulation Results

The explicit analytical expressions derived in the preceding sections provide a convenient tool to evaluate the long-term average volumes of overflow and stormwater capture efficiencies of rain gardens. Several assumptions were made in the derivation of these expressions. To verify the acceptability of these assumptions and to illustrate the accuracy of the derived expressions, a set of continuous SWMM (Version 5.0) simulations were performed for rain gardens with different $r$ and $S_d$ values. The 61-year hourly rainfall record of Atlanta was used as the rainfall input to the continuous simulations. The Horton infiltration method was selected to simulate the infiltration process of the rain gardens in SWMM simulations.

The values of the major hydrologic and hydraulic parameters of the test rain gardens are listed in Table 3.3.

**Table 3.3 Input parameter values used in SWMM and the analytical equation**

| Parameters | SWMM Simulations | Analytical Equation |
|---|---|---|
| $r$ (unitless) | 5-45 | 5-45 |
| $S_d$ (mm) | 100-800 | 100-800 |
| $E_a$ (mm/h) | 0.13 | 0.13 |
| $f_c$ or $K$ (mm/h) | 10.9 | 10.9 |
| $f_m$ (mm/h) | 101.9 | N/N* |
| $k$ (1/h) | 4.14 | N/N* |
| $D$ (day) | 7.8 | N/N* |

Notes:

$f_c$ is the final constant infiltration rate of the fill media, $K$ used in the analytical equation is made equal to $f_c$;

$f_m$ is the maximum infiltration capacity of the fill media;

$k$ is the infiltration capacity decay coefficient;

$D$ is a decay coefficient for the infiltration capacity recovery curve;

* indicates that the parameter is not needed.

From the continuous SWMM simulations, the total volumes of inflow and overflow over the 61 years can be obtained. Using the total volumes of inflow and overflow, the SWMM model simulated stormwater capture efficiency of a test rain garden ( $C_{eSWMM}$ ) can be calculated as

$$C_{eSWMM} = \frac{V_{in} - V_{over}}{V_{in}} \tag{3.20}$$

where $V_{in}$ and $V_{over}$ are the total volumes of inflow and overflow, respectively.

Results from the continuous simulations [Equation (3.20)] and those from the analytical expression [Equation (3.19)] were compared in Figures 3.8 and 3.9. Figure 3.8 shows the comparison for rain gardens with a fixed $r$ of 20:1 and $S_d$ changing from 100 mm to 800 mm. As shown in Figure 3.8, stormwater capture efficiencies calculated using the analytical equation are very close to those from continuous simulations when $S_d$ changes from 100 mm to 600 mm. When $S_d$ is greater than 600 mm, the difference between the analytical and continuous simulation results gets larger. This may be caused by the assumption that the surface depression of the rain garden is completely full at the start of the current cycle. As mentioned previously, this assumption will cause the analytical expression [Equation (3.19)] to underestimate the stormwater capture efficiencies. The larger the $S_d$, the more conservative the estimation by Equation (3.19). This is reflected by the trend revealed in Figure 3.8. By fixing $S_d$ to 300 mm and changing $r$ from 5:1 to 45:1, Figure 3.9 shows a close agreement between results from the analytical equation and the SWMM simulations.

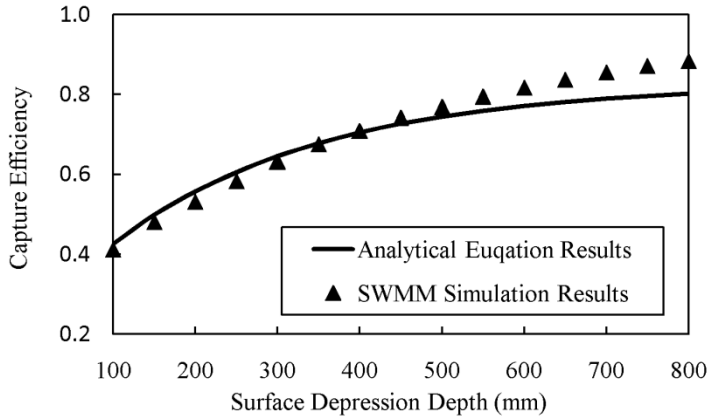


**Figure 3.8 Comparison of analytical and SWMM simulation results ($r = 20:1$)**

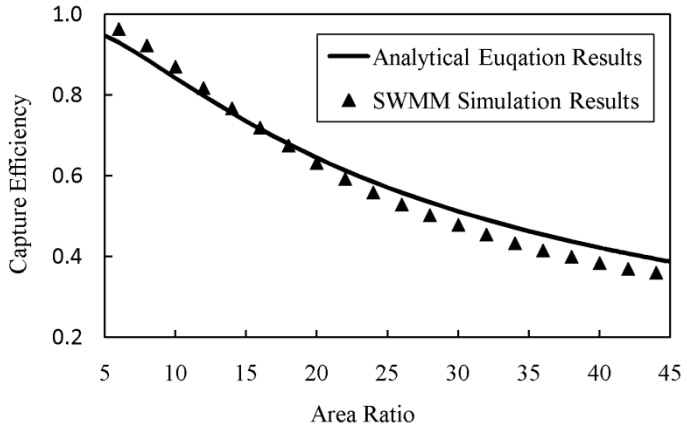


**Figure 3.9 Comparison of analytical and SWMM results ($S_d = 300$ mm)**

Figures 3.8 and 3.9 show that, as long as $S_d$ and $r$ are within practically suitable ranges ( $0 < S_d \le 800$ mm and $5:1 < r \le 45:1$ ), the difference between the results from the analytical expression and the SWMM simulations should be less than about 10%. Since this level of accuracy is acceptable for planning and design purposes, the analytical expressions may be used as an alternative to continuous simulations for the estimation of long-term average stormwater capture efficiencies. The overall close

agreement also verifies that the fitted exponential distribution models of rainfall event characteristics and the independence assumptions about these rainfall event characteristics for the rainfall data of Atlanta are acceptable. For specific locations of interest, many more sets of continuous simulations may be conducted to better quantify the level of accuracies of the analytical equations.

## 3.4 Example Application of the Analytical Probabilistic Expression

In Equation (3.19), the $C_e$ of a rain garden is expressed as a function of its two critical dimensions (i.e., $r$ and $S_d$), its average evapotranspiration rate ($E_a$), the hydraulic conductivity of the fill media ($K$), and the three parameters (i.e., $\zeta$, $\lambda$, and $\psi$) describing the local rainfall conditions. To illustrate the effects of the $K$, $r$ and $S_d$ of a rain garden on its $C_e$, example applications of the analytical expression were made for Atlanta and Flagstaff, which represent humid and dry climate conditions respectively. Thus, the variations of $C_e$ caused by climate differences can also be shown in these example applications. The $E_a$ of rain gardens located in Atlanta and Flagstaff was estimated to be 0.13 mm/h and 0.18 mm/h, respectively, based on the annual pan evaporation data from NOAA (1982). In the example applications, the $C_e$ of rain gardens with various $K$, $r$ and $S_d$ were

calculated using the rainfall statistics of Atlanta and Flagstaff. Results are plotted in Figures 3.10-3.12.

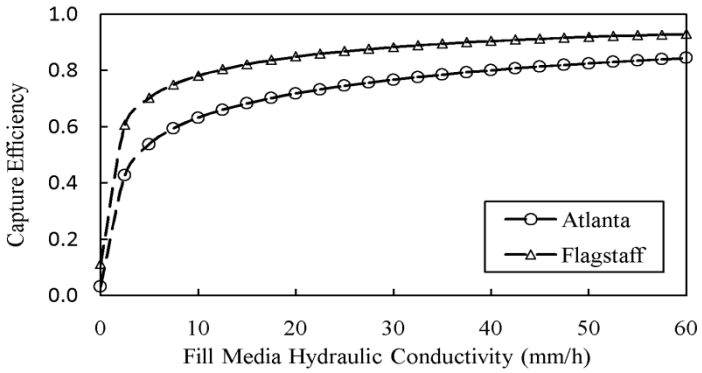


**Figure 3.10 The capture efficiency achievable as a function of the fill media's hydraulic conductivity (with $r = 20$ and $S_d = 300$ mm)**

As shown in Figure 3.10, the capture efficiency increases quickly when the hydraulic conductivity of fill media increases from 0 to about 10 mm/h. Further increases in hydraulic conductivity beyond 10 mm/h do not result in significant increases in capture efficiency. This indicates that there are points of diminishing returns (around 10 mm/h) on the fill media hydraulic conductivity versus rain garden stormwater capture efficiency curves. This is part of the reason why sandy loam with a hydraulic conductivity of about 10.9 mm/h (Rawls et al. 1983) is used as the fill media of rain gardens (Dietz and Clausen 2005; Li et al. 2009; Davis et al. 2009).

Figure 3.11 shows the effect of the area ratio on $C_e$. Higher $C_e$ values can be obtained with smaller area ratios (i.e., larger rain garden surface areas),

and $C_e$ can approach very closely to its maximum value (i.e., 1.0) when the area ratio decreases. The figure also shows the effect of climate differences on $C_e$. In Atlanta, which has a humid climate, the $C_e$ achieved is lower than that in Flagstaff, which has a dry continental climate. In other words, to achieve the same level of stormwater capture efficiency, a larger rain garden needs to be constructed in Atlanta than in Flagstaff to serve the same contributing area. For example, according to Figure 3.11, one needs to build a 16 $m^2$ rain garden in Atlanta to capture 80% of the stormwater generated from a 200 $m^2$ roof or parking lot. While in Flagstaff, a rain garden with an area of 10 $m^2$ can achieve the same stormwater capture efficiency.

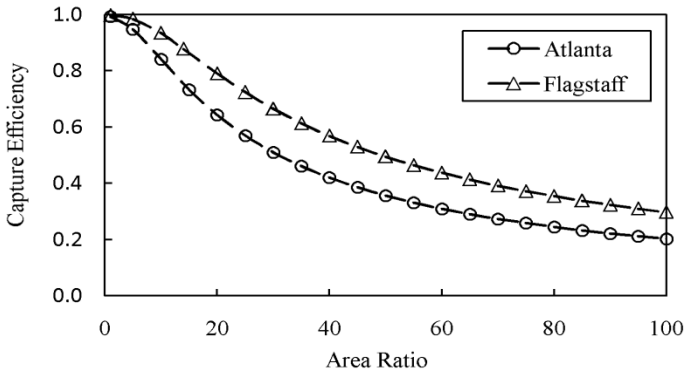


**Figure 3.11 The capture efficiency achievable as a function of the area ratio (with $K = 10.9$ mm/h and $S_d = 300$ mm)**

The effect of the surface depression depth on $C_e$ is illustrated in Figure 3.12. It is obvious that the $C_e$ of a rain garden increases with its surface depression depth. However, beyond a depth of about 500 mm, further increases in the surface depression depth only translate to marginal increases

in $C_e$. Moreover, there exist significant differences between the two locations. A deeper rain garden needs to be constructed in Atlanta than in Flagstaff to obtain the same stormwater capture efficiency. For example, to capture 70% of the stormwater generated from a 200 $m^2$ roof or parking lot, the surface depression depth of a 10 $m^2$ rain garden should be about 400 mm in Atlanta and only about 200 mm in Flagstaff.

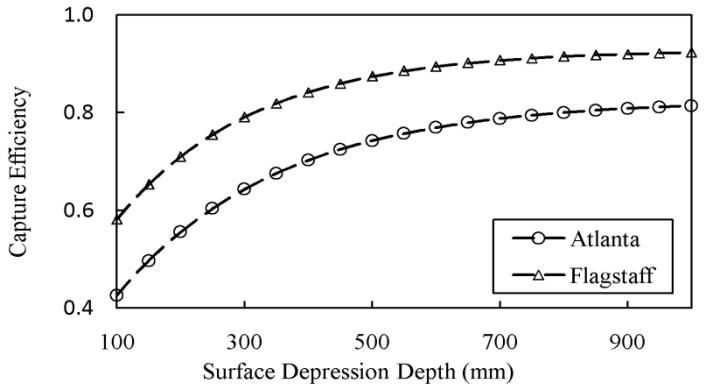


**Figure 3.12 The capture efficiency achievable as a function of the surface depression depth (with $r = 20$ and $K = 10.9$ mm/h)**

## 3.5 Summary and Conclusion

An explicit analytical equation was derived for calculating the long-term average stormwater capture efficiency of rain gardens. The derivation was based on the exponential probability density functions representing local rainfall conditions and a simplified representation of the hydrologic processes involved in the operation of rain gardens. The simplified representation of the hydrologic processes was based on the following four assumptions: (1) the

contributing impervious area converts 100% of the rainfall into surface runoff; (2) proper site selection of rain gardens or installation of underdrains ensures that impermeable or less permeable subsoil layers and groundwater tables do not impede the infiltration of water through the fill media; (3) infiltration takes place at a rate equaling the hydraulic conductivity of the fill media when there is water held in, or when there is sufficient inflow coming into, the surface depression; and (4) the surface depression is completely full at the end of a random rainfall event.

Results from the analytical equation were compared to those from continuous SWMM simulations using the 61-year rainfall record of Atlanta, Georgia as rainfall input. The close agreement between the results from the analytical equation and the SWMM simulations indicates that the simplifying assumptions made in this study are acceptable for practical design purposes. The fourth assumption would usually result in conservative estimations of stormwater capture efficiencies of rain gardens. As shown in Figure 3.8, the inaccuracy caused by this and other assumptions increases with the increase of the surface depression depth. Since surface depression depths commonly range from 150 to 520 mm (Davis et al. 2012), where the difference between analytical and continuous simulation results is relatively small, the fourth assumption is acceptable for practical purposes. As design tools, figures similar to Figures 3.10−3.12 for different locations may be easily developed

using the analytical equations.

In the application of Equation (3.19), it should be noted that the stormwater capture efficiency of a rain garden is defined as the fraction of stormwater captured by its surface depressions. For rain gardens with no underdrain systems, the stormwater captured by surface depressions will be infiltrated into native soils or depleted through ET. For rain gardens with underdrain systems, the stormwater captured may also be discharged through the underdrain systems and returned as runoff to surface waters. Since water that is infiltrated into native soils, depleted through ET, or discharged through underdrain systems all receives some degree of treatment, the stormwater capture efficiency calculated using Equation (3.19) is suitable for both types of rain gardens when their overall water quality control performance is the main concern. However, if the runoff volume reduction rate needs to be calculated, which would require a separate accounting of volumes carried away by the underdrains, Equation (3.19) is only suitable for rain gardens without underdrains. This is because the portion of water that may be drained away through underdrains was not separately considered in deriving the analytical equations. For rain gardens located on low permeable native soils and with no underdrain systems, Equations (3.17) and (3.19) may provide inaccurate estimates because the second assumption may be violated and infiltration of water through the fill media may be impeded if the footprints of the rain

gardens are not large enough. Future studies may take into consideration the moisture condition of the fill media and the infiltration capacity of the underlying native soils in deriving more sophisticated analytical expressions.

**ACKNOWLEDGEMENTS:** This work was supported by the Natural Sciences and Engineering Research Council of Canada and the China Scholarship Council.

## References

Abi Aad, M. P., Suidan, M. T., and Shuster, W. D. (2010). Modeling techniques of best management practices: rain barrels and rain gardens using EPA SWMM-5. *Journal of Hydrologic Engineering*, 15(6), 434–443.

Adams, B. J., and Papa, F. (2000). *Urban Stormwater Management Planning with Analytical Probabilistic Models*, John Wiley & Sons, Inc., New York, USA.

Adams, B. J., Fraser, H. G., Howard, C. D. D., and Hanafy, M. S. (1986). Meteorologic data analysis for drainage system design. *Journal of Environmental Engineering*, ASCE, 112(5), 827–848.

American Society of Civil Engineers (ASCE), (2012). *Design of Urban Stormwater Controls*, *Manuals of Practice* (MOP) 87, McGraw-Hill Inc., New York, USA.

Aravena, J. E., and Dussaillant, A. (2009). Storm-water infiltration and focused recharge modeling with finite-volume two-dimensional Richards Equation: application to an experimental rain garden. *Journal of Hydraulic Engineering*, 135(12), 1073–1080.

Ashkar, F., and Rousselle, J. (1987). Partial duration series modeling under the assumption of a Poissonian Flood Count. *Journal of Hydrology*, 90(1-2), 135-144.

Asleson, B. C., Nestingen, R. S., Gulliver, J. S., Hozalski, R. M., and Nieber, J. L. (2009). Performance assessment of rain gardens. *Journal of the*

*American Water Resources Association*, 45(4),1019–1031.

Bacchi, B., Balistrocchi, M., and Grossi, G. (2008). Proposal of a semi-probabilistic approach for storage facility design. *Urban Water Journal*, 5(3), 195–208.

Balistrocchi, M., Grossi, G., and Bacchi, B. (2009). An analytical probabilistic model of the quality efficiency of a sewer tank. *Water Resources Research*, 45, W12420, doi:10.1029/2009WR007822.

Benjamin, J. R., and Cornell, C. A. (1970). *Probability, Statistics and Decision for Civil Engineers*, McGraw-Hill, New York, USA.

Clar, M. L., and Green, R. (1993). *Design manual for use of bioretention in stormwater management*, Dept. of Environmental Resources, Prince George's County, USA.

Cruise, J. F., and Arora, K. (1990). A hydroclimatic application strategy for the Poisson partial duration model. *Water Resources Bulletin*, American Water Resources Association 26(3), 431-442.

Cunnane, C. (1979). A note on the Poisson assumption in partial duration series models. *Water Resources Research*, 15(2), 489-494.

Davis, A. P. (2008). Field performance of bioretention: Hydrology impact. *Journal of Hydrologic Engineering*, 13(2), 90–95.

Davis, A. P., Hunt, W. F., Traver, R. G., and Clar, M. (2009). Bioretention technology: overview of current practice and future needs. *Journal of Environmental Engineering*, 135(3), 109–117.

Davis, A. P., Shokouhian, M., Sharma, H., and Minami, C. (2001). Laboratory study of biological retention for urban stormwater management. *Water Environment Research*, 73, 5–14.

Davis, A. P., Shokouhian, M., Sharma, H., Minami, C., and Winogradoff, D. (2003). Water quality improvement through bioretention: Lead, copper, and zinc. *Water Environment Research*, 75(1), 73–82.

Davis, A. P., Traver, R. G., Hunt, W. F., Lee, R., Brown, R. A., and Olszewski, J. O. (2012). Hydrologic performance of bioretention storm-water control measures. *Journal of Hydrologic Engineering*, 17(5), 604–614.

DeBusk, K. M., Hunt, W. F., and Line, D. E. (2011). Bioretention outflow: does it mimic nonurban watershed shallow interflow? *Journal of Hydrologic Engineering*, 16(3), 274–279.

Delaware Natural Resources and Environmental Control (DNREC). (2005). *Green technology: The Delaware urban runoff management approach*, Delaware Department of Natural Resources and Environmental Control, Division of Soil and Water Conservation, Dover, Delaware, USA.

Dietz, M. E., and Clausen, J. C. (2005). A field evaluation of rain garden flow and pollutant treatment. *Water, Air, Soil Pollutant*, 167, 123–138.

Dietz, M. E., and Clausen, J. C. (2006). Saturation to improve pollutant retention in a rain garden flow. *Environmental Science & Technology*, 40, 1335–1340.

Dussaillant, A. R., Wu, C. H., and Potter, K. W. (2004). Richards equation model of a rain garden. *Journal of Hydrologic Engineering*, 9(3), 219–

225.

Eagleson, P. S. (1972). Dynamics of flood frequency. *Water Resources Research*, 8(4), 878–898.

Eagleson, P. S. (1978). Climate, soil, and vegetation, 2, the distribution of annual precipitation derived from observed storm sequences. *Water Resources Research*, 14(5), 713–721.

Emerson, C. H., and Traver, R. G. (2008). Multi-year and seasonal variation of infiltration from stormwater best management practices. *Journal of Irrigation and Drainage Engineering*, 134(5), 598–605.

Guo, Y. (2001). Hydrologic design of urban flood control detention ponds. *Journal of Hydrologic Engineering*, 6(6), 472–479.

Guo, Y., and Adams, B. J. (1998a). Hydrologic analysis of urban catchments with event-based probabilistic models. Part I: Runoff volume. *Water Resources Research*, 34(12), 3421–3431.

Guo, Y., and Adams, B. J. (1998b). Hydrologic analysis of urban catchments with event-based probabilistic models. Part II: Peak discharge rate. *Water Resources Research*, 34(12), 3433–3443.

Guo, Y., and Adams, B. J. (1999a). Analysis of detention ponds for storm water quality control. *Water Resources Research*, 35(8), 2447–2456.

Guo, Y., and Adams, B. J. (1999b). An analytical probabilistic approach to sizing flood control detention facilities. *Water Resources Research*, 35(8), 2457–2468.

Guo, Y., and Baetz, B. W. (2007). Sizing of rainwater storage units for green building applications. *Journal of Hydrologic Engineering*, 12(2), 197–205.

Guo, Y., Hansen, D., and Li, C. (2009). Probabilistic approach to estimating the effects of channel reaches on flood frequencies. *Water Resources Research*, 45, W08404, doi: 10.1029/2008WR007387.

Hager, M. C. (2003). Low-impact development, lot-level approaches to stormwater management are gaining ground. *Stormwater, the Journal for Surface Water Quality Professionals*, 4(1), 12–25.

He, Z., and Davis, A. P. (2011). Process modeling of storm-water flow in a bioretention cell. *Journal of Irrigation and Drainage Engineering*, 137(3), 121–131.

Heasom, W., Traver, R., and Welker, A. (2006). Hydrologic modeling of a bioinfiltration best management practice. *Journal of the American Water Resources Association*, 42(5), 1329–1347.

Howard, C. D. D. (1976). Theory of storage and treatment plant overflows. *Journal of the Environmental Engineering Division*, ASCE, 102(EE4), 709–722.

Hsieh, C. H., and Davis, A. P. (2005). Evaluation and optimization of bioretention media for treatment of urban storm water runoff. *Journal of Environmental Engineering*, 131(11), 1521–1531.

Hunt, W. F., and Lord, W. G. (2006). *Bioretention performance, design, construction, and maintenance*, North Carolina Cooperative Extension,

Raleigh, NC, USA.

Hunt, W. F., Smith, J. T., Jadlocki, S. J., Hathaway, J. M., and Eubanks, P. R. (2008). Pollutant removal and peak flow mitigation by a bioretention cell in urban Charlotte, NC. *Journal of Environmental Engineering*, 134(5), 403–408.

James, M. and Dymond, R. (2012). Bioretention hydrologic performance in an urban stormwater network. *Journal of Hydrologic Engineering*, 17(3), 431–436.

Jenkins, J. K. G., Wadzuk, B. M., and Welker, A. L. (2010). Fines accumulation and distribution in a storm-water rain garden nine years postconstruction. *Journal of Irrigation and Drainage Engineering*, 136(12), 862–869.

Kim, H., Seagren, E. A., and Davis, A. P. (2003). Engineered bioretention for removal of nitrate from stormwater runoff. *Water Environment Research*, 75(4), 355–367.

Klein, R. D. (1979). Urbanization and stream quality impairment. *Water Resources Bulletin*, American Water Resources Association, 15(4), 948–963.

Li, H., Sharkey, L. J., Hunt, W. F., and Davis, A. P. (2009). Mitigation of impervious surface hydrology using bioretention in North Carolina and Maryland. *Journal of Hydrologic Engineering*, 14(4), 407–415.

Loganathan, G. V., and Delleur, J. W. (1984). Effects of urbanization on frequencies of overflows and pollutant loadings from storm sewer

overflows: A derived distribution approach. *Water Resources Research*, 20(7), 857–865.

Maryland Department of the Environment (MDE). (2000). *2000 Maryland stormwater design manual*, Vols. I and II, Center for Watershed Protection and the Maryland Department of the Environment, Water Management Administration, Baltimore, MD, USA.

Muthanna, T. M., Viklander, M. and Thorolfsson, S. T. (2008). Seasonal climatic effects on the hydrology of a rain garden. *Hydrological Processes*, 22, 1640–1649.

National Oceanic and Atmospheric Administration (NOAA) (1982). *Mean Monthly, Seasonal, and Annual Pan Evaporation for the United States*. Washington, D.C. (http://www.nws.noaa.gov/oh/hdsc/PMP_related_studies/TR34.pdf)

Pennsylvania Department of Environmental Protection (PDEP). (2006). *Pennsylvania stormwater best management practices manual*. *PA DEP Rep. No. 363-0300-002*, Harrisburg, PA, USA.

Prince George's County, Department of Environmental Protection (PGC DEP). (1993). *Design Manual for Use of Bioretention in Stormwater Management.* Prince George's County (MD) Government, Department of Environmental Protection. Watershed Protection Branch, Landover, MD, USA.

Rawls, W. J., Brakensiek, D. L., and Miller, N. (1983). Green-Ampt infiltration parameters from soils data. *Journal of Hydraulic Engineering*, 109(1), 62–70.

Restrepo-Posada, P. J., and Eagleson, P. S. (1982). Identification of independent rainstorms. *Journal of Hydrology,* 55(1-4), 303-319

Roy-Poirier, A., Champagne, P., and Filion, Y. (2010). Review of bioretention system research and design: past, present, and future. *Journal of Environmental Engineering*, 136(9), 878–889.

Sharkey, L. J. (2006). The performance of bioretention areas in North Carolina: A study of water quality, water quantity, and soil media. M.A.Sc Thesis, North Carolina State University, Raleigh, NC, USA.

Smith, D. I. (1980). Probability of storage overflow for stormwater management. M.A.Sc thesis, Department of Civil Engineering, University of Toronto, Toronto, ON, Canada.

Tholin, A. L., and Kiefer, C. J. (1960). The hydrology of urban runoff. *Trans. of ASCE*, 125, 1308–1379.

Trowsdale, S. A., and Simcock, R. (2011). Urban stormwater treatment using bioretention. *Journal of Hydrology*, 397(3-4), 167–174.

Yang, H., Florence, D. C., McCoy, E. L., Dick, W. A. and Grewal, P. S. (2009). Design and hydraulic characteristics of a field-scale bi-phasic bioretention rain garden system for storm water management. *Water Science & Technology*, 59(9), 1863–1872.

Zhang, S., and Guo Y. (2013). An analytical probabilistic model for evaluating the hydrologic performance of green roofs. *Journal of Hydrologic Engineering*, 18(1), 19–28.

# Chapter 4

## Stormwater Capture Efficiency of Bioretention Systems

**Shouhong Zhang and Yiping Guo**

**Abstract:** Bioretention systems are increasingly being used to control the adverse effects of urbanization on stormwater quantity and quality. The stormwater capture efficiency of a bioretention system, defined as the fraction of stormwater volume captured by the system, can be used as an important index of its stormwater management performance. In this paper, an analytical probabilistic expression (APE) is derived for estimating the long-term average stormwater capture efficiency of bioretention systems. The derivation is based on the probability distribution functions of the input rainfall event characteristics and the rainfall-runoff-overflow transformations occurring on a bioretention system and its contributing catchment. In the derivation, instead of simply adopting the Howard's conservative assumption as used in many previous studies, an approximate expected value of the surface depression water contents of a bioretention system at the end of a random rainfall event [denoted as $E(S_{dw})$] is derived and used. The accuracy of the resulting APE is verified by comparing its results with those determined from continuous simulations. The use of $E(S_{dw})$ is proven to be

advantageous than the use of the Howard's conservative assumption, it demonstrates that similar methods may be developed to analytically evaluate the stormwater management performance of other types of storage facilities for which the Howard's conservative assumption was employed previously.

**Key Words:** Urban Stormwater Management; Bioretention System; Stormwater Capture Efficiency; Analytical Probabilistic Approach; Howard's conservative assumption.

## 4.1 Introduction

Rapid urbanization has resulted in greater volumes and peaks of surface runoff (Sreeja and Gupta 2007; Misra 2011) and less evapotranspiration and groundwater recharge (Rose and Peters 2001; DeBusk et al. 2011). Water quality can also be influenced by urban development because of the changes of pollutants transport pathways, the decreases in water residence times and the introduction of new contaminant sources (Barron et al. 2013). These adverse effects associated with urbanization are common problems in urban stormwater management (Cheng et al. 2010). Bioretention systems are increasingly being used (Davis 2008; Denich and Bradford 2010; Trowsdale and Simcock 2011) as they have the potential to achieve many stormwater management objectives (Zhang and Guo 2013b). These objectives include controlling volumes and peaks of surface runoff (Davis et al. 2012; James and Dymond 2012), maintaining evapotranspiration and groundwater recharge (Li et al. 2009; Denich and Bradford 2010), and reducing pollution of water bodies (Kim et al. 2003; Hunt et al. 2008).

A bioretention system generally consists of a vegetated ponding area underlaid by a pervious media layer (Figure 4.1). The ponding area provides a storage space for stormwater and more time for the infiltration of captured stormwater. The vegetation planted in a bioretention system provides aesthetic and ecological values and also enhances the stormwater management

performance of the system (Aravena and Dussaillant 2009). The pervious media layer should be highly permeable to avoid overly-long standing of water on the surface of the bioretention system (Clar and Green 1993).

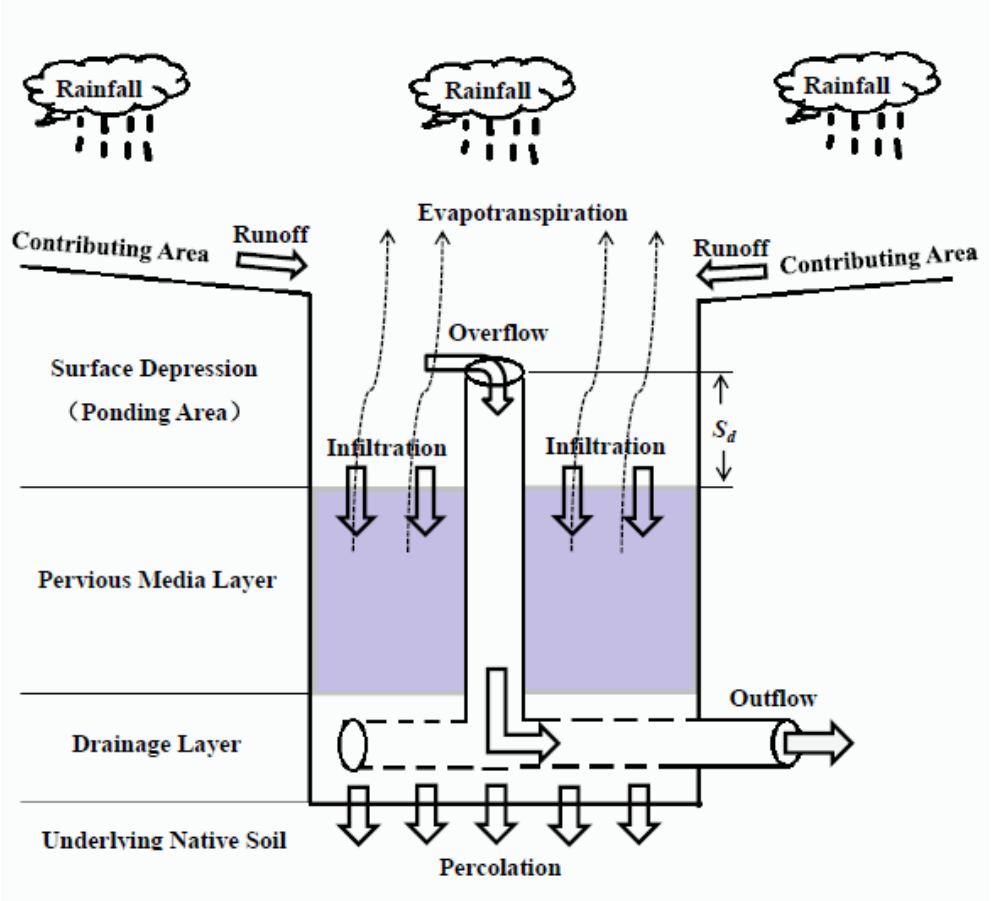


**Figure 4.1 A schematic diagram of bioretention systems and the associated flows**

Bioretention systems are often located right beside their contributing catchments. A fraction of the volumes of stormwater generated from the contributing catchment could be captured by its bioretention system, and the rest may bypass the system as overflow. As the captured stormwater is gradually infiltrated and evapotranspirated, most of the pollutants carried in it are adsorbed, filtered and accumulated in the bioretention system rather than

flow into the receiving water bodies. Thus, the stormwater capture efficiency of a bioretention system, defined as the fraction of stormwater volume captured by the system, demonstrates both its water quantity and quality control performances (Zhang and Guo 2013b). The stormwater capture efficiency of bioretention systems varies largely due to differences in design (Li et al. 2009; Davis et al. 2012) and climatic conditions (Muthanna et al. 2008; Emerson and Traver 2008). To guarantee that optimum bioretention systems are created, accurate and reliable methods are needed to estimate the stormwater capture efficiency of bioretention systems.

Extensive laboratory and field monitoring methods (e.g., Li et al. 2009; Davis et al. 2012) and many hydrologic models (e.g., Heasom et al. 2006; Aravena and Dussaillant 2009; He and Davis 2011) have been employed to evaluate the hydrologic performance of bioretention systems. Given the small spatial scale, it may not be justified to use continuous simulations with extensive data and time requirements for the majority of actual design cases. The analytical probabilistic approach (Eagleson 1972; Adams and Papa 2000) may be used as a computationally efficient alternative to continuous simulations and monitoring studies for estimating the long-term average hydrologic performance of bioretention systems. This approach has been employed to derive expressions which can be used to estimate the values of not only the volumes and peaks of runoff from small urban watersheds (e.g., Guo and Adams 1998a, 1998b) but also the performance indices of stormwater

management facilities (e.g., Guo and Adams 1999a, 1999b; Guo and Baetz 2007; Balistrocchi et al. 2009; Zhang and Guo 2013a).

In applying the analytical probabilistic approach to assess the efficiency of a stormwater management system involving a storage facility, it is important to obtain the storage facility's initial condition, e.g., the available stormwater storage capacity of the facility. Depending on the conditions preceding a random rainfall event, the storage facility may be completely or partly empty when the rainfall event starts. Theoretically, the stationary probability distribution of the available storage capacity of the facility at the beginning of a random rainfall event exists. However, previous studies (Smith 1980; Chen and Adams 2005) indicated that such a probability distribution cannot be obtained analytically. For simplification, two types of assumptions have been adopted in many previous studies. The first type assumes that the storage facility is completely full at the end of the rainfall event preceding the random rainfall event under analysis (e.g., Loganathan and Delleur 1984; Guo and Baetz 2007). This type of assumption was first adopted by Howard (1976) and could give rise to a conservative estimation of the performance of storage facilities. Therefore, it is referred to as the Howard's conservative assumption (Adams and Papa 2000). The other type assumes that the storage facility is completely empty when the analyzed random rainfall event starts (Bacchi et al. 2008; Balistrocchi et al. 2009).

Although these two types of assumptions could be justified and are acceptable for specific types of facilities operating under particular circumstances, they may result in systematic underestimations or overestimations of the performance of the facilities. Moreover, the inaccuracies caused by these assumptions could be aggravated in some unusual design cases, e.g., cases where the storage capacity of the facility is extremely large or extremely small.

Adopting the Howard's conservative assumption, Zhang and Guo (2013b) derived an analytical equation which can be used to estimate the stormwater capture efficiency of rain gardens. That analytical equation was derived for rain gardens receiving stormwater generated only from impervious areas such as building roofs and parking lots. Stormwater captured in the surface depression of rain gardens was assumed to infiltrate at a constant rate. The analytical equation derived in Zhang and Guo (2013b) is not suitable for bioretention systems receiving stormwater from catchments which are comprised of both pervious and impervious areas. The inaccuracy of that analytical equation may increase with the depth of the surface depressions due to the use of Howard's conservative assumption.

This study presents methods for derivation of a closed-form analytical probabilistic expression (APE) which can be used to evaluate the stormwater

capture efficiency of bioretention systems receiving stormwater from both pervious and impervious areas. In the derivation of this APE, the Horton infiltration equation is used to depict the infiltration processes. The magnitude and duration of the rainfall event preceding the analyzed random rainfall event are also taken into consideration for the purpose of deriving an approximate expected value of the water content of the bioretention system's surface depression at the end of the rainfall event preceding the analyzed random rainfall event [denoted as $\mathrm{E}(S_{dw})$]. Compared to the adoption of the Howard's conservative assumption, a more accurate estimation of the stormwater capture efficiency of bioretention system is achieved by using $\mathrm{E}(S_{dw})$.

## 4.2 Probabilistic Models of Rainfall

A rainfall series can be viewed as consisting of consecutive rainfall events and inter-event dry periods (Guo et al. 2012). The consecutive rainfall events are characterized by their volumes and durations. The rainfall volumes, rainfall durations and inter-event dry periods are generally assumed to be independent of each other and exponentially distributed (Adams et al. 1986; Balistrocchi et al. 2009). The exponential probability density functions (PDFs) can be expressed as

$$f(v) = \zeta \exp(-\zeta v), \qquad v \geq 0 \tag{4.1}$$

$$f(t) = \lambda \exp(-\lambda t), \qquad t \geq 0 \tag{4.2}$$

$$f(b) = \psi \exp(-\psi b), \qquad b \geq 0 \tag{4.3}$$

where $v$, $t$ and $b$ are the rainfall event volume, rainfall event duration and inter-event dry period, respectively; while $\zeta$, $\lambda$ and $\psi$ are the distribution parameters and their values can be estimated as the inverse of, respectively, the mean values of rainfall event volumes ($mm^{-1}$), duration ($h^{-1}$), and inter-event dry periods ($h^{-1}$).

The derivations in this study focus on a random rainfall event cycle including a $b$-hour dry period and a $t$-hour rainfall event with a volume of $v$ mm. Hereafter this rainfall event cycle and the rainfall event of this cycle are referred to as the current cycle and the current rainfall event (CRE), respectively. The rainfall event preceding the dry period of the current cycle is named as the previous rainfall event (PRE). In each cycle, $v$, $t$ and $b$ are assumed to be independent of each other. The potential limitations of this independent assumption are discussed in Adams and Papa (2000).

As an example, the 61-year (1945-2005) historical rainfall record of the Boston station in Boston, Massachusetts is used for testing the goodness-of-fit of the exponential PDFs and for verifying the APE derived in this study. An

inter-event time definition (IETD) of 6 h and a rainfall volume threshold of 3 mm are selected to separate consecutive rainfall events from the continuous rainfall record (Guo et al. 2012). The histograms and fitted exponential PDFs of *v*, *t* and *b* are compared in Figures 4.2–4.4, respectively. As shown in these figures, the exponential PDFs fit well with the observed histograms. The exponential distribution parameters were estimated to be $\zeta = 1/16.5$ $mm^{-1}$, $\lambda = 1/10.6$ $h^{-1}$ and $\psi = 1/135.0$ $h^{-1}$.

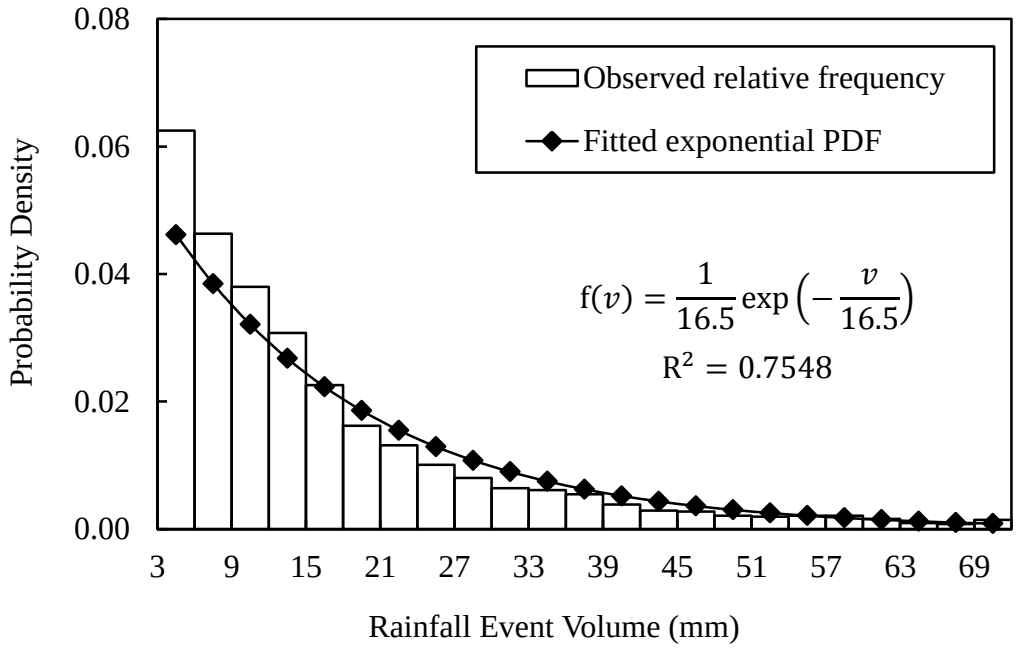


**Figure 4.2 Histogram and PDF of rainfall event volume at Boston**

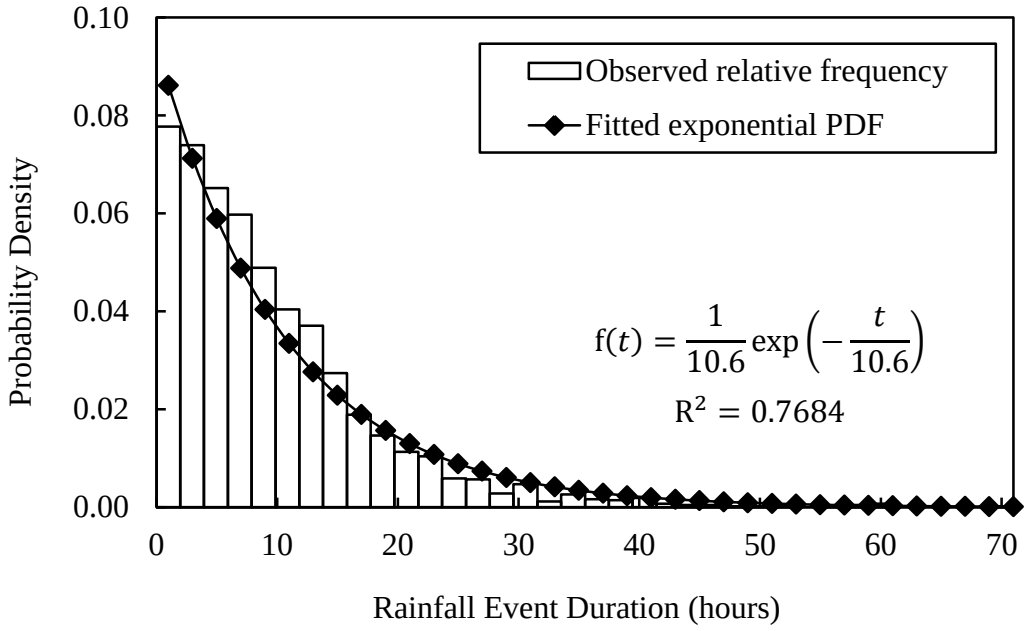


**Figure 4.3 Histogram and PDF of rainfall event duration at Boston**

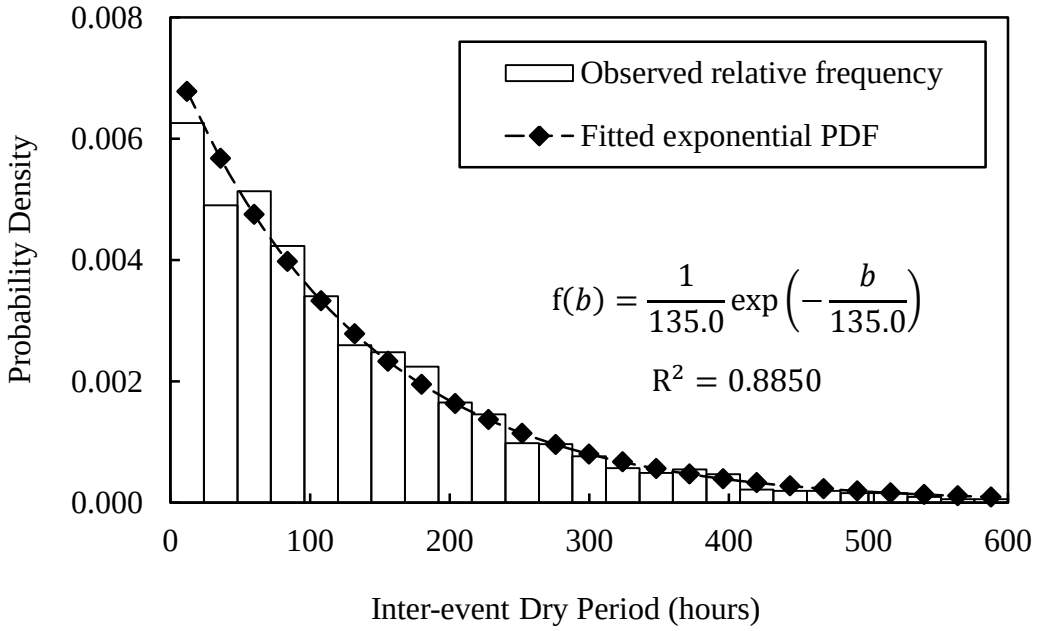


**Figure 4.4 Histogram and PDF of inter-event dry period at Boston**

## 4.3 Stormwater Capture Efficiency of Bioretention Systems

### 4.3.1 Water Balance Equation and Stormwater Capture Efficiency

The amount of stormwater captured by a bioretention system within the current cycle is controlled by the volumes of inflow, infiltration and evapotranspiration (ET) during the current cycle, and the available storage capacity of the system at the beginning of the CRE (Zhang and Guo 2013b). The rate of ET during a rainfall event is very small when it is compared to the high infiltration capacity of the fill media used for bioretention systems. Therefore, the volume of ET during a rainfall event may be negligible and the event-based water balance equation of a bioretention system can be expressed as:

$$v_o = v_i - F_t - R_c \tag{4.4}$$

In Equation (4.4), $v_i$ and $v_o$ are, respectively, the volumes of inflow into and overflow from the bioretention system during the CRE; $F_t$ is the volume of infiltration through the fill media layer of the bioretention system during the CRE; $R_c$ is the available storage or retention capacity of the bioretention system's surface depression when the CRE starts. All the terms in Equation (4.4) are expressed in mm of water over the bioretention system's surface area.

Using the derived probability distribution theory (Benjamin and Cornell

1970), the expected values of $v_i$ and $v_o$ per rainfall event can be derived. With these expected values, the long-term average stormwater capture efficiency of the bioretention system $C_e$ can be calculated as

$$C_e = \frac{\mathrm{E}(v_i) - \mathrm{E}(v_o)}{\mathrm{E}(v_i)} \tag{4.5}$$

where $\mathrm{E}(v_i)$ and $\mathrm{E}(v_o)$ are the expected values of $v_i$ and $v_o$ per rainfall event, respectively.

### 4.3.2 Volume of Inflow

When a rainfall event occurs on a bioretention system's contributing catchment, part of the rain water does not contribute to surface runoff due to initial losses caused by interceptions and depression storages. When these initial losses are satisfied, surface runoff begins. Due to further losses through infiltration, only part of the remaining rain water from the contributing catchment flows into the bioretention system as surface runoff. This conceptualization of the rainfall-runoff transformation is expressed as

$$v_r = \begin{cases} 0\,, & v \le S_{dc} \\ \phi(v - S_{dc})\,, & v > S_{dc} \end{cases} \tag{4.6}$$

where $v_r$ is the volume of surface runoff generated from the contributing catchment, expressed in mm of water over the catchment; $S_{dc}$ (in mm of

water over the catchment) and $\phi$ (dimensionless) are, respectively, the surface depression storage capacity and the runoff coefficient of the catchment.

As shown in Figure 4.1, the volume of stormwater entering a bioretention system consists of two parts, i.e., the volume of rain water directly falling on the system ($v$) and the volume of surface runoff generated from the contributing catchment ($v_r$). Given the area ratio *r* (dimensionless) between the contributing catchment and the bioretention system surface, the volume of stormwater entering a bioretention system (expressed in depth of water over the bioretention system's surface area itself) can be calculated as

$$v_i = v + rv_r = \begin{cases} v, & v \le S_{dc} \\ (r\phi + 1)v - r\phi S_{dc}, & v > S_{dc} \end{cases} \tag{4.7}$$

Based on the PDF of *v* and the functional relationship between $v_i$ and *v* as expressed respectively in Equations (4.1) and (4.7), the expected value of $v_i$ can be derived as

$$\mathrm{E}(v_i) = \int_0^\infty v_i \exp(-\zeta v)\, dv = \frac{\left[1 + r\phi \exp(-\zeta S_{dc})\right]}{\zeta} \tag{4.8}$$

### 4.3.3 Volume of Overflow

As shown in Equation (4.4), the volume of overflow $v_o$ is controlled by

$v_i$, $R_c$, and $F_t$. $v_i$ can be estimated using Equation (4.7). $R_c$ depends on (1) the amount of stormwater retained in the bioretention system's surface depression when the current cycle starts or the PRE ends (hereafter denoted as $S_{dw}$, in mm of water over the bioretention system's surface area); and (2) the infiltration & ET rates during the *b*-hour dry period. $F_t$ is determined by the CRE duration, the fill media's infiltration capacity, and the availability of stormwater for infiltration.

#### *4.3.3.1 Stormwater in the Surface Depression of a Bioretention System at the Start of the Current Cycle*

To estimate $R_c$, the value of $S_{dw}$ needs to be known. The value of $S_{dw}$ is dependent on many factors including the available storage capacity of the surface depression when the PRE starts, the magnitude and duration of the PRE and the fill media's infiltration capacity. As a result, the surface depression may be empty, partly empty, or full at the beginning of the current cycle (i.e., $0 \le S_{dw} \le S_d$, where $S_d$ is the design storage capacity of the surface depression of the bioretention system, which is in the same unit as $S_{dw}$). The expected value of $S_{dw}$ is needed in order to determine the expected value of $v_o$. The expected value of $S_{dw}$ exists but cannot be obtained through the analytical approaches (Chen and Adams 2005). Similar problems have also been encountered in many previous studies where a

storage facility that operates in a similar way as the surface depression of this study is involved (e.g., Howard 1976; Loganathan and Delleur 1984; Adams and Papa 2000; Chen and Adams 2005; Guo and Baetz 2007; Zhang and Guo 2013b). For simplification, it was assumed in these previous studies that the storage facility is full at the beginning of the current cycle (i.e., $S_{dw} = S_d$). The inaccuracy caused by this assumption will be aggravated when the capacity of the storage facility increases. To improve accuracy, the approximate expected value of $S_{dw}$ is derived here by taking into consideration the design storage capacity of the bioretention system, the infiltration capacity of the fill media and the magnitude and duration of the PRE.

Although rainfall events that occurred prior to the PRE all have an impact on $S_{dw}$, the value of $S_{dw}$ is mainly determined by the volumes of inflow and infiltration occurred during the PRE and the available storage capacity of the surface depression at the start of the PRE. To obtain an approximate expected value of $S_{dw}$, only the PRE is taken into consideration and two simplifying assumptions are made while analyzing processes associated with the PRE. The two assumptions are (1) the surface depression is empty when the PRE starts; and (2) infiltration takes place at a constant rate $f_c$ (i.e., the fill media's ultimate infiltration rate, in mm/h), whenever there is water held in the surface depression. For the majority of fill medium types, assumption (1)

may be justified because highly permeable fill media layer are usually used in bioretention systems to allow stormwater held in the surface depression to be drained out during average dry periods (Zhang and Guo 2013b). Assumption (2) may be justified since for materials with high permeability, the initially higher infiltration capacity of the material is relatively close to its ultimate infiltration capacity. Based on these two assumptions, $S_{dw}$ can be estimated as

$$S_{dw} = \begin{cases} 0, & v_{ip} \le f_c t_p \\ v_{ip} - f_c t_p, & f_c t_p < v_{ip} \le f_c t_p + S_d \\ S_d, & v_{ip} > f_c t_p + S_d \end{cases} \tag{4.9}$$

where $t_p$ (in h) is the duration of the PRE; $v_{ip}$ (in the same unit as $v_i$) is the volume of inflow entering the system resulting from the PRE.

The volume of inflow entering the bioretention system resulting from the PRE can be expressed in the same form of Equation (4.7) as

$$v_{ip} = \begin{cases} v_p, & v_p \le S_{dc} \\ (r\phi + 1)v_p - r\phi S_{dc}, & v_p > S_{dc} \end{cases} \tag{4.10}$$

where $v_p$ is the volume of the PRE, in mm.

Since a bioretention system is usually designed to capture stormwater runoff from its contributing catchment, there should be no standing water in the surface depression of the system when there is no runoff generated from

the contributing catchment. This is equivalent to say that when the volume of a rainfall event is less than $S_{dc}$, the bioretention system should be able to infiltrate all the rainwater that falls directly on the system, i.e., $S_{dc} \le f_c t_p$. However, it is worth to note that $S_{dc} \le f_c t_p$ may not be true for other types of stormwater management facilities from which the outflow rate is low and the surface depression storage of the contributing catchments ($S_{dc}$) is large. For simplification, $S_{dc} \le f_c t_p$ is assumed to be always true for bioretention systems in order to obtain an approximate expected value of $S_{dw}$. Incorporating this assumption, $S_{dw}$ can be expressed by substituting Equation (4.10) into Equation (4.9) as

$$S_{dw} = \begin{cases} 0, & v_p \le \dfrac{f_c t_p + r\phi S_{dc}}{r\phi + 1} \\ (r\phi + 1)v_p - r\phi S_{dc} - f_c t_p, & \dfrac{f_c t_p + r\phi S_{dc}}{r\phi + 1} < v_p \le \dfrac{f_c t_p + r\phi S_{dc} + S_d}{r\phi + 1} \\ S_d, & v_p > \dfrac{f_c t_p + r\phi S_{dc} + S_d}{r\phi + 1} \end{cases} \quad (4.11)$$

The volume and duration of the PRE (i.e., $v_p$ and $t_p$) also follow the same PDFs as shown in Equations (4.1) and (4.2), respectively. Given the PDFs of $v_p$ and $t_p$, the approximate expected value of $S_{dw}$ can be derived based on Equation (4.11) as

$$\begin{aligned} \mathrm{E}(S_{dw}) &= \int_{\frac{S_{dc}}{f_c}}^{\infty} \int_0^{\infty} S_{dw} \zeta \exp(-\zeta v_p) \lambda \exp(-\lambda t_p) dv_p dt_p \\ &= \frac{\lambda (r\phi + 1)^2}{\zeta [\lambda (r\phi + 1) + \zeta f_c]} \exp[-\frac{S_{dc}(\zeta f_c + \lambda)}{f_c}][1 - \exp(-\frac{\zeta S_d}{r\phi + 1})] \end{aligned} \quad (4.12)$$

In developing the probabilistic models, the value of $S_{dw}$ for all storm events is treated as a constant equaling $\mathrm{E}(S_{dw})$. This treatment of $S_{dw}$ is expected to improve the accuracy of the estimation of the long-term average volume of overflows as compared to other simplification methods.

#### *4.3.3.2 Available Retention Capacity of the Surface Depression at the Start of the Current Rainfall Event*

During the dry period of the current cycle, water retained in the surface depression [i.e., $\mathrm{E}(S_{dw})$ ] is depleted simultaneously through ET and infiltration. For most cases, the infiltration capacity shortly approaches the constant rate ( $f_c$ ) if there is sufficient amount of inflow (Guo and Adams 1998a). Thus, it is reasonable to assume that the fill media of the bioretention system, which receives a large amount of water from both the contributing catchment and the system itself, has an infiltration capacity equaling $f_c$ at the end of the PRE. Denoting the average ET rate as $E_a$ (in mm/h), the time needed to completely drain out the surface depression, $t_d$ (in h), can therefore be estimated as

$$t_d = \frac{\mathrm{E}(S_{dw})}{E_a + f_c} \tag{4.13}$$

Depending upon how long the dry period is, the available retention capacity of the surface depression of a bioretention system can be recovered to different levels when the CRE starts. In the cases in which the dry period is longer than the time needed to drain out water in the surface depression (i.e., $b > t_d$), the surface depression will be empty when the CRE starts. Thus, the design retention capacity of surface depression is 100% available (i.e., $R_c = S_d$). Otherwise $R_c$ varies depending on how much stormwater is held in the surface depression at the end of the PRE and how much of this stormwater is depleted during the *b*-hour dry period. In summary, $R_c$ can be expressed as:

$$R_c = \begin{cases} S_d - \mathrm{E}(S_{dw}) + (E_a + f_c)b, & b \le t_d \\ S_d, & b > t_d \end{cases} \tag{4.14}$$

#### *4.3.3.3 Volume of Infiltration through a Bioretention System during the Current Rainfall Event*

The volume of infiltration through the bioretention system during the CRE (i.e., $F_t$) can be calculated as the sum of two parts, i.e., volume of infiltrated water needed to wet the fill media layer and volume of water infiltrated at a constant rate ( $f_c$ ) during the CRE. The validity of the above two-part infiltration-loss notion can be illustrated by the Horton infiltration

equation (Guo and Adams 1998a). With sufficient inflow water, the maximum possible infiltration volume during the CRE $F_m$ can be calculated using the Horton infiltration equation as follows:

$$F_m = f_c t + \int_0^t (f_0 - f_c)\exp(-kT_p)dT_p = f_c t + \frac{(f_0 - f_c)}{k}[1-\exp(-kt)] \qquad (4.15)$$

In Equation (4.15), $T_p$ is the time elapsed since the CRE starts, in h; $f_0$ is the initial infiltration capacity when the CRE starts, in mm/h; *k* is the infiltration capacity decay coefficient, in $h^{-1}$.

The second term in Equation (4.15) represents the volume of infiltrated water needed to wet the fill media layer, denoted as $F_{iw}$, and is given as:

$$F_{iw} = \frac{(f_0 - f_c)}{k}[1-\exp(-kt)] \qquad (4.16)$$

As expressed in the Horton infiltration model, infiltration capacity of most soils decreases exponentially towards $f_c$. As a result, $F_{iw}$ would be satisfied within a short time after the rainfall event starts. It is therefore assumed that $F_{iw}$ must be satisfied before any overflow occurs for each rainfall event.

The value of $f_0$ in Equation (4.16) may change from storm to storm and is dependent on how much the fill media's infiltration capacity is regenerated during the dry period preceding the CRE. For the SWMM model,

Huber and Dickinson (1988) developed a procedure to estimate the regeneration of infiltration capacity during dry periods. The procedure is described using the following equation:

$$f_{Ts} = f_m - (f_m - f_c)\exp[-Rk(T_s - T_w)] \qquad (4.17)$$

In Equation (4.17), $T_s$ is the time at which the simulation starts, in h; $f_{T_s}$ is the infiltration capacity at time $T_s$, in mm/h; $f_m$ is the soil's maximum infiltration capacity, in mm/h; $T_w$ is a hypothetical projected time at which $f_{T_s}$ equals $f_c$ on the recovery curve, in h; and *R* is a constant ratio.

As mentioned previously, it is reasonable to assume that the fill media of the bioretention system has an infiltration capacity equaling its ultimate value $f_c$ at the end of a random rainfall event; and the ultimate value of the fill media's infiltration capacity will last until there is no stormwater retained in the surface depression. Taking $T_s$ as the time when the CRE begins, $f_{T_s}$ calculated in Equation (4.17) can be used as the $f_0$ in Equation (4.16). For cases in which the stormwater held in the surface depression is completely depleted within the *b*-hour dry period, $T_w$ in Equation (4.17) corresponds to the time when the ponding of water resulting from the PRE ends. Under this situation, $(T_s - T_w)$ in Equation (4.17) equals to $(b - t_d)$. For other cases where the water held in the surface depression is not completely depleted within the *b*-hour dry period, there is no time left for the regeneration of

infiltration capacity during the dry period. Under this situation, $(T_s - T_w)$ equals to zero. Therefore, $(T_s - T_w)$ can be expressed as:

$$T_s - T_w = \begin{cases} 0, & b \le t_d \\ b - t_d, & b > t_d \end{cases} \tag{4.18}$$

Substituting Equations (4.17) and (4.18) into Equation (4.16) and noting that $f_{T_s}$ is the $f_0$ for the CRE, $F_{iw}$ can be calculated as:

$$F_{iw} = \begin{cases} 0, & b \le t_d \\ \dfrac{(f_m - f_c)}{k}[1-\exp(-kt)]\{1-\exp[-Rk(b-t_d)]\}, & b > t_d \end{cases} \tag{4.19}$$

Based on the PDFs of $b$ and $t$ and the functional relationship as expressed in Equation (4.19), the expected value of $F_{iw}$, $\mathrm{E}(F_{iw})$, can be determined as follows:

$$\mathrm{E}(F_{iw}) = \int_0^\infty \int_0^\infty F_{iw} \psi \exp(-\psi b) \lambda \exp(-\lambda t) db dt = \frac{Rk(f_m - f_c)\exp(-\psi t_d)}{(\lambda + k)(\psi + Rk)} \tag{4.20}$$

The value of $F_{iw}$ for all storm events is treated as a constant equaling $\mathrm{E}(F_{iw})$. This may balance out the variations from event to event and simplifies the final result. The value of $F_t$ can then be estimated as:

$$F_t = f_c t + \frac{Rk(f_m - f_c)\exp(-\psi t_d)}{(\lambda + k)(\psi + Rk)} \tag{4.21}$$

### *4.3.3.4 Volume of Overflow per Rainfall Event*

Substituting Equations (4.7), (4.14) and (4.21) into Equation (4.4), the volume of overflow $v_o$ can finally be determined as

$$v_o = \begin{cases} 0, & (v \le S_{dc}) \text{ or} \\ & \left[ b \le t_d \text{ and } S_{dc} < v \le \dfrac{(r\phi S_{dc} + R_{c1} + F_t)}{r\phi + 1} \right] \text{ or} \\ & \left[ b > t_d \text{ and } S_{dc} < v \le \dfrac{(r\phi S_{dc} + S_d + F_t)}{r\phi + 1} \right] \\ (r\phi + 1)v - r\phi S_{dc} - R_{c1} - F_t, & \left[ b \le t_d \text{ and } v > \dfrac{(r\phi S_{dc} + R_{c1} + F_t)}{r\phi + 1} \right] \\ (r\phi + 1)v - r\phi S_{dc} - S_d - F_t, & \left[ b > t_d \text{ and } v > \dfrac{(r\phi S_{dc} + S_d + F_t)}{r\phi + 1} \right] \end{cases} \tag{4.22}$$

where $R_{c1} = S_d - \mathrm{E}(S_{dw}) + (E_a + f_c)b$, as shown in Equation (4.14).

Using the derived probability distribution theory, the expected value of $v_o$ can be derived on the basis of the rainfall-runoff-overflow transformations expressed in Equation (4.22) as

$$\begin{aligned} \mathrm{E}(v_o) &= \int_0^\infty \int_0^\infty \int_0^\infty v_o \zeta \exp(-\zeta v) \psi \exp(-\psi b) \lambda \exp(-\lambda t) dv db dt \\ &= \frac{(r\phi + 1)}{\zeta} C_1 C_3 [C_2 C_4 (1 - C_5) + \exp(-\psi t_d)] \end{aligned} \tag{4.23}$$

where $C_1$ through $C_5$ are all dimensionless constants introduced in order to simplify the expression for $\mathrm{E}(v_o)$. The values of these constants can be

determined as shown below when the design of the bioretention system, the characteristics of the contributing catchment, and the mean values of the local rainfall event characteristics are known.

$$C_1 = \frac{\lambda(r\phi+1)}{\lambda(r\phi+1)+\zeta f_c}$$

$$C_2 = \frac{\psi(r\phi+1)}{\psi(r\phi+1)+\zeta(E_a + f_c)}$$

$$C_3 = \exp\left\{-\frac{\zeta\left[r\phi S_{dc} + S_d + \mathrm{E}(F_{iw})\right]}{r\phi+1}\right\}$$

$$C_4 = \exp\left[\frac{\zeta \mathrm{E}(S_{dw})}{r\phi+1}\right]$$

$$C_5 = \exp\left[-\frac{\psi(r\phi+1)+\zeta(E_a + f_c)}{r\phi+1} t_d\right]$$

Knowing the expected values of the volumes of inflow and overflow per rainfall event [as shown in Equations (4.8) and (4.23), respectively], the long-term average stormwater capture efficiency of a bioretention system can be estimated according to Equation (4.5). The final result is,

$$C_e = 1 - \frac{(r\phi+1)C_1C_3[C_2C_4(1-C_5)+\exp(-\psi t_d)]}{\left[1+r\phi\exp(-\zeta S_{dc})\right]} \qquad (4.24)$$

The above explicit expression for $C_e$ is referred to as the APE (analytical

probabilistic expression). This APE provides an efficient means for estimating the long-term average stormwater capture efficiency of bioretention systems.

## 4.4 Comparison with Continuous Simulations

To prove the acceptability of the simplifying assumptions adopted in developing the rainfall-runoff-overflow transformations for a bioretention system and to illustrate the accuracy of the APE, results calculated using the APE are compared to those determined from continuous simulations. The SWMM 5 software (USEPA 2005), which does not need the same simplifying assumptions adopted in the derivation of the APE, was chosen for continuous simulations.

### 4.4.1 Development of Continuous Simulation Models

In a SWMM model, runoff from a subcatchment may drain to a node of a drainage network or another subcatchment (USEPA 2005). A bioretention system can therefore be modeled as a subcatchment (hereafter referred to as Subcatchment A representing the bioretention system itself) which receives rain water directly falling onto it and the surface runoff generated from a larger contributing subcatchment (hereafter referred to as Subcatchment B). Subcatchment A has a large surface depression storage and a highly permeable

soil layer, which are characteristics of bioretention systems. A subcatchment in a SWMM model is an area of land which is divided into impervious and pervious subareas using the parameter known as imperviousness ( $h$ , dimensionless). The impervious subarea of a subcatchment is characterized by only its surface depression storage ( $S_{di}$, in mm) and has no infiltration or any other losses. For the pervious subarea, surface water can be captured by its surface depression storage ( $S_{dp}$, in mm) and can also infiltrate into the soil zone.

The Horton Model was selected to simulate the infiltration processes on pervious subareas in the continuous simulations because it was also used in the derivation of the APE. The parameters required for the infiltration simulation are the maximum infiltration rate ( $f_m$ ), the minimum infiltration rate ( $f_c$ ), the infiltration capacity decay coefficient ( $k$ ) and the drying time ( $D$, in days). The drying time is used in infiltration capacity recovery calculations.

Subcatchment A, which represents a bioretention system, consists of highly permeable soil layers and contains no impervious subareas, i.e., $h = 0$. The surface depression storages of bioretention systems commonly range from 150 to 520 mm (Davis et al. 2012). To cover all the possibilities, the surface depression storage on the pervious subarea of Subcatchment A was changed from 100 to 600 mm in this research. The infiltration parameters ( $f_m$, $f_c$,

$k$, and $D$) of Subcatchment A can all be determined for each type of fill media selected for a bioretention system.

For Subcatchment B, which represents the contributing catchment, $h$ can change from 0 to 1 according to the degree of urbanization of the catchment. The surface depression storages on impervious subareas are usually smaller than 3 mm (ASCE 2012). The depths of surface depression storage of pervious subareas may range from zero to several millimeters. The infiltration parameters ( $f_m$, $f_c$, $k$, and $D$) of Subcatchment B can all be determined for a specific type of soil. Area ratios ($r$) between the contributing catchment's area and the bioretention system's surface area usually range from 5 to 45 (Davis et al. 2009). Accordingly, with the area of Subcatchment B fixed at 0.4 ha, the areas of Subcatchment A were changed from 0.008 to 0.08 ha in this research to represent all possibilities.

Using a long period of rainfall record as input to a SWMM model, the total volumes of runoff generated from both Subcatchments A and B over the period can be obtained from continuous simulations. When the total volumes of rainfall and runoff are obtained, the long-term average stormwater capture efficiency of Subcatchment A, which represents a bioretention system in the continuous simulations, can be calculated as

$$C_{eSWMM} = \frac{V_{rain} + V_{runoffB} - V_{runoffA}}{V_{rain} + V_{runoffB}} \quad (4.25)$$

where $V_{rain}$ is the total volume of rainfall; $V_{runoffA}$ and $V_{runoffB}$ are the total volumes of runoff from Subcatchments A and B, respectively. With the units of all these three terms converted to mm of water over the area of Subcatchment A, $(V_{rain} + V_{runoffB})$ and $V_{runoffA}$ in Equation (4.25) represent, respectively, the inflow to and overflow from the simulated bioretention system.

### 4.4.2 Relationship between APE and SWMM Input Parameters

The parameters required by the APE and the SWMM models are not identical because of their differences in representing the rainfall-runoff-overflow transformations of bioretention systems. To ensure that a specific bioretention system as represented by the APE is the same as that simulated by a SWMM model, parameter values for the bioretention system and the contributing catchment should be the same or properly related.

In deriving the APE, the volume of rainfall is transformed into volume of runoff from the contributing catchment of a bioretention system by two parameters (i.e., $S_{dc}$ and $\phi$). Having the imperviousness ($h$) of a contributing catchment and the surface depression storages of its impervious

and pervious subareas (i.e., $S_{di}$ and $S_{dp}$, respectively) input to the SWMM model, the surface depression depth ($S_{dc}$) of the contributing catchment required by the APE can be estimated using the area-weighted average method:

$$S_{dc} = hS_{di} + (1-h)S_{dp} \tag{4.26}$$

The value of $\phi$ can also be expressed using the catchment parameters of the SWMM model. Based on the relationship between $v_r$ and $v$ as described in Equation (4.6), the expected value of $v_r$ can be determined as

$$\mathrm{E}(v_r) = \int_0^\infty v_r \zeta \exp(-\zeta v) dv = \frac{\phi}{\zeta} \exp(-\zeta S_{dc}) \tag{4.27}$$

To ensure that a contributing catchment simulated by a SWMM model and that represented by the corresponding APE are largely the same, the volumes of runoff estimated using Equation (4.27) and that determined from SWMM simulation should be the same. Taking into account almost the same rainfall-runoff generation processes as modeled by a SWMM model using the Horton infiltration equation, Guo and Adams (1998a) developed an analytical equation to estimate the expected runoff event volume from a catchment. This analytical equation is expressed as

$$\mathrm{E}(v_r)_g = \frac{h}{\zeta}\exp(-\zeta S_{di}) + \frac{\lambda(1-h)}{\zeta(\zeta f_c + \lambda)}\exp\{-\zeta[S_{dp} + \frac{(f_m - f_c)Rk}{(k+\lambda)(\psi + Rk)}]\} \quad (4.28)$$

where $\mathrm{E}(v_r)_g$ is the expected value of runoff event volume generated from a catchment. According to Huber and Dickinson (1988), $R$ can be expressed as a function of $D$ and $k$ and it can be calculated as

$$R = -\frac{\ln(0.02)}{24Dk} \quad (4.29)$$

Since Equation (4.28) has been demonstrated to be able to provide long-term average runoff event volumes close to those determined from SWMM simulations, it is used to estimate the equivalent value of $\phi$ by letting $\mathrm{E}(v_r) = \mathrm{E}(v_r)_g$. As a result, $\phi$ can be estimated as

$$\phi = h\exp[\zeta(1-h)(S_{dp} - S_{di})] + \frac{\lambda(1-h)}{\zeta f_c + \lambda}\exp\{-\zeta[\frac{0.16\times(f_m - f_c)}{(k+\lambda)(D\psi + 0.16)} + h(S_{dp} - S_{di})]\} \quad (4.30)$$

In the derivation of the APE, the rainfall-runoff-overflow transformations of bioretention systems are described using the parameters such as the area ratio ($r$), the surface depression depth ($S_d$) and the Horton infiltration parameters. According to its definition, $r$ equals the ratio between the areas of Subcatchments B and A in the continuous SWMM simulations. The $S_d$ used in the APE is equivalent to the $S_{dp}$ of Subcatchment A in the corresponding SWMM model. The Horton infiltration parameters required

by the APE are all the same as those in the SWMM model. The parameters $R$ needed for the APE is expressed in Equation (4.29).

It can be seen from the previous descriptions that some of the input parameters for the continuous SWMM simulations are the same as those used in the APE and others are closely related. Establishment of their relationships based on their definitions ensures that an APE-represented bioretention system is physically the same as that modeled by the corresponding SWMM model. Comparison of results from the two different approaches can therefore be used to verify the simplifying assumptions made in the derivation of the APE.

### 4.4.3 Comparison of SWMM and APE Results

The 61-year historical rainfall record of the Boston station analyzed in Section 2 was used in the SWMM simulations. Four area ratios (10, 20, 30 and 40), two types of fill media (sand and sandy loam), and surface depression depths changing from 100 to 600 mm were evaluated in the simulations. These bioretention systems receive stormwater from the contributing catchments with different types of soils (sand, silt, and clay) and different levels of imperviousness. The simulated imperviousness levels (30%, 50%, and 70%) represent different degrees of urbanization. The input parameter values for the bioretention systems and the contributing catchments are listed,

respectively, in Tables 4.1 and 4.2. The APE input parameter values, as shown in the tables, are either the same as the corresponding SWMM input parameter values or calculated using Equations (4.26), (4.29), or (4.30) according to the related SWMM input parameter values.

Stormwater capture efficiencies calculated using the APE for all the possible combinations of bioretention systems (listed in Table 4.1) and contributing catchments (listed in Table 4.2) are compared to those determined from the corresponding continuous simulations. Typical comparisons are summarized in Figures 4.5–4.7. As shown in Figures 4.5–4.7, both the APE and the continuous simulations illustrate that the stormwater capture efficiency of a bioretention system decreases as $h$ and $r$ increase. This is because higher imperviousness of the contributing catchment and larger area ratio can generate more surface runoff into a bioretention system with a fixed capacity.

The differences between the stormwater capture efficiencies calculated using the two approaches are smaller than 7% for all the possible combinations of cases listed in Tables 4.1 and 4.2. To save space, not all of these cases are included in Figures 4.5–4.7. This close agreement verifies that the simplifying assumptions adopted in establishing the event-based transformation of rainfall-runoff-overflow which is employed in the derivation of the APE are acceptable.

**Table 4.1 Input parameters of bioretention systems**

| Models | SWMM | | APE | |
|---|---|---|---|---|
| Fill Media | Sand | Sandy Loam | Sand | Sandy Loam |
| $r$ (unitless) | 5-45 | 5-45 | 5-45 | 5-45 |
| $S_d$ (mm) | 100-600 | 100-600 | 100-600 | 100-600 |
| $E_a$ (mm/h) | 0.11 | 0.11 | 0.11 | 0.11 |
| $f_m$ (mm/h) | 127.0 | 101.9 | 127.0 | 101.9 |
| $f_c$ (mm/h) | 36.0 | 10.9 | 36.0 | 10.9 |
| $K$ (1/h) | 3.0 | 4.0 | 3.0 | 4.0 |
| $R$ (fraction) | N/N* | N/N* | 0.014 | 0.005 |
| $D$ (day) | 4.0 | 7.8 | N/N* | N/N* |

* Not needed

**Table 4.2 Input parameters of contributing catchments**

| Soil Type | SWMM | | | | | | | APE | |
|---|---|---|---|---|---|---|---|---|---|
| | $h$ (%) | $S_{dp}$ (mm) | $S_{di}$ (mm) | $f_m$ (mm/h) | $f_c$ (mm/h) | $k$ (1/h) | $D$ (day) | $S_{dc}$ (mm) | $\phi$ |
| Sand | 30 | 3 | 2 | 127.0 | 36.00 | 3.0 | 4 | 2.7 | 0.320 |
| | 50 | 3 | 2 | 127.0 | 36.00 | 3.0 | 4 | 2.5 | 0.520 |
| | 70 | 3 | 2 | 127.0 | 36.00 | 3.0 | 4 | 2.3 | 0.715 |
| Silt | 30 | 3 | 2 | 76.2 | 3.60 | 4.5 | 8 | 2.7 | 0.416 |
| | 50 | 3 | 2 | 76.2 | 3.60 | 4.5 | 8 | 2.5 | 0.588 |
| | 70 | 3 | 2 | 76.2 | 3.60 | 4.5 | 8 | 2.3 | 0.756 |
| Clay | 30 | 3 | 2 | 25.4 | 0.36 | 6.0 | 12 | 2.7 | 0.788 |
| | 50 | 3 | 2 | 25.4 | 0.36 | 6.0 | 12 | 2.5 | 0.851 |
| | 70 | 3 | 2 | 25.4 | 0.36 | 6.0 | 12 | 2.3 | 0.912 |

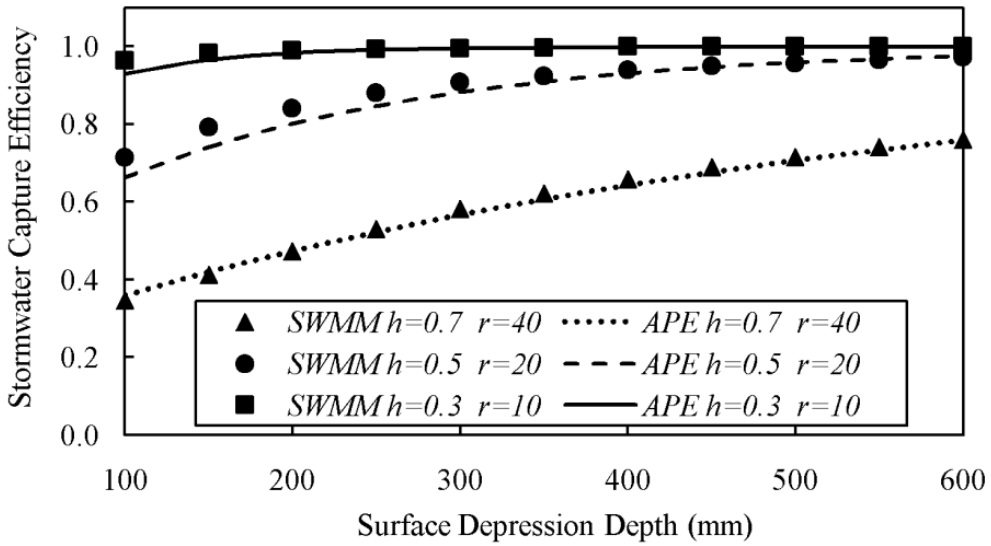


**Figure 4.5 Comparison of the APE and SWMM results (contributing catchment soil type: sand; bioretention system fill media: sandy loam)**

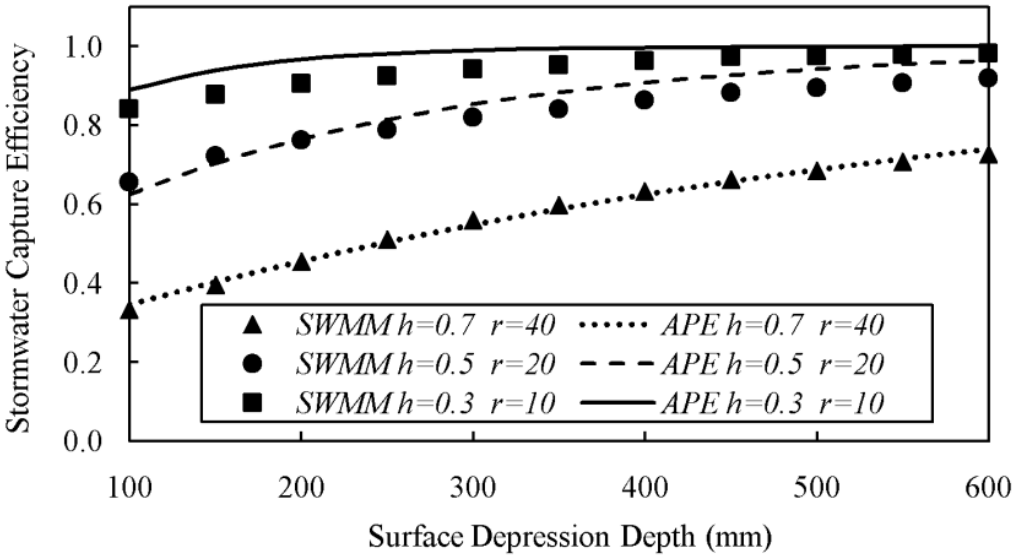


**Figure 4.6 Comparison of the APE and SWMM results (contributing catchment soil type: silt; bioretention system fill media: sandy loam)**

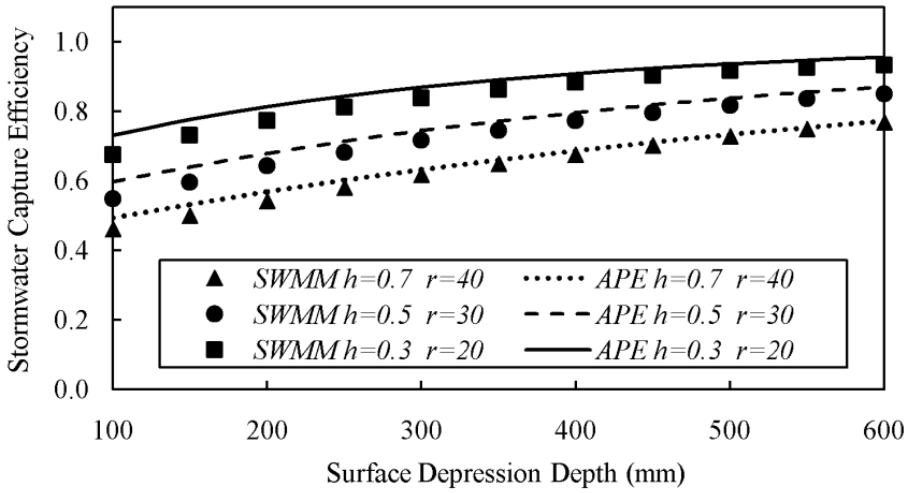


**Figure 4.7 Comparison of the APE and SWMM results (contributing catchment soil type: clay; bioretention system fill media: sand)**

## 4.5 Discussion

As mentioned in Section 4.3.3.1, in deriving the analytical equation to assess the efficiency of a stormwater storage facility, simplifying assumptions about the initial state of the facility had to be made in previous studies (e.g., Loganathan and Delleur 1984; Chen and Adams 2005; Balistrocchi et al. 2009; Zhang and Guo 2013b). One of the widely used assumptions is referred to as the Howard's conservative assumption. Howard (1976) analyzed the problem of runoff diverted to a storage reservoir and assumed that the reservoir is full at the end of the rainfall event preceding the analyzed random rainfall event. This assumption usually results in underestimations of the capture efficiency of storage facilities. Moreover, the inaccuracy caused by this assumption may be aggravated when the storage capacity of the facility

increases significantly and the outflow rate from the facility becomes disproportionally small.

Smith (1980) extended the Howard's method (Howard 1976) by solving for the steady-state PDFs of the water levels of the storage facility at the end of the rainfall event preceding the analyzed random rainfall event. This work eliminated the need for the Howard's conservative assumption but required a numerical solution procedure (Adams and Papa 2000). Although more accurate results could be obtained from the Smith (1980) method, the numerical procedure required in the analysis limited its practical application. For simplification, the Howard's conservative assumption was still employed by many other researchers to evaluate the performance of stormwater management facilities.

Rather than following the Smith (1980) method, what we did in Section 4.3.3.1 is the derivation of an analytical expression which provides an approximate expected value of the water contents of a storage facility at the end of the rainfall event preceding the analyzed random rainfall event. The approximate expected value is then used as the initial condition of the analyzed random rainfall cycle. This method not only retains the calculation efficiency of the analytical probabilistic approach, but also alleviates the inaccuracy problems associated with the Howard's conservative assumption.

The approximate expected value of the water contents in a bioretention system's surface depression at the end of the PRE [i.e., $E(S_{dw})$ ] was employed in the estimation of $C_e$ of bioretention systems. The $C_e$ calculated using the APE derived incorporating $E(S_{dw})$ and the $C_e$ estimated using the analytical probabilistic expression derived based on the Howard's conservative assumption (referred to as the APEH) are both compared to those determined from continuous simulations. The comparisons illustrated in Figures 4.8 and 4.9 show that, for almost all cases, the $C_e$ calculated using the APE is closer than the $C_e$ calculated using the APEH to that determined by the SWMM simulations. Moreover, it can be seen from Figures 4.8 and 4.9 that, as $S_d$ increases or as the fill medium becomes less permeable (from sand to sandy loam) the difference between the $C_e$ calculated using the APEH and the $C_e$ obtained from the SWMM simulations generally increases, whereas the results from the APE do not show these trends.

The surface depression depth and the infiltration rate of the fill media layer of a bioretention system are equivalent to, respectively, the storage capacity and the outflow rate of a general stormwater management system. The comparisons (Figures 4.8 and 4.9) therefore illustrate the shortcomings of the Howard's conservative assumption, i.e., increased inaccuracies with larger storage capacity and smaller outflow rate. These results demonstrate that the

approach taken in this study is viable and advantageous. Since the basic hydrologic operation of a bioretention system is similar to that of many other types of storage facilities used in stormwater management, the method developed in this study is worthy of further investigation and may also be employed in evaluating the performance of other types of stormwater storage facilities.

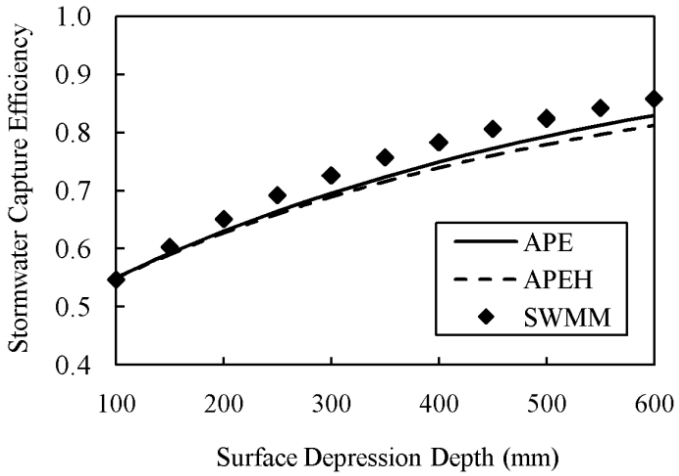


**Figure 4.8 Comparison of the APE, APEH and SWMM results ($h = 1.0$, $r = 30$, bioretention system fill media: sand)**

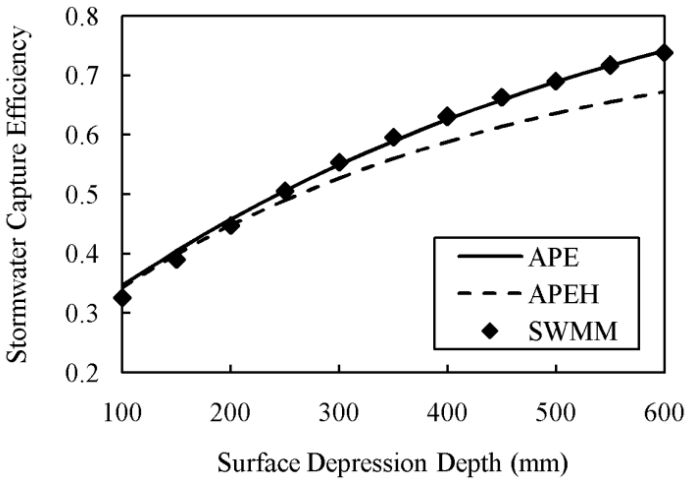


**Figure 4.9 Comparison of the APE, APEH and SWMM results ($h = 1.0$, $r = 30$, bioretention system fill media: sandy loam)**

## 4.6 Summary and Conclusions

The ratio or percentage of stormwater captured by a bioretention system is referred to as its stormwater capture efficiency ($C_e$). The value of $C_e$ can be used as an important metric of the stormwater management performance of a bioretention system. To calculate the long-term average $C_e$ of bioretention systems, an analytical probabilistic expression (APE) is derived in this study. The derivation is based on the exponential probabilistic models characterizing local rainfall conditions and the mathematical representations depicting the hydrologic processes occurring on a bioretention system and its contributing catchment. The mathematical manipulations required in the derivation process are quite complex, but the end result is an easy-to-use and mathematically closed-form expression requiring few input parameters.

A suite of SWMM models of hypothetical bioretention systems were developed. Continuous simulations were conducted for these bioretention systems with different types of fill media, different area ratios and various surface depression depths. These bioretention systems were assumed to receive stormwater from contributing catchments with different levels of imperviousness and various soil types. The long-term average $C_e$ of bioretention systems determined by continuous simulation results were

compared to those calculated using the APE. In these comparisons, the input parameter values required by the APE are either the same as those input to the corresponding SWMM model or calculated from the related SWMM model input parameters based on physical grounds. Close agreement between the APE and SWMM simulation results demonstrates the accuracy of the APE in calculating the $C_e$ of bioretention systems.

The APE derived in this study provides an efficient means which can be used to assist in the hydrologic design of bioretention systems for preliminary design purposes. The approximate expected value of water contents in a bioretention system's surface depression at the end of a rainfall event was derived and used in deriving the APE. More accurate estimations of $C_e$ were achieved by using this approximate expected value than by employing the Howard's conservative assumption. Similar methods may be developed to evaluate the performance of other types of stormwater storage facilities for which the Howard's conservative assumption was previously employed.

**ACKNOWLEDGEMENTS:** This work was supported by the Natural Sciences and Engineering Research Council (NSERC) of Canada and the China Scholarship Council (CSC).

## References

Adams, B. J., Fraser, H. G., Howard, C. D. D., and Hanafy, M. S. (1986). Meteorologic data analysis for drainage system design. *Journal of Environmental Engineering*, ASCE, 112(5), 827–848.

Adams, B. J. and Papa, F. (2000). *Urban Stormwater Management Planning with Analytical Probabilistic Models*, John Wiley & Sons, Inc., New York, USA.

American Society of Civil Engineers (ASCE). (2012). *Design of Urban Stormwater Controls*, *Manuals of Practice* (MOP) 87, McGraw-Hill Inc., New York, USA.

Aravena, J. E., and Dussaillant, A. (2009). Storm-water infiltration and focused recharge modeling with finite-volume two-dimensional Richards Equation: application to an experimental rain garden. *Journal of Hydraulic Engineering*, 135(12), 1073–1080.

Bacchi, B., Balistrocchi, M., and Grossi, G. (2008). Proposal of a semi-probabilistic approach for storage facility design. *Urban Water Journal*, 5(3), 195–208.

Balistrocchi, M., Grossi, G., and Bacchi, B. (2009). An analytical probabilistic model of the quality efficiency of a sewer tank. *Water Resources Research*, 45, W12420, doi:10.1029/2009WR007822.

Barron, O. V., Donn, M. J., Barr, A. D. (2013). Urbanisation and shallow groundwater: predicting changes in catchment hydrological responses. *Water Resources Management,* 27, 95–115. doi:10.1007/s11269-012-

0168-0.

Benjamin, J. R., and Cornell, C. A. (1970). *Probability, Statistics and Decision for Civil Engineers*, McGraw-Hill, New York, USA.

Chen, J., and Adams, B. J. (2005). Analysis of storage facilities for urban stormwater quantity control. *Advances in Water Resources*, 28, 377–392.

Cheng, S. J., Lee, C. F., and Lee, J. H. (2010). Effects of urbanization factors on model parameters. *Water Resources Management* 24(4),775–794.

Clar, M. L., and Green, R. (1993). *Design manual for use of bioretention in stormwater management*, Dept. of Environmental Resources, Prince George's County, USA.

Davis, A. P. (2008). Field performance of bioretention: Hydrology impact. *Journal of Hydrologic Engineering*, 13(2), 90–95.

Davis, A. P., Hunt, W. F., Traver, R. G., and Clar, M. (2009). Bioretention technology: overview of current practice and future needs. *Journal of Environmental Engineering*, 135(3), 109–117.

Davis, A. P., Traver, R. G., Hunt, W. F., Lee, R., Brown, R. A., and Olszewski, J. O. (2012). Hydrologic performance of bioretention storm-water control measures. *Journal of Hydrologic Engineering*, 17(5), 604–614.

DeBusk, K. M., Hunt, W. F., and Line, D. E. (2011). Bioretention outflow: does it mimic nonurban watershed shallow interflow? *Journal of Hydrologic Engineering*, 16(3), 274–279.

Denich, C., and Bradford, A. (2010). Estimation of evapotranspiration from

bioretention areas using weighing lysimeters. *Journal of Hydrologic Engineering*, 15(6), 522-530.

Eagleson, P. S. (1972). Dynamics of flood frequency. *Water Resources Research*, 8(4), 878–898.

Emerson, C. H., and Traver, R. G. (2008). Multi-year and seasonal variation of infiltration from stormwater best management practices. *Journal of Irrigation and Drainage Engineering*, 134(5), 598–605.

Guo, Y., and Adams, B. J. (1998a). Hydrologic analysis of urban catchments with event-based probabilistic models. Part I: Runoff volume. *Water Resources Research*, 34(12), 3421–3431.

Guo, Y., and Adams, B. J. (1998b). Hydrologic analysis of urban catchments with event-based probabilistic models. Part II: Peak discharge rate. *Water Resources Research*, 34(12), 3433–3443.

Guo, Y., and Adams, B. J. (1999a). Analysis of detention ponds for storm water quality control. *Water Resources Research*, 35(8), 2447–2456.

Guo, Y., and Adams, B. J. (1999b). An analytical probabilistic approach to sizing flood control detention facilities. *Water Resources Research*, 35(8), 2457–2468.

Guo, Y., and Baetz, B. W. (2007). Sizing of rainwater storage units for green building applications. *Journal of Hydrologic Engineering*, 12(2), 197–205.

Guo, Y., Liu, S., and Baetz, B. W. (2012). Probabilistic rainfall-runoff transformation considering both infiltration and saturation excess runoff

generation processes. *Water Resources Research*, 48: W06513. doi:10.1029/2011WR011613

He, Z., and Davis, A. P. (2011). Process modeling of storm-water flow in a bioretention cell. *Journal of Irrigation and Drainage Engineering*, 137(3), 121–131.

Heasom, W., Traver, R., and Welker, A. (2006). Hydrologic modeling of a bioinfiltration best management practice. *Journal of the American Water Resources Association*, 42(5), 1329–1347.

Howard, C. D. D. (1976). Theory of storage and treatment plant overflows. *Journal of the Environmental Engineering Division*, ASCE, 102(EE4), 709–722.

Huber, W. C., and Dickinson, R. E. (1988). *Stormwater Management Model, Version 4: User's Manual*. U.S. Environmental Protection Agency, Washington, D.C., USA.

Hunt, W. F., Smith, J. T., Jadlocki, S. J., Hathaway, J. M., and Eubanks, P. R. (2008). Pollutant removal and peak flow mitigation by a bioretention cell in urban Charlotte, NC. *Journal of Environmental Engineering*, 134(5), 403–408.

James, M. and Dymond, R. (2012). Bioretention hydrologic performance in an urban stormwater network. *Journal of Hydrologic Engineering*, 17(3), 431–436.

Kim, H., Seagren, E. A., and Davis, A. P. (2003). Engineered bioretention for removal of nitrate from stormwater runoff. *Water Environment Research*,

75(4), 355–367.

Li, H., Sharkey, L. J., Hunt, W. F., and Davis, A. P. (2009). Mitigation of impervious surface hydrology using bioretention in North Carolina and Maryland. *Journal of Hydrologic Engineering*, 14(4), 407–415.

Loganathan, G. V., and Delleur, J. W. (1984). Effects of urbanization on frequencies of overflows and pollutant loadings from storm sewer overflows: A derived distribution approach. *Water Resources Research*, 20(7), 857–865.

Misra, A. K. (2011). Impact of urbanization on the hydrology of Ganga Basin (India). *Water Resources Management*, 25(2), 705–719.

Muthanna, T. M., Viklander, M. and Thorolfsson, S. T. (2008). Seasonal climatic effects on the hydrology of a rain garden. *Hydrological Processes*, 22, 1640–1649.

Rose, S., and Peters, N. E. (2001). Effects of urbanization on streamflow in the Atlanta area (Georgia, USA): a comparative hydrological approach. *Hydrological Processes*, 15(8),1441–1457.

Smith, D. I. (1980). Probability of storage overflow for stormwater management. M.A.Sc thesis, Department of Civil Engineering, University of Toronto, Toronto, ON, Canada.

Sreeja, P., and Gupta, K. (2007). An alternate approach for transient flow modeling in urban drainage systems. *Water Resources Management*, 21, 1225–1244.

Trowsdale, S. A., and Simcock, R. (2011). Urban stormwater treatment using

bioretention. *Journal of Hydrology*, 397, 167–174.

U.S. Environmental Protection Agency (USEPA). (2005). Stormwater management model user's manual, Version 5.0, Rep. EPA/600/R-05/040. Off. of Res. and Dev., Cincinnati, Ohio

Zhang, S., and Guo Y. (2013a). An analytical probabilistic model for evaluating the hydrologic performance of green roofs. *Journal of Hydrologic Engineering*, 18(1), 19–28.

Zhang, S., and Guo, Y. (2013b). An explicit equation for estimating the stormwater capture efficiency of rain gardens. *Journal of Hydrologic Engineering*, 18(12), 1739-1748.

# Chapter 5

# An Analytical Equation for Evaluating the Stormwater Volume Control Performance of Permeable Pavement Systems

**Shouhong Zhang and Yiping Guo**

**Abstract:** Permeable pavement systems have been increasingly used for on-site stormwater management. In this study, an analytical equation is derived for calculating the long-term average stormwater capture efficiency of permeable pavement systems. This analytical equation is obtained by using the derived probability distribution theory on the basis of the probabilistic models of rainfall event characteristics and the mathematical representations of the hydrologic processes occurring in permeable pavement systems. Simplifying assumptions are made in establishing these mathematical representations. The validity of these assumptions and the accuracy of the analytical equation are demonstrated by comparing the analytical equation results with those determined from a series of continuous simulations.

**Key Words:** Permeable pavement system; Stormwater management; Stormwater capture efficiency; Probabilistic methods.

## 5.1 Introduction

The presence and creation of impervious surfaces in urban and urbanizing areas commonly lead to disrupted natural hydrological processes resulting in increased surface runoff and peak flow and decreased base flow and ground water recharge. Problems such as flooding, stream bank erosion, and degradation of aquatic habitats associated with urbanization have been recognized for decades (Hammer 1972; Hollis 1975; Booth and Jackson 1997). The reduction of the water-retaining capacity of the soil reservoirs underneath impervious urban landscapes is the fundamental cause of nearly all these problems (Booth and Leavitt 1999). Traditional efforts to address these problems focused on the use of structural devices (e.g., detention ponds) to partly mimic the functions of soil reservoirs. However, many of the structural techniques are designed solely to avoid downstream flooding and therefore rarely incorporate features that promote on-site infiltration (Dreelin et al. 2006). Compared to the native soil reservoirs, these structural techniques are reported to be ineffective in many aspects due to the limitations in construction, operation and maintenance (Booth and Leavitt 1999; Kwiatkowski et al. 2007).

Permeable pavements, which allow stormwater to infiltrate through the pavements and partly preserve the functions of soil reservoirs, have been

increasingly used for on-site stormwater control (Pratt et al. 1989; USEPA 1999; Brattebo and Booth 2003; Sansalone et al. 2012). The use of permeable pavements reflects an effort to change the apparently inevitable relationship between urbanization and increased impervious surface areas (Booth and Leavitt 1999). Numerous studies have shown that permeable pavements can reduce surface runoff volumes as well as peak flows (Dreelin et al. 2006; Bean et al. 2007a; Collins et al. 2008; Ball and Rankin 2010), maintain base flows and ground water recharge (USEPA 1999; Bean et al. 2007b), and improve stormwater quality (Pratt et al. 1995; Sansalone and Buchberger 1995; Rushton 2001; Fassman and Blackbourn 2011). In addition to their stormwater management benefits, permeable pavements can also assist in improving the safety for vehicular traffic because of reduced splash and spray, better visibility, and better traction (Berbee et al. 1999; Barrett et al. 2006) under precipitation conditions. Using as an alternative to impermeable asphalt and concrete surfaces, permeable pavements are particularly useful in high density urban areas because they do not consume any additional urban lands.

A permeable pavement system is a structural Low Impact Development (LID) practice which generally consists of a permeable pavement layer underlain by a stone reservoir (USEPA 1999; PDEP 2006; NCDWQ 2007; CVC and TRCA 2010). The surface pavement layer may be comprised of

pervious concrete, porous asphalt, or different types of porous structural pavers. The pavement layer is usually highly permeable with permeabilities ranging from tens to thousands of millimeters per hour (Bean et al. 2007b; Kuang et al. 2011). Uniformly graded coarse aggregate is usually recommended to form the stone reservoir which provides temporary storage for peak flow and stormwater volume control purposes (USEPA 1999). The stone reservoir is usually designed with an overflow control device so that the water level inside the stone reservoir cannot rise to the pavement level or the surface of the pavement during any large storm events (PDEP 2006). This overflow control device is commonly referred to as the underdrain of a permeable pavement system. For permeable pavement systems without underdrains, the in-situ soil needs to be highly permeable and with low clay contents [e.g., less than 30%, USEPA (1999)].

Permeable pavement systems are primarily designed to provide treatment for the rainwater that falls directly onto their surfaces (NCDWQ 2007), but can also be designed to receive stormwater generated from adjacent conventionally-paved areas and building roofs (Kwiatkowski et al. 2007). Some jurisdictions specify that the impervious area, which contributes surface runoff to a permeable pavement system, should not exceed certain times of the area of the permeable pavement system itself [e.g., 1.2 times as specified by CVC and TRCA (2010)]. To avoid potential clogging of the permeable

pavement system, it is usually discouraged to use permeable pavements to control stormwater generated from pervious areas. Reduction of stormwater volume is one of the main stormwater management roles that permeable pavements play (Pratt et al. 1989, 1995; Dreelin et al. 2006; Collins et al. 2008; Ball and Rankin 2010). The stormwater capture efficiency of a permeable pavement system is defined as the fraction of stormwater captured by the system; it can be used to demonstrate both its stormwater quantity and quality control performances. Due to differences in design and climate conditions, observed stormwater capture efficiencies of permeable pavement systems vary significantly as shown in Table 5.1. To assist in the hydrologic design of permeable pavement systems, accurate and reliable methods are needed to evaluate their stormwater capture efficiencies.

Many laboratory experiments and field monitoring studies have been conducted to assess the stormwater management performance of permeable pavement systems (e.g., Pratt et al. 1995; Booth and Leavitt 1999; Bean et al. 2007a; Collins et al. 2008; Welker et al. 2013). Although a significant amount of work is required in these studies to observe a large number of storm events, unavoidable uncertainty is still contained in the final assessment of a system's long-term average performance. Based on Erwin, an icon-driven rainfall-runoff model containing modules needed for evaluating the performance of sustainable urban drainage systems (AWS, 1998), Schluter and

**Table 5.1 Observed stormwater capture efficiencies of permeable pavement systems**

| Location | Depth of Stone Reservoir | Availability of Underdrain | Type of Subsoil | Stormwater Capture Efficiency | Reference |
|---|---|---|---|---|---|
| Nottingham, UK | 30-40 cm | Yes | N/I** | 53-66% | Pratt et al. (1995) |
| Reze, France | 45 cm | No | N/A* | 97% | Legret and Colandani (1999) |
| Tampa, US-FL | N/A* | No | sandy loam | 40-45% | Rushton (2001) |
| Renton, US-PA | N/A* | No | N/A* | >97% | Brattebo and Booth (2003) |
| Athens, US-GA | 25.4 cm | Yes | clay | 93% | Dreelin et al. (2006) |
| Waterford, US-CT | 20 cm | No | sandy loam | 72% | Gilbert and Clausen (2006) |
| Villanova,US- PA | 46-76 cm | Yes | silty sand | 90% | Kwiatkowski et al. (2007) |
| Kinston, US-NC | 28-35 cm | Yes | sandy loam | 36-64% | Collins et al. (2008) |

Notes: * Not available; ** No Infiltration into the subsoil.

Jefferies (2002) developed a hydrologic model for evaluating the performance of permeable pavement systems. In the hydrologic model, a permeable pavement system is modeled as a combination of a road, a trench-soakaway, and a reservoir. The hydrologic model was shown to be able to simulate the outflow from permeable pavement systems as long as several parameters of the model were accurately determined through the parameter calibration process. The U.S. Environmental Protection Agency recently added an LID module to the Storm Water Management Model Version 5 (referred to as SWMM) which has the capability of simulating the stormwater management performance of permeable pavement systems (Rossman 2010). Using the

long-term continuous simulation results from a SWMM model, the long-term average performance of a permeable pavement system can be accurately assessed.

The analytical probabilistic approach (Eagleson 1972, 1978; Adams and Papa 2000) can be used as a computationally efficient alternative to continuous simulation for modeling the general rainfall-runoff processes. This approach has been successfully used to derive analytical equations for urban stormwater management purposes. For example, derived analytical equations can be used to directly calculate the values of runoff volumes and flood peaks from small urban watersheds (Guo and Adams 1998a, b; Guo et al. 2012). Derived equations can also be used to evaluate the performance of stormwater management facilities such as detention ponds (Guo and Adams 1999a, b), stormwater storage tanks (Bacchi et al. 2008; Balistrocchi et al. 2009), rain barrels (Guo and Baetz 2007), rain gardens (Zhang and Guo 2013b) and green roofs (Zhang and Guo 2013a).

In this research, the analytical probabilistic approach is applied to investigate the hydrologic operation of permeable pavement systems. The objective is to develop an analytical equation which can be used to calculate the long-term average stormwater capture efficiencies of different types of permeable pavements. The probabilistic models of rainfall event

characteristics are introduced first, followed by an analysis of the hydrologic processes involved in the operation of permeable pavement systems. An Analytical equation which can be used as a design tool is then derived based on the probabilistic models of rainfall event characteristics and the mathematical representations of the hydrologic processes. The validity of this probabilistic approach is demonstrated by comparing its outcomes with the results of a series of continuous simulations using long-term rainfall data from Charlotte, North Carolina as an example.

## 5.2 Derivation of the Analytical Equation

### 5.2.1 Statistical Representation of Rainfall Data

Probabilistic models of local rainfall event characteristics are used to represent the rainfall conditions of a location of interest. In order to obtain these probabilistic models of rainfall event characteristics, a continuous rainfall series is separated into individual rainfall events by applying two discretization thresholds: an interevent time definition (IETD) and a minimum volume (e.g., Guo and Adams 1998a; Adams and Papa 2000; Balistrocchi et al. 2011). The IETD represents the minimum dry period needed to assume that two consecutive rainfall pulses are statistically independent and the minimum volume threshold is set to equal the minimum rainfall volume that must be exceeded in order to have an appraisable rainfall or runoff event (Balistrocchi

and Bacchi 2011; Guo et al. 2012).

Each rainfall event isolated from a continuous rainfall series is characterized by its rainfall volume ($v$), rainfall duration ($t$), and interevent time ($b$). For a specific location, histograms of $v$, $t$, and $b$ can be prepared and probability density functions (PDFs) can be fitted to these histograms. Exponential PDFs have been found to provide good fits to the resulting histograms (e.g., Eagleson 1972; Howard 1976; Adams and Papa 2000), although the Weibull distribution was found to better fit the histogram of $v$ under some climate conditions (Bacchi et al. 2008; Balistrocchi et al. 2009). The exponential PDFs of rainfall event characteristics used in this study are expressed as:

$$f(v) = \zeta \exp(-\zeta v), \quad v \geq 0 \tag{5.1}$$

$$f(t) = \lambda \exp(-\lambda t), \quad t \geq 0 \tag{5.2}$$

$$f(b) = \psi \exp(-\psi b), \quad b \geq 0 \tag{5.3}$$

In Equations (5.1) – (5.3), $\zeta$, $\lambda$, and $\psi$ are distribution parameters; their values for a specific location may be estimated as the inverses of the mean of rainfall event volume ($\bar{v}$), the mean of rainfall event duration ($\bar{t}$), and the mean of interevent time ($\bar{b}$), respectively.

These exponential PDFs will be used in the derivation of the analytical

equation which can be used to quantitatively evaluate the stormwater volume control performance of permeable pavement systems. The derivation focuses on a random dry and wet cycle starting from a *b*-hour dry period followed by a *t*-hour rainfall event with a volume of $v$ mm. Hereafter, for ease of reference, this dry and wet cycle is referred to as the current cycle and the rainfall event in the cycle is referred to as the current rainfall event. For each cycle, the time of the dry period, the rainfall duration and the volume of the rainfall event are treated as independent random variables following their respective probability distributions. The potential limitations of this approach are noted and a more complete discussion could be found in Adams et al. (1986) and Adams and Papa (2000).

For illustration purposes, hourly rainfall data (1945-2005) of Charlotte, North Carolina were used in verifying the accuracy of the analytical equation derived in this paper. In each year, the non-winter period rainfall data from March through November were analyzed. An IETD of 12 hours and a volume threshold of 2 mm were applied to separate individual rainfall events from the continuous rainfall series and the means used to estimate the distribution parameters of the exponential PDFs were found to be: $\bar{v} = 17.7$ mm, $\bar{t} = 11.6$ h and $\bar{b} = 134.7$ h. The histograms and the fitted exponential PDFs of $v$, $t$, and $b$ are shown in Figures 5.1– 5.3, respectively. These figures indicate that exponential PDFs fit reasonably well with the observed

histograms of rainfall event characteristics at Charlotte.

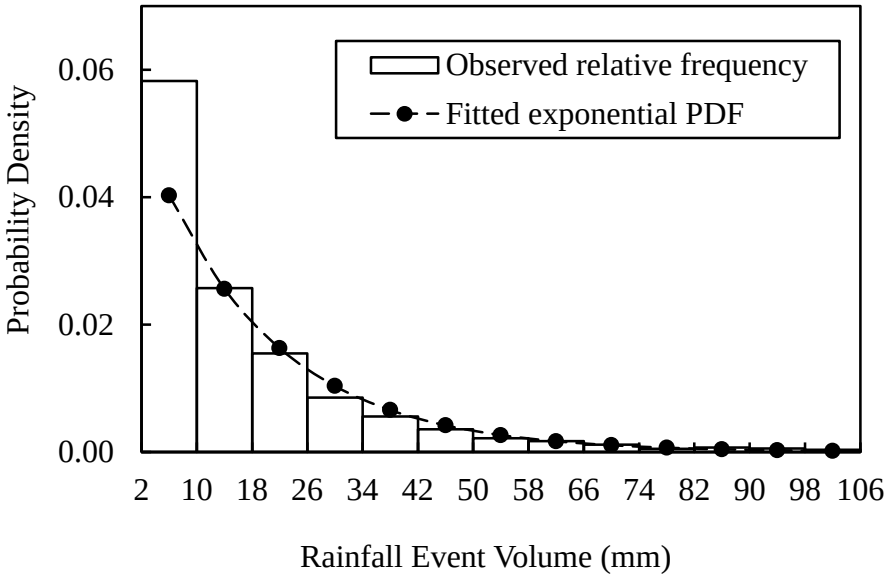


**Figure 5.1 Histogram and PDF of rainfall event volume at Charlotte**

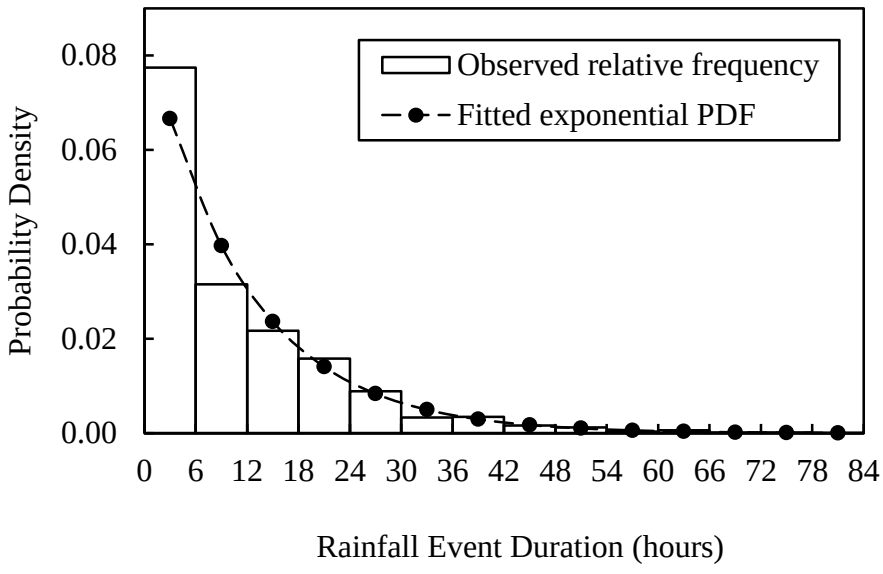


**Figure 5.2 Histogram and PDF of rainfall event duration at Charlotte**

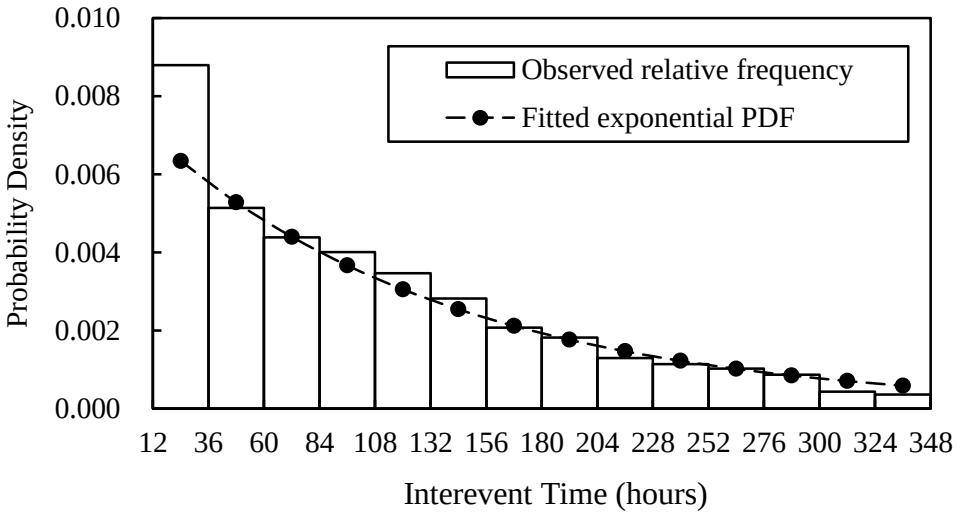


**Figure 5.3 Histogram and PDF of inter-event time at Charlotte**

### 5.2.2 Hydrologic Processes Involved

The hydrologic processes involved in the operation of permeable pavement systems are depicted schematically in Figure 5.4. The inflow entering a permeable pavement system which receives surface runoff generated from adjacent impervious areas may include two parts: (1) the surface runoff generated from the contributing impervious area, and (2) the rainwater directly falling onto the permeable pavement. As rain falls onto the contributing impervious area, depending on the volume of the rainfall event, a portion or all of the rainwater can be trapped by the small depressions on the surface of the impervious area. If the volume of rainwater ($v$) is greater than the storage capacity of these surface depressions (denoted as $S_{di}$, in mm of water over the impervious area), the remainder of the rainwater after filling up

the storage capacity of the surface depressions will flow to the permeable pavement. If $v$ is not greater than $S_{di}$, there will be no surface runoff generated from the impervious area and the inflow water to the permeable pavement consists of only the rainwater directly falling on it. A permeable pavement system which does not receive stormwater from adjacent impervious areas can be viewed as a special case in which the inflow water into the system includes only the rainwater directly falling onto its surface.

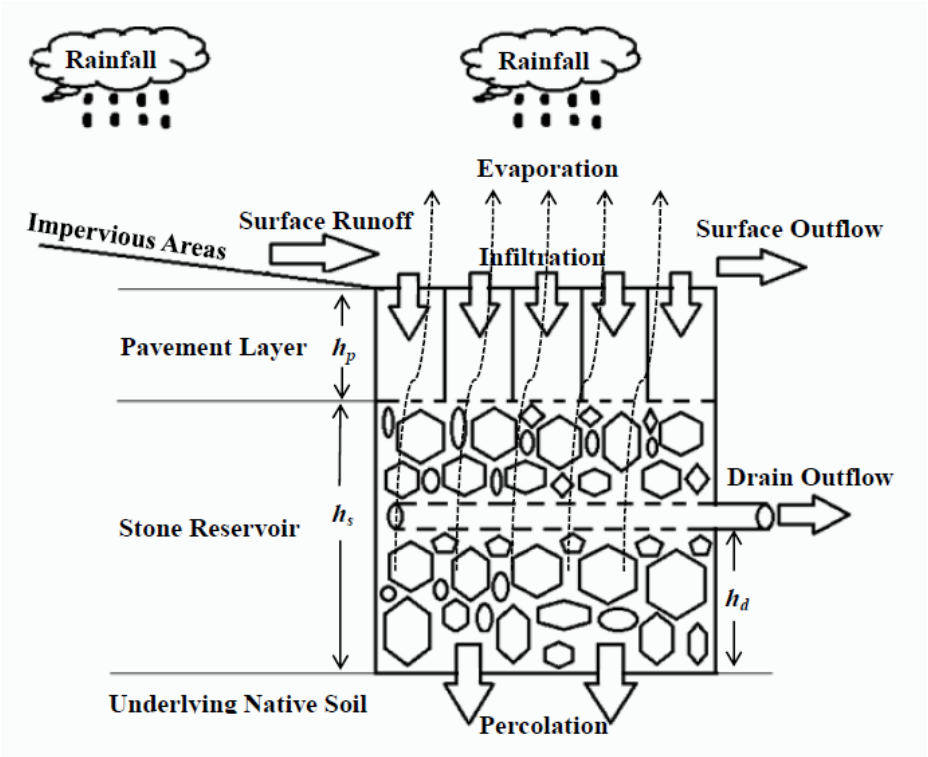


**Figure 5.4 Hydrologic processes involved in the operation of permeable pavement systems**

As inflow accumulates on a permeable pavement surface, a portion of the inflow water can be trapped by small depressions on the surface or

adsorbed by the pavement layer. The rest of the inflow may either infiltrate through the pavement layer into the stone reservoir or flow away from the system as surface outflow. Due to the extremely high permeability of the pavement layer, surface outflow seldom occurs (Brattebo and Booth 2003; Collins et al. 2008). As the infiltrated water moves downward in the stone reservoir, a very little portion of the water is adsorbed by the stones and the rest will percolate through the bottom of the reservoir into the underlying native soils. When the inflow rate into the stone reservoir exceeds the infiltration capacity of the native soil, accumulation of stormwater occurs in the reservoir and the water level of the reservoir rises. During a large and intense storm, the water level may reach the underdrain pipe or even rise up to the surface of the pavement layer. The excess stormwater after filling up the storage capacity of the system and satisfying the requirement for percolation into the native soil will either be drained away through the underdrain as drain outflow (if there is an underdrain installed in the system) or flow away over the surface of the system as surface outflow. When a rainfall event ceases, the rainwater retained in the entire permeable pavement system is depleted through both percolation through the bottom of the stone reservoir and evaporation.

### 5.2.3 Water Balance Equation and Stormwater Capture Efficiency

Focusing on a random b-hour dry period followed by a $t$-hour rainfall event cycle referred to as the current cycle, the volume of stormwater captured by a permeable pavement system during the current rainfall event is controlled by the volumes of inflow, infiltration through the surface of the pavement layer, percolation through the bottom of the stone reservoir, evaporation from the system, and the available storage capacity of the system at the beginning of the current rainfall event. The rate of evaporation from a permeable pavement system during wet weather period is very small (Nemirovsky et al. 2013) when it is compared to the infiltration capacity of the soil underneath the system. Therefore, the volume of evaporation during a rainfall event may be negligible and the water balance equation of a permeable pavement system over the current rainfall event can be expressed as:

$$v_o = v_i - F_t - R_c \tag{5.4}$$

In Equation (5.4), $v_i$ and $v_o$ are, respectively, the volumes of inflow into and outflow from the system during the current rainfall event; $F_t$ is the volume of percolation through the bottom of the stone reservoir into the native soil during the current rainfall event; $R_c$ is the available storage or retention capacity of the system at the start of the current rainfall event. All the terms in Equation (5.4) are expressed in mm of water over the system's surface area.

For a permeable pavement system without underdrains, $v_o$ is the volume of surface outflow from the system; for a permeable pavement system with underdrains, $v_o$ is the sum of the volumes of the surface outflow and drain outflow from the system.

Using the derived probability distribution theory (Benjamin and Cornell 1970), the PDFs of $v_i$ and $v_o$ can be derived on the basis of the PDFs of $v$, $t$, and $b$. Based on the derived PDFs of $v_i$ and $v_o$, the expected values of them can be calculated. Given the expected values of $v_i$ and $v_o$ of a permeable pavement system for a random rainfall event, the long-term average stormwater capture efficiency of the system can be calculated as

$$C_e = \frac{E(v_i) - E(v_o)}{E(v_i)} \tag{5.5}$$

where $E(v_i)$ and $E(v_o)$ are the expected values of $v_i$ and $v_o$, respectively; and $C_e$ is the long-term average stormwater capture efficiency of the permeable pavement system.

### 5.2.4 Expected Value of the Inflow Volume

As described previously, the inflow entering a permeable pavement system which receives stormwater from adjacent impervious area may include two parts: (1) surface runoff generated from the contributing impervious area, and (2) rainwater directly falling onto the system itself. Under the current

rainfall event, the volume of surface runoff generated from the contributing impervious areas (denoted as $v_r$, in mm of water over the surface area of the contributing impervious areas) can be calculated as

$$v_r = \begin{cases} 0, & v \le S_{di} \\ v - S_{di}, & v > S_{di} \end{cases} \tag{5.6}$$

Taking the ratio (denoted as *r*, dimensionless) between the contributing impervious area and the permeable pavement area into consideration and combining the two parts of inflow into the system, the total volume of inflow ($v_i$) into the permeable pavement system can be expressed as

$$v_i = \begin{cases} v, & v \le S_{di} \\ (r+1)v - rS_{di}, & v > S_{di} \end{cases} \tag{5.7}$$

For a permeable pavement which does not receive stormwater from any impervious areas (i.e., $r = 0$), Equation (5.7) can still be used to calculate the total volume of inflow. In this case, Equation (5.7) can be simplified as $v_i = v$. Based on the PDF of $v$ [Equation (5.1)] and the functional relationship between $v_i$ and $v$ [Equation (5.7)], the expected value of $v_i$ can be calculated as

$$E(v_i) = \int_0^{S_{di}} v\zeta \exp(-\zeta v)dv + \int_{S_{di}}^{\infty} [(r+1)v - rS_{di}]\zeta \exp(-\zeta v)dv = \frac{1 + r\exp(-\zeta S_{di})}{\zeta} \tag{5.8}$$

### 5.2.5 Expected Value of the Outflow Volume

As shown in Equation (5.4), $v_o$ is controlled by $v_i$, $F_t$, and $R_c$. Equation (5.7) can be used to calculate $v_i$. The value of $F_t$ depends on the infiltration capacity of the underlying native soil, the duration of the current rainfall event, and the availability of stormwater for percolation into the native soil. The value of $R_c$ is determined by the volume of stormwater stored in the entire permeable pavement system at the beginning of the current cycle (denoted as $v_s$, in mm of water over the permeable pavement area), and the volumes of evaporation from the system and percolation into the native soil during the *b*-hour dry period of the current cycle.

The value of $v_s$ is required in order to determine $R_c$. For the current rainfall event which is just a random rainfall event under consideration, the value of $v_s$ varies and depends on many factors including the characteristics of the rainfall events preceding the current cycle, the infiltration rate of the native soil, and the maximum storage or retention capacity of the permeable pavement system (denoted as $R_{c\max}$, in mm of water over the permeable pavement area). As a result, a permeable pavement system may be empty (i.e., $v_s = 0$), or fully filled with stormwater (i.e., $v_s = R_{c\max}$), or partly filled with stormwater (i.e., $0 < v_s < R_{c\max}$) at the start of the current cycle. Theoretically, $v_s$ may be treated as a random variable and its expected value

may be used in estimating the expected value of $R_c$. However, it has been found that such an expected value cannot be derived analytically (Smith 1980; Adams and Papa 2000). For simplification, it is assumed that the permeable pavement system is fully filled with stormwater at the end of the previous rainfall event which is the beginning of the current cycle (i.e., $v_s = R_{c\max}$). This assumption will result in an over-estimation of stormwater remaining in the permeable pavement system at the beginning of the current rainfall event and therefore a conservative estimation of the stormwater capture efficiency of the permeable pavement system. Similar conservative assumptions were also adopted by Howard (1976), Loganathan and Delleur (1984), Adams and Papa (2000), Guo and Baetz (2007), and Zhang and Guo (2013b) in studying other urban stormwater management problems.

For a permeable pavement system without underdrains, its stormwater retention capacity ($R_{c\max}$) consists of three parts, i.e., the surface depressions of the pavement, the void space of the pavement layer and the void space of the stone reservoir. Therefore, its $R_{c\max}$ can be calculated as

$$R_{c\max} = S_d + n_p h_p + n_s h_s \tag{5.9}$$

where $S_d$ is the surface depression storage of the permeable pavement, in mm of water over the surface area of the pavement; $n_p$ and $n_s$ (dimensionless) are, respectively, the porosities of the pavement layer and the

stone reservoir; $h_p$ and $h_s$ (as shown in Figure 5.4) are, respectively, the depths of the pavement layer and the stone reservoir, in mm.

For a permeable pavement system with underdrains, stormwater held in the void space of the pavement layer and the void space of the part of stone reservoir which is above the underdrains can be quickly drained away through the underdrains. Therefore, the retention capacity of the system ($R_{c\max}$) only consists of the surface depressions of the system and the void space of the part of stone reservoir which is below the underdrains. Thus, its $R_{c\max}$ can be estimated as

$$R_{c\max} = S_d + n_s h_d \tag{5.10}$$

where $h_d$ (in mm) is the depth of the stone reservoir that is below the underdrain.

During the dry period of the current cycle, stormwater held in the permeable pavement system is depleted through evaporation and percolation. It is assumed that percolation takes place at a constant rate $K$ (i.e., the constant infiltration rate or the saturated hydraulic conductivity of the native soil, in mm/h) when there is water held in, or inflow into, the permeable pavement system. Given that the permeable pavement system is completely filled at the beginning of the current cycle, the time needed (denoted as $t_d$, in h) to regenerate the entire retention capacity of the system can be calculated as

$$t_d = \frac{R_{cmax}}{E_a + K} \tag{5.11}$$

where $E_a$ is the average evaporation rate from the permeable pavement system, in mm/h. Depending on the magnitude of $t_d$ and *b*, the available retention capacity ($R_c$) of the permeable pavement system at the beginning of the current rainfall event can be calculated as

$$R_c = \begin{cases} (E_a + K)b, & b \le t_d \\ R_{cmax}, & b > t_d \end{cases} \tag{5.12}$$

Knowing the duration of the current rainfall event $t$ and the percolation rate through the bottom of the stone reservoir $K$, the volume of potential percolation into the native soil during the current rainfall event ($F_t$) can be estimated as

$$F_t = Kt \tag{5.13}$$

Equation (5.13) is valid only when there is enough water to be percolated. This has to be recognized when substitute Equation (5.13) into Equation (5.14).

Since typical values of $S_{di}$ are very small, usually changing from 1.27 mm to 2.54 mm (ASCE 2012), there should be no outflow generated from a permeable pavement when there is no surface runoff generated from its contributing impervious area (i.e., whenever $v \le S_{di}$, $v_o = 0$). Considering this while substituting Equations (5.7), (5.12) and (5.13) into Equation (5.4),

the volume of outflow $v_o$ resulting from the current rainfall event can be estimated as:

$$v_o = \begin{cases} 0, & (v \le S_{di}) \text{ or} \\ & \left[ b \le t_d \text{ and } S_{di} < v \le \dfrac{rS_{di} + (E_a + K)b + Kt}{r+1} \right] \text{ or} \\ & \left[ b > t_d \text{ and } S_{di} < v \le \dfrac{rS_{di} + R_{c\max} + Kt}{r+1} \right] \\ (r+1)v - rS_{di} - (E_a + K)b - Kt, & \left[ b \le t_d \text{ and } v > \dfrac{rS_{di} + (E_a + K)b + Kt}{r+1} \right] \\ (r+1)v - rS_{di} - R_{c\max} - Kt, & \left[ b > t_d \text{ and } v > \dfrac{rS_{di} + R_{c\max} + Kt}{r+1} \right] \end{cases} \tag{5.14}$$

Equation (5.14) establishes the rainfall-outflow relationship for a permeable pavement system; it is the basis for deriving the PDF of $v_o$ through the use of the derived probability distribution theory. Since the expression for the PDF of $v_o$ is lengthy, the following notations are introduced in order to simplify its presentation:

$$C_1 = \exp\left( -\frac{\zeta r S_{di}}{r+1} \right)$$

$$C_2 = \frac{\lambda(r+1)}{\lambda(r+1) + \zeta K}$$

$$C_3 = \frac{\psi(r+1)}{\psi(r+1) + \zeta(E_a + K)}$$

$$C_4 = \exp\left\{-\frac{\left[\psi(r+1)+\zeta(E_a+K)\right]R_{c\max}}{(r+1)(E_a+K)}\right\}$$

Based on Equations (5.1), (5.2), (5.3), and (5.14), the PDF of $v_o$ was derived to be

$$f(v_o)=\begin{cases}\{1-C_1C_2[C_3+(1-C_3)C_4]\}\delta(v_o) & v_o=0\\ \dfrac{\zeta}{r+1}\exp\left(-\dfrac{\zeta v_o}{r+1}\right)C_1C_2[C_3+(1-C_3)C_4], & v_o>0\end{cases} \quad (5.15)$$

where $\delta(v_o)$ is the Dirac delta function whose integral is unity. $\delta(v_o)$ is used to simplify the notation of the impulse probability at $v_o=0$. Based on the PDF of $v_o$ as expressed in Equation (5.15), the expected value of $v_o$ per rainfall event can be calculated as

$$E(v_o)=\int_0^\infty v_o f(v_o)\,dv_o=\frac{(r+1)}{\zeta}C_1C_2[C_3+(1-C_3)C_4] \quad (5.16)$$

### 5.2.6 Long-term Average Stormwater Capture Efficiency

Given the expected values of the volumes of inflow and outflow per rainfall event, as shown in Equations (5.8) and (5.16), respectively, the long-term average stormwater capture efficiencies of permeable pavement systems can be estimated using Equation (5.5). The final result is as follows:

$$C_e=\frac{E(v_i)-E(v_o)}{E(v_i)}=1-\frac{(r+1)C_1C_2\left[C_3+(1-C_3)C_4\right]}{1+r\exp(-\zeta S_{di})} \quad (5.17)$$

Equation (5.17) provides an efficient method of estimating the long-term average stormwater capture efficiencies of all types of permeable pavement systems. For permeable pavement systems without underdrains, Equation (5.9) should be used to calculate $R_{c\max}$; for permeable pavement systems with underdrains, Equation (5.10) should be used to calculate $R_{c\max}$. For permeable pavement systems which receive stormwater from adjacent impervious areas, the value of *r* in the equations represents the ratio between the contributing impervious area and the permeable pavement area. For permeable pavement systems which do not receive stormwater from adjacent impervious areas, the value of *r* in the equations should be set to 0.

## 5.3 Comparison with Continuous Simulation Results

Several simplifying assumptions were made in the above-described derivations. To verify the acceptability of the simplifying assumptions and to illustrate the accuracy of Equation (5.17), a set of continuous SWMM simulations using the LID module were performed for different types of permeable pavement systems. To model the rainfall-outflow transformations of permeable pavement systems, the LID module of SWMM does not require the same simplifying assumptions invoked in the development of Equation (5.17). Thus, results from the SWMM continuous simulations using long-term historical rainfall records can be viewed as relatively accurate

values.

The input parameters required by Equation (5.17) and the SWMM model are not identical due to their differences in representing the rainfall-outflow transformations of permeable pavement systems. The parameters required in the LID-SWMM simulations and their values or ranges of values used in this study are listed in Table 5.2. Table 5.3 presents the parameters required by Equation (5.17) and their values or ranges of values. To ensure that a particular permeable pavement system as simulated by a SWMM model is the same as that represented by using Equation (5.17), parameter values used in the two approaches are the same if the parameters are the same, or properly related if the definitions of the parameters are not exactly the same but the parameters are related. For example, the porosity of the pavement layer ( $n_p$ ) used in the analytical approach is calculated based on the void ratio of the pavement layer used in the corresponding SWMM model. The relationships between other parameters used in the two approaches can be identified by examining their values presented in Tables 5.2 and 5.3.

Using the 61-year hourly rainfall record of Charlotte as input to the SWMM simulations, the total volumes of inflow ($V_{in}$, in mm), surface outflow ($V_{sr}$, in mm) and drain outflow ($V_{dr}$, in mm) of a permeable pavement system over the 61 years can be obtained. Given the values of $V_{in}$, $V_{sr}$, and $V_{dr}$,

**Table 5.2 Parameters used in the LID-SWMM simulations**

| | Parameter | Value |
|---|---|---|
| surface layer | storage depth | 1.0 mm |
| | vegetative cover fraction | 0 |
| | surface roughness | 0.015 |
| | surface slope | 1% |
| pavement layer | thickness | 100 mm |
| | void ratio | 0.165 |
| | impervious surface fraction | 0 |
| | permeability | 254 mm/h |
| | clogging factor | 0 |
| storage layer | height | 0-450 mm |
| | void ratio | 0.625 |
| | filtration rate | 3.3[(a)] or 10.9[(b)] mm/h |
| | clogging factor | 0 |
| underdrain system | drain coefficient | 1000 |
| | drain exponent | 0.5 |
| | drain offset height | 0-450 mm |
| native soil | suction head | 88.9[(a)] or 109.9[(b)] mm |
| | conductivity | 3.3[(a)] or 10.9[(b)] mm/h |
| | initial deficit | 0 |
| other parameters of the permeable pavement systems | area | 1000 $m^2$ |
| | width | 30 m |
| | ET rate | 0.1 mm/h |
| contributing impervious areas | area | 0[(c)] or 1500[(d)] $m^2$ |
| | imperviousness | 100% |
| | depression storage | 2 mm |

Notes: (a) Values for permeable pavements with loam as native soil;

(b) Values for permeable pavements with sandy loam as native soil;

(c) Value for permeable pavement not receiving stormwater from any impervious areas;

(d) Value for permeable pavements receiving stormwater from adjacent impervious areas.

**Table 5.3 Parameters used in the analytical equations**

| | Parameter | Value |
|---|---|---|
| surface layer | storage depth ($S_d$) | 1.0 mm |
| pavement layer | depth ($h_p$) | 100 mm |
| | porosity ($n_p$) | 0.141 |
| storage layer | depth ($h_s$) | 0-450 mm |
| | porosity ($n_s$) | 0.385 |
| underdrain system | drain offset height ($h_d$) | 0-450 mm |
| native soil | hydraulic conductivity ($K$) | 3.3[(a)] or 10.9[(b)] mm/h |
| other parameters | area ratio ($r$) | 0[(c)] or 1.5[(d)] |
| | ET rate ($E_a$) | 0.1 mm/h |
| impervious areas | depression storage ($S_{di}$) | 2 mm |

Notes: (a) Values for permeable pavements with loam as native soil;
(b) Values for permeable pavements with sandy loam as native soil;
(c) Value for permeable pavement systems not receiving stormwater from any impervious areas;
(d) Value for permeable pavement systems (with an area of 1000 $m^2$) receiving stormwater from 1500 $m^2$ impervious areas.

the SWMM-determined long-term average stormwater capture efficiency of the permeable pavement system, $C_{eSWMM}$, can be calculated as

$$C_{eSWMM} = \frac{V_{in} - V_{sr} - V_{rd}}{V_{in}} \tag{5.18}$$

It is worth noting that, for a permeable pavement system which receives stormwater from adjacent impervious areas, $V_{in}$ includes both the stormwater generated from the contributing impervious areas and the input rainfall. Otherwise, $V_{in}$ equals to the total volume of the input rainfall.

Results determined from the continuous simulations and those calculated using Equation (5.17) are compared in Figures 5.5 and 5.6. Figure 5.5 shows

the comparison for permeable pavement systems with underdrains and loam soil underneath the stone reservoirs. As shown in Figure 5.5, for both types of permeable pavement systems which receive ($r = 1.5$) and do not receive ($r = 0$) stormwater from adjacent impervious areas, the stormwater capture efficiencies calculated using the analytical equation are very close to those determined from SWMM continuous simulations when $h_d$ changes from 0 mm to 450 mm. For permeable pavement systems without underdrains and with sandy loam underneath the systems, Figure 5.6 also shows a close agreement between the results from the analytical equation and SWMM continuous simulations when $h_s$ changes from 0 mm to 450 mm.

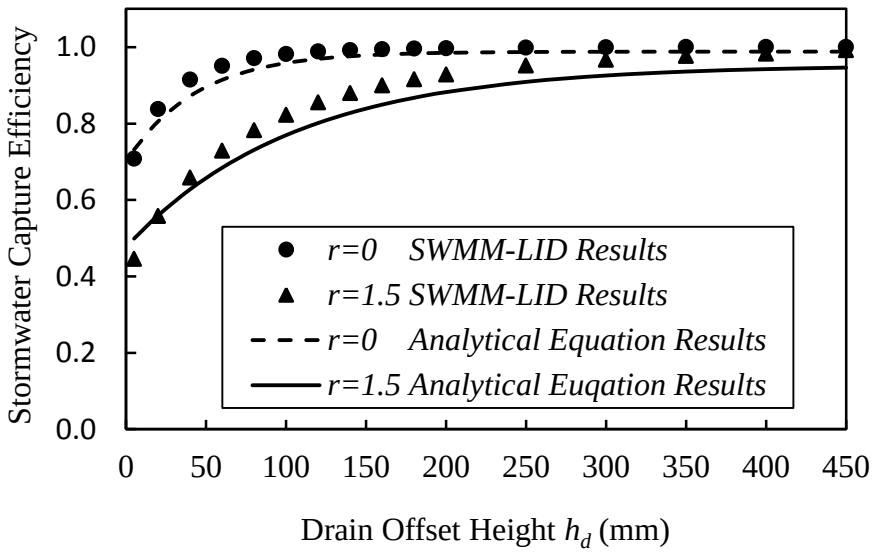


**Figure 5.5 Comparison of the analytical equation and SWMM results for permeable pavement systems with underdrains**

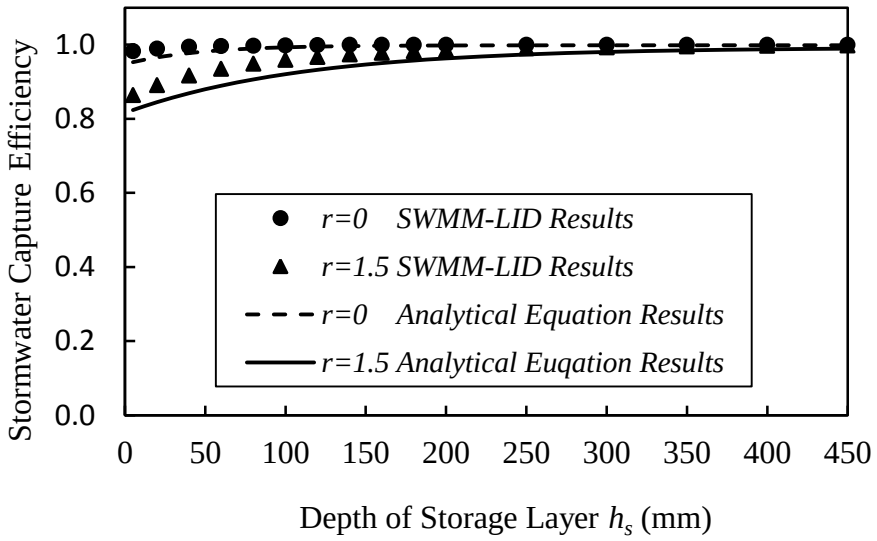


**Figure 5.6 Comparison of the analytical equation and SWMM results for permeable pavement systems without underdrains**

In Figures 5.5 and 5.6, both the analytical equation and the continuous simulation results indicate that the stormwater capture efficiencies of permeable pavement systems increase with the increase of $h_d$ or $h_s$. This is due to the fact that higher $h_d$ and $h_s$ result in larger retention capacity available for capturing stormwater. For most of the cases, the stormwater capture efficiencies calculated using the analytical equation are slightly smaller than those determined from continuous simulations. This is partly caused by the assumption that the permeable pavement systems are fully filled with stormwater at the beginning of the current cycle (i.e., $v_s = R_{c\max}$). As mentioned previously, this assumption will cause the analytical equation to slightly underestimate the stormwater capture efficiencies.

The differences between the stormwater capture efficiencies of permeable pavement systems calculated using the two approaches are smaller than 6% for all the cases shown in Figures 5.5 and 5.6. This close agreement demonstrates that the analytical equation derived on the basis of the event-based rainfall-outflow transformations [i.e., Equation (5.14)] and the fitted exponential distributions of rainfall event characteristics [i.e., Equations (5.1), (5.2), and (5.3)] can generate results close to those determined from continuous simulations. It also indicates that the simplifying assumptions made in establishing the event-based rainfall-outflow transformations are generally acceptable.

## 5.4 Summary and Conclusions

In this study, an analytical equation which can be used to calculate the long-term average stormwater capture efficiencies of permeable pavement systems was derived based on the probabilistic models of local rainfall event characteristics and mathematical representations of the hydrologic processes included in the operation of permeable pavement systems. This analytical equation is suitable for various types of permeable pavement systems having or not having underdrains, receiving or not receiving stormwater from adjacent impervious areas. Once the required local rainfall statistics are obtained, the applications of this analytical equation are simple and straightforward.

The mathematical representations of the hydrologic processes occurring in permeable pavement systems were established on the basis of the following four main assumptions: (1) the infiltration capacity of the pavement layer and the stone reservoir of the permeable pavement system is always greater than the rate of inflow into the system; (2) percolation into the native soils takes place at a rate equaling the hydraulic conductivity of the native soil when there is water held in, or when there is sufficient inflow coming into, the permeable pavement system; (3) evaporation during wet weather periods is negligible and evaporation takes place at its average rate during dry weather periods; and (4) the permeable pavement system is fully filled with stormwater at the end of a random rainfall event.

A set of continuous SWMM simulations using the LID module were performed for different types of permeable pavement systems with the 61-year hourly rainfall data from Charlotte, NC as rainfall input. The continuous simulation results were compared to those calculated using the analytical equation [Equation (5.17)]. The small differences between the results from the SWMM simulations and the analytical equation indicate that the analytical equation can be used as an alternative to continuous simulations for calculating the stormwater capture efficiencies of permeable pavement systems. The comparisons also demonstrate that the assumptions made in developing the analytical equation are acceptable for practical purposes. It is

desirable if the analytical equation results could also be verified using observed data. However, long-term observed data are seldom available. As these data become available in the future, the analytical probabilistic approach may be further verified or improved as well.

**ACKNOWLEDGEMENTS:** This work has been supported by the Natural Sciences and Engineering Research Council of Canada and the China Scholarship Council.

## References

Adams, B. J., and Papa, F. (2000). *Urban Stormwater Management Planning with Analytical Probabilistic Models*, John Wiley & Sons, Inc., New York, USA.

Adams, B. J., Fraser, H. G., Howard, C. D. D., and Hanafy, M. S. (1986). Meteorologic data analysis for drainage system design. *Journal of Environmental Engineering*, ASCE, 112(5), 827–848.

American Society of Civil Engineers (ASCE). (2012). *Design of Urban Stormwater Controls*, *Manuals of Practice* (MOP) 87, McGraw-Hill Inc., New York, USA.

Abertay Waste Solutions (AWS). (1998). *Erwin User Guide Version 3.0, English*. Urban Water Technology Centre, University of Abertay, Dundee, Scotland.

Bacchi, B., Balistrocchi, M., and Grossi, G. (2008). Proposal of a semi-probabilistic approach for storage facility design. *Urban Water Journal*, 5(3), 195–208.

Balistrocchi, M., and Bacchi, B. (2011). Modelling the statistical dependence of rainfall event variables through copula functions. *Hydrology and Earth System Sciences*, 15, 1959–1977.

Balistrocchi, M., Grossi, G., and Bacchi, B. (2009). An analytical probabilistic model of the quality efficiency of a sewer tank. *Water Resources Research*, 45, W12420, doi:10.1029/2009WR007822.

Ball, J. E., and Rankin, K. (2010). The hydrological performance of a permeable pavement. *Urban Water Journal*, 7(2), 79–90.

Barrett, M., Kearfott, P., and Malina, J. F. (2006). Stormwater quality benefits of a porous friction course and its impact on pollutant removal by roadside shoulders. *Water Environmental Research*, 78(11), 2177–2185.

Bean, E. Z., Hunt, W. F., and Bidelspach, D. A. (2007a). Evaluation of four permeable pavement sites in eastern North Carolina for runoff reduction and water quality impacts. *Journal of Irrigation and Drainage Engineering*, 133(6), 583–592.

Bean, E. Z., Hunt, W. F., and Bidelspach, D. A. (2007b). Field survey of permeable pavement surface infiltration rates. *Journal of Irrigation and Drainage Engineering*, 133(3), 247–255.

Benjamin, J. R., and Cornell, C. A. (1970). *Probability, Statistics and Decision for Civil Engineers*, McGraw-Hill, New York, USA.

Berbee, R., Rijs, G., Dde Brouwer, R., Van Velzen, L. (1999). Characterization and treatment of runoff from highways in the Netherlands paved with impervious and pervious asphalt. *Water Environmental Research*, 71 (2), 183–190.

Booth, D. B., and Leavitt, J. (1999). Field evaluation of permeable pavement systems for improved stormwater management. *Journal of American Planning Association*, 65 (3), 314–325.

Booth, D. B., and Jackson, C. R. (1997). Urbanization of aquatic systems: degradation thresholds, stormwater detection, and the limits of mitigation. *Journal of American Water Resources Association*, 33(5), 1077–1090.

Brattebo, B. O., and Booth, D. B. (2003). Long-term stormwater quantity and quality performance of permeable pavement systems. *Water Research*, 37(18), 4369–4376.

Collins, K. A., Hunt, W. F., and Hathaway, J. M. (2008). Hydrologic

comparison of four types of permeable pavement and standard asphalt in eastern North Carolina. *Journal of Hydrological Engineering*, 13(12), 1146–1157.

Credit Valley Conservation Authority and Toronto and Region Conservation Authority (CVC and TRCA), (2010). *Low impact development stormwater management planning and design guide*. CVC and TRCA, Downsview and Mississauga, ON, Canada.

Dreelin, E. A., Fowler, L., and Carroll, C. R. (2006). A test of porous pavement effectiveness on clay soils during natural storm events. *Water Research*, 40(4), 799–805.

Eagleson, P. S. (1972). Dynamics of flood frequency. *Water Resources Research*, 8(4), 878–898.

Eagleson, P. S. (1978). Climate, soil, and vegetation, 2, the distribution of annual precipitation derived from observed storm sequences. *Water Resources Research*, 14(5), 713–721.

Fassman, E. A., and Blackbourn, S. D. (2011). Road runoff water-quality mitigation by permeable modular concrete pavers. *Journal of Irrigation and Drainage Engineering*, 137 (11), 720–729.

Gilbert, J., and Clausen, J. (2006). Stormwater runoff quality and quantity from asphalt, paver and crushed stone driveways in Connecticut. *Water Research*, 40(4), 826–832.

Guo, Y., and Adams, B. J. (1998a). Hydrologic analysis of urban catchments with event-based probabilistic models. Part I: Runoff volume. *Water Resources Research*, 34(12), 3421–3431.

Guo, Y., and Adams, B. J. (1998b). Hydrologic analysis of urban catchments with event-based probabilistic models. Part II: Peak discharge rate. *Water*

*Resources Research*, 34(12), 3433–3443.

Guo, Y., and Adams, B. J. (1999a). Analysis of detention ponds for storm water quality control. *Water Resources Research*, 35(8), 2447–2456.

Guo, Y., and Adams, B. J. (1999b). An analytical probabilistic approach to sizing flood control detention facilities. *Water Resources Research*, 35(8), 2457–2468.

Guo, Y., and Baetz, B. W. (2007). Sizing of rainwater storage units for green building applications. *Journal of Hydrological Engineering*, 12(2), 197–205.

Guo, Y., Liu, S., and Baetz, B. W. (2012). Probabilistic rainfall-runoff transformation considering both infiltration and saturation excess runoff generation processes. *Water Resources Research*, 48, W06513, doi:10.1029/2011WR011613.

Hammer, T. H. (1972). Stream channel enlargement due to urbanization. *Water Resources Research*, 8(6), 1530–1540.

Hollis, G. E. (1975). The effect of urbanization on floods of different recurrence interval. *Water Resources Research*, 11(3), 431–435.

Howard, C. D. D. (1976). Theory of storage and treatment plant overflows. *Journal of Environmental Enineering Division.*, ASCE, 102(EE4), 709–722.

Kuang, X., Sansalone, J., Ying, G., and Ranieri, V. (2011). Pore-structure models of hydraulic conductivity for porous pavement. *Journal of Hydrology*, 399(3–4), 148–157.

Kwiatkowski, M., Welker, A. L., Traver, R. G., Vanacore, M., and Ladd, T. (2007). Evaluation of an infiltration best management practice utilizing

pervious concrete. *Journal of American Water Resources Association*, 43(5), 1208–1222.

Legret, M., and Colandani, V. (1999). Effects of a porous pavement structure with a reservoir structure on runoff water: water quality and fate of metals. *Water Science and Technology*, 39(2), 111–117.

Loganathan, G. V., and Delleur, J. W. (1984). Effects of urbanization on frequencies of overflows and pollutant loadings from storm sewer overflows: A derived distribution approach. *Water Resources Research*, 20(7), 857–865.

Nemirovsky, E. M., Welker, A. L., and Lee, R. (2013). Quantifying evaporation from pervious concrete systems: methodology and hydrologic perspective. *Journal of Irrigation and Drainage Engineering*, 139 (4), 271–277.

North Carolina Division of Water Quality (NCDWQ). (2007). *Stormwater best management practices manual.* North Carolina Department of Environment and Natural Resources, Raleigh, NC, USA.

Pennsylvania Department of Environmental Protection (PDEP). (2006). *Pennsylvania stormwater best management practices manual.* PA DEP, Rep. No. 363-0300-002, Harrisburg, PA, USA.

Pratt, C. J., Mantle, J. D. G., and Schofield, P. A. (1989). Urban stormwater reduction and quality improvement through the use of permeable pavements. *Water Science and Technology*, 21(8), 769–778.

Pratt, C. J., Mantle, J. D. G., and Schofield, P. A. (1995). UK research into the performance of permeable pavement, reservoir structures in controlling stormwater discharge quantity and quality. *Water Science and Technology*, 32(1), 63–69.

Rossman, L. A. (2010). *Storm Water Management Model User's Manual, Version 5.0*, EPA/600/R-05/040, U.S. Environmental Protection Agency, Cincinnati, OH, USA.

Rushton, B. T. (2001). Low-impact parking lot design reduces runoff and pollutant loads. *Journal of Water Resources Planning and Management*, ASCE, 127(3), 172–179.

Sansalone, J. J., and Buchberger, S. G. (1995). An infiltration device as a best management practices for immobilizing heavy metals in urban highway runoff. *Water Science and Technology*, 32(1), 119–125.

Sansalone, J., Kuang, X., Ying, G., Ranieri, G. (2012). Filtration and clogging of permeable pavement loaded by urban drainage." *Water Research*, 46 (20), 6763–6774

Schluter, W., and Jefferies, C. (2002). Modelling the outflow from a porous pavement. *Urban Water*, 4(3), 245-253.

Smith, D. I. (1980). Probability of storage overflow for stormwater management. M.A.Sc thesis, Department of Civil Engineering, University of Toronto, Toronto, ON, Canada.

United States Environmental Protection Agency (USEPA). (1999). Storm Water Technology Fact Sheet: Porous Pavement. EPA 832-F-99-023.

Welker, A. L., Jenkins, J. K. G., McCarthy, L., and Nemirovsky, E. (2013). Examination of the material found in the pore spaces of two permeable pavements. *Journal of Irrigation and Drainage Engineering*, 139 (4), 278–284.

Zhang, S., and Guo, Y. (2013a). An analytical probabilistic model for evaluating the hydrologic performance of green roofs. *Journal of Hydrological Engineering*, 18(1), 19–28.

Zhang, S., and Guo, Y. (2013b). An explicit equation for estimating the stormwater capture efficiency of rain gardens. *Journal of Hydrological Engineering*, 18(12), 1739-1748.

# Chapter 6

# Conclusions and Recommendations for Future Research

## 6.1 Conclusions

In this thesis, the analytical probabilistic approach was employed to develop a set of analytical models which can be used as computationally efficient alternatives to continuous simulation for the planning and preliminary design of LID practices including green roofs, rain gardens, bioretention systems and permeable pavement systems. The analytical models were derived on the basis of exponential probability density functions (PDF) representing local rainfall characteristics and mathematical representations of the hydraulic and hydrologic processes occurring in association with LID practices. Exponential PDFs are found to provide good fits to the histograms of rainfall characteristics of five cities which are located in different climatic zones. These five cities are Detroit (Michigan), Atlanta (Georgia), Flagstaff (Arizona), Boston (Massachusetts) and Charlotte (North Carolina). This demonstrates that the analytical LID models can be used in many different regions.

The rainfall-runoff transformation of green roofs, the rainfall-inflow-infiltration-overflow transformations of rain gardens, biretention systems and permeable pavement systems used in the development of the analytical LID

models are all physically based. Most of the input parameters used to characterize the hydraulic and hydrologic processes in the analytical LID models are the same as those required in commonly used numerical models such as the SWMM model (Rossman 2010). Simplifying assumptions are made in order to establish the mathematical representations of the hydraulic and hydrologic processes. These assumptions are demonstrated to be reasonable and acceptable in order to obtain the estimations of the long-term average performances of the LID practices.

The accuracy of the analytical model for green roofs is verified by comparing the results from the analytical model with both observations from a real case study and results determined from long-term SWMM simulations. Due to the lack of suitable long-term hydrologic data, the overall accuracy of the analytical models developed for rain gardens, bioretention systems and permeable pavement systems are only demonstrated by comparing the results from these analytical models with results determined from long-term SWMM simulations. In the comparisons, the input parameter values of the analytical LID models are either directly taken or calculated based on physical grounds from corresponding and related parameters required by the SWMM model. The long-term rainfall data from the above-mentioned five locations and a variety of LID practices design configurations are used in the comparisons. The relative differences between the results calculated using the analytical LID models and those determined from corresponding SWMM simulations are all less than 10%.

The Howard's conservative assumption (Howard 1976; Adams and Papa 2000) was adopted in the development of the analytical models for rain gardens and permeable pavement systems. It was found that this assumption results in underestimations of the stormwater capture efficiency of rain gardens and permeable pavement systems, and that the inaccuracy caused by this assumption may be aggravated when the storage capacity of the LID practices increases significantly and the outflow rate from them becomes disproportionally small. Instead of simply adopting the Howard's conservative assumption, an approximate expected value of the surface depression water content of a bioretention system at the end of a random rainfall event [denoted as $E(S_{dw})$] was derived and used in the development of the analytical model for bioretention systems. The use of $E(S_{dw})$ was proven to be advantageous over the use of the Howard's conservative assumption.

As illustrated in the application examples, the application of the analytical LID models can be easy and efficient. For a specific location of interest, with a goodness-of-fit examination of the exponential PDFs to local rainfall data and verification of the accuracy of the analytical LID models, the models may be used as a convenient planning, design, and management tool for LID practices. For example, a municipality may have the analytical LID models coded into spreadsheets. Using these spreadsheets, the runoff reduction rates of green roofs, stormwater capture efficiency of rain gardens, bioretention systems and permeable pavements can be easily estimated for various types of design configurations. Presented in tabular or graphical

form, all this information is very helpful for the planning, design, and operation of these LID practices.

## 6.2 Recommendations for Future Research

### 6.2.1 Further Validation of the Analytical LID Models

Due to the lack of suitable long-term hydrologic data of LID practices, three out four of the analytical LID models are only tested against results determined from continuous SWMM simulations. As in the application of any other models, it would be better if the models developed here could first be calibrated using observed data for multiple objectives. As longer-term field data become available, the analytical LID models can be further verified.

### 6.2.2 Regional Distributions of Statistics of Rainfall Characteristics

In this thesis, statistics of rainfall characteristics and goodness-of-fit of the exponential PDFs are provided for five cities. It should be easy and convenient for designers in these five locations to apply the analytical LID models since the statistics of the rainfall characteristics are given and the accuracy of the analytical LID models are tested for these five locations. For other locations, however, statistical analyses are required in order to obtain the statistics of rainfall characteristics from long-term continuous rainfall records and to test the goodness-of-fit of the exponential PDFs before the application

of the analytical LID models. It would be much easier and more convenient for designers in other locations if the goodness-of-fit of the exponential PDFs are tested for more locations and the regional distributions of the statistics of rainfall characteristics are made available.

The statistics of rainfall characteristics of locations throughout Canada were presented in Adams and Papa (2000). Guo and Baetz (2007) listed the the U.S. regional summer rainfall statistics based on the data from USEPA (1986). However, these statistics were either not specifically tested for the analytical LID models or not calculated based on the most recent rainfall data. Regional distributions of the statistics of rainfall characteristics obtained on the basis of the updated rainfall data for the analytical LID models will be needed for the convenience of using these models in the panning and design of LID practices.

### 6.2.3 Initial Status of Stormwater Management Storage Facilities

In the application of the analytical probabilistic approach to assess the performance of stormwater management systems involving storage elements, it is necessary to specify the initial conditions (e.g., the initial water level or the initial moisture content) of the storage elements at the end/beginning of a random rainfall event. In Chapter 2, the moisture content of the growing media of green roofs at the end of a random rainfall event was assumed to be

equal to the average of its field capacity and wilting point. This assumption could result in either underestimation or overestimation of the performances of the green roofs depending on the types of growing medium and the climatic conditions. In Chapter 3 and Chapter 5, the Howard's conservative assumption (Howard 1976; Adams and Papa, 2000) was employed in order to obtain the initial water contents in rain gardens and permeable pavement systems. The Howard's conservative assumption could result in overestimation of overflows from rain gardens and permeable pavements and thus conservative estimation of their stormwater capture efficiencies.

In Chapter 4, an approximate expected value of the surface depression water content of bioretention systems at the end of a random rainfall event [denoted as $\mathrm{E}(S_{dw})$] was derived and used in the development of the analytical model for bioretention systems. $\mathrm{E}(S_{dw})$ was derived by assuming that the surface depression of a bioretention system is completely empty at the beginning of the rainfall event preceding the random rainfall event under analysis. Although the use of $\mathrm{E}(S_{dw})$ was proven to be advantageous than the use of the Howard's conservative assumption, systematic errors still exist due to the introduction of another assumption.

Smith (1980) alleviated the Howard's conservative assumption by solving the steady-state probability distribution of reservoir contents at the end of the rainfall event preceding the analyzed random rainfall event (Adams and

Papa, 2000). However, the numerical solution required in Smith's method makes it complicated and may limit its practical applications. Using a stochastic method, Rodriguez-Iturbe and co-workers (e.g., Rodriguez-Iturbe et al. 1999a, 199b; Laio et al. 2001) analytically obtained the steady-state probability distributions for soil moisture. Similar stochastic method may be employed in future researches to analytically determine the initial conditions of the stormwater storage facilities.

### 6.2.4 Stormwater Control Benefits of Impervious Surface Disconnection

Runoff from an urban catchment depends largely on not only the area of impervious surfaces but also the connectivity of these surfaces to stormwater drainage systems (Lee and Heaney 2003). Routing stormwater runoff from impervious surfaces (e.g., rooftops) onto pervious surfaces (e.g., lawns) is one of the LID strategies that can help mitigate the increases in runoff volume resulting from urbanization (Mueller and Thompson 2009). The runoff generation and routing processes from these disconnected impervious areas (i.e., impervious areas which are not directly connected to drainage systems) are not explicitly considered in any of the rainfall-runoff transformation representations of earlier analytical models (e.g., Adams and papa, 2000; Guo and Adams 1998a, b; Chen and Adams 2006; Guo et al. 2012). As the LID strategies are increasingly being implemented, it may be worthwhile to extend the earlier analytical models by considering the generation and routing processes of runoff from disconnected impervious areas.

### 6.2.5 Hydrologic Modeling of LID Practices in a Watershed Scale

LID practices are usually small in scale and distributed around an urban catchment to control stormwater quality and quantity close to the source areas. The effects of individual LID practices have been evaluated and modelled more extensively at small scales (e.g., lot levels). The collective effects of different types of LID practices at large scales (e.g., watershed scales) are expected to vary spatially and temporarily (Ahiablame et al. 2012). On the basis of the analytical LID models developed in this thesis for individual LID practices, using appropriate lumping (Guo et al. 2012) or aggregation (Elliott et al. 2009) methods, the analytical probabilistic approach can also be used to develop analytical LID models for investigating the collective effects of different combinations of various types of LID practices at watershed scales in future studies.

## References

Adams, B. J. and Papa, F. (2000). *Urban Stormwater Management Planning with Analytical Probabilistic Models*, John Wiley & Sons, Inc., New York, USA.

Ahiablame, L., Engel, B., and Chaubey, I. (2012). Effectiveness of Low Impact Development practices: literature review and suggestions for future research. *Water, Air, and Soil Pollution*, 223(7), 4253-4273.

Chen, J., and Adams, B. J. (2006). A framework for urban storm water modeling and control analysis with analytical models. *Water Resources Research*, 42(6), W06419.

Elliott, A. H., Trowsdale, S. A., and Wadhwa, S. (2009). Effect of aggregation of on-site storm-water control devices in an urban catchment model. *Journal of Hydrologic Engineering*, 14(9), 975–983.

Guo, Y., and Adams, B. J. (1998a). Hydrologic analysis of urban catchments with event-based probabilistic models. Part I: Runoff volume. *Water Resources Research*, 34(12), 3421–3431.

Guo, Y., and Adams, B. J. (1998b). Hydrologic analysis of urban catchments with event-based probabilistic models. Part II: Peak discharge rate. *Water Resources Research*, 34(12), 3433–3443.

Guo, Y., and Baetz, B. W. (2007). Sizing of rainwater storage units for green building applications. *Journal of Hydrological Engineering*, 12(2), 197–205.

Guo, Y., Liu, S., and Baetz, B. W. (2012). Probabilistic rainfall-runoff

transformation considering both infiltration and saturation excess runoff generation processes, *Water Resources Research*, 48, W06513, doi:10.1029/2011WR011613.

Howard, C. D. D. (1976). Theory of storage and treatment plant overflows. *Journal of Environmental Engineering Division*, ASCE, 102(EE4), 709–722.

Laio, F., Porporato, A., Ridolfi, L., and Rodriguez-Iturbe, I. (2001). Plants in water-controlled ecosystems: active role in hydrologic processes and response to water stress II. Probabilistic soil moisture dynamics. *Advances in Water Resources*, 24,707–723.

Lee, J. G., and Heaney, J. P. (2003). Estimation of urban imperviousness and its impacts on storm water systems. *Journal of Water Resources Planning and Management*, 129(5), 419–426.

Mueller, G. D., and Thompson, A. M. (2009). The ability of urban residential lawns to disconnect impervious area from municipal sewer systems. *Journal of American Water Resources Association*, 45 (5), 1116–1126.

Rodriguez-Iturbe, I., D'Odorico, P. D., Porporato, A., and Ridolfi, L. (1999a). Probabilistic modelling of water balance at a point: the role of climate, soil and vegetation. *Proceedings of the Royal Society London A*, A455, 3789–3805.

Rodriguez-Iturbe, I., D'Odorico, P.D., Porporato, A., and Ridolfi, L. (1999b). On the spatial and temporal links between vegetation, climate and soil moisture. *Water Resources Research*, 35 (12), 3709–3722.

Rossman, L. A. (2010). *Storm Water Management Model User's Manual, Version 5.0,* EPA/600/R-05/040, U.S. Environmental Protection Agency, Cincinnati, OH, USA .

Smith, D. I. (1980), Probability of storage overflow for stormwater management, M.A.Sc thesis, Department of Civil Engineering, University of Toronto, Toronto, ON, Canada.

U.S. Environmental Protection Agency (USEPA). (1986). *Methodology for analysis of detention basins for control of urban runoff quality*. EPA440/5-87-001, Washington D.C., USA.

# Appendix A (Thesis Related Paper)

# SWMM Simulation of the Stormwater Volume Control Performance of Permeable Pavement Systems

**Shouhong Zhang and Yiping Guo**

**Abstract:** The reliability of the Low Impact Development (LID) module of the widely used Storm Water Management Model (SWMM) for modeling the hydrologic performance of permeable pavement systems was evaluated through example applications. The method of calculating infiltration through the pavement layers of permeable pavement systems of the LID module was found to be inadequate which causes the LID-SWMM results to be overly sensitive to computational time steps and also causes the depth of the pavement layer to have an erroneous impact on runoff generation from permeable pavements. An alternative method of representing permeable pavement systems as equivalent regular subcatchments is proposed. Using this method, the hydrologic operation of permeable pavement systems can be modeled by SWMM or other hydrologic models.

**Key Words:** Permeable pavement; Stormwater management; Runoff reduction; SWMM; LID.

## A.1 Introduction

A permeable pavement system (Figure A.1) is a structural Low Impact Development (LID) practice which generally consists of a permeable pavement layer underlain by a stone reservoir (USEPA 1999; PDEP 2006; NCDWQ 2007; CVC and TRCA 2010). The surface pavement layer may be comprised of pervious concrete, porous asphalt, or different types of structural pavers. These pavement layers are usually highly permeable with permeabilities ranging from tens to thousands of millimeters per hour (Bean et al. 2007; Kuang et al. 2011). Washed coarse aggregate is used to form the stone reservoir to provide temporary storage for peak flow and stormwater volume control purposes (USEPA 1999; CVC and TRCA 2010). Depending on the infiltration capacity of the native soils, a permeable pavement system may be designed with no underdrain for full infiltration, with an underdrain for partial infiltration, or with an impermeable liner and underdrain for no infiltration to the native soils (CVC and TRCA 2010).

Permeable pavements have emerged as a widely used technology for on-site stormwater control (Pratt et al. 1989; Booth and Leavitt 1999; USEPA 1999; Brattebo and Booth 2003; Sansalone et al. 2012). Reduction of runoff volume is one of the main stormwater management roles that permeable pavements play (Dreelin et al. 2006; Collins et al. 2008; Ball and Rankin

2010). The runoff reduction rate of a permeable pavement system is defined as the fraction or percentage of runoff volume reduced by the system over the long term, it varies significantly due to differences in design, climatic and operating conditions (Brattebo and Booth 2003; Gilbert and Clausen 2006; Collins et al. 2008; Drake et al. 2012). Accurate and reliable methods are needed to estimate the long-term average runoff reduction rates of permeable pavement systems to ensure that optimum systems can be designed and constructed.

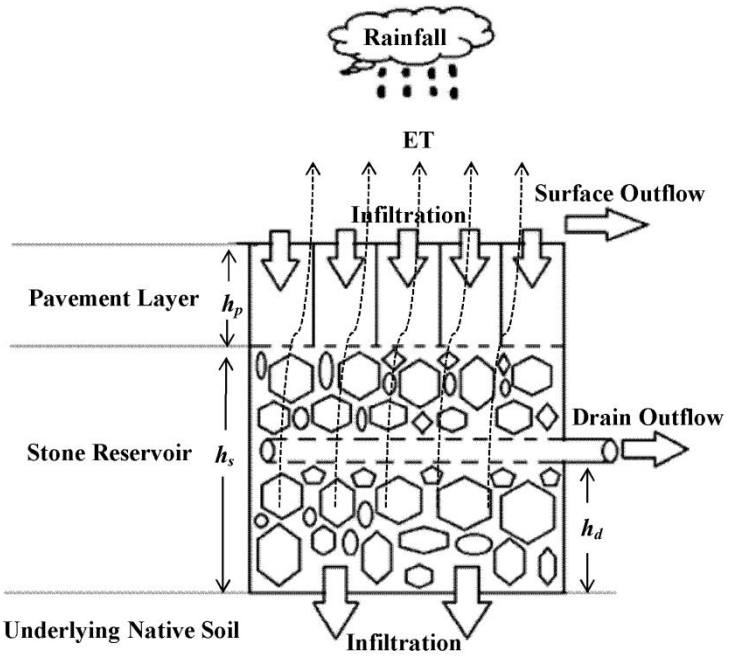


**Figure A.1 Diagram of a permeable pavement system and the hydrological processes involved**

The Storm Water Management Model Version 5 (referred to as SWMM) developed by the U. S. Environmental Protection Agency (EPA) is widely

used for single event and continuous simulation of runoff quantity and quality from urban catchments (Rossman 2010). The newly added LID module (SWMM Version 5.0.022) is expected to have the capability of simulating the stormwater management performance of various types of LID practices including permeable pavements. In this note, the reliability of the LID module of SWMM for simulating the runoff reduction performance of permeable pavements is examined and its unstable behavior is demonstrated. An alternative method based on the basic SWMM algorithms is proposed for evaluating the long-term average runoff reduction rates of permeable pavement systems.

## A.2 Methodology

### A.2.1 Hydrological Processes Involved

The hydrological processes occurring in a permeable pavement during non-winter seasons are depicted schematically in Figure A.1. As rain falls onto a permeable pavement system, part of the rainwater is trapped by small depressions on the surface or adsorbed by the pavement layer. The rest of the rainwater may either move downward through the pavement layer into the stone reservoir or flow away from the site as surface runoff. Due to the extremely high permeability of the pavement layers, surface runoff seldom occurs (Brattebo and Booth 2003; Collins et al. 2008). As rainwater moves

downward into the stone reservoir, a very little portion of the rainwater is adsorbed by the aggregates in the stone reservoir and the rest will percolate through the bottom of the reservoir into the underlying native soil. When the inflow rate exceeds the infiltration capacity of the native soil, accumulation of water occurs in the reservoir and the water level of the reservoir rises. During a large and intense storm, the water level may reach the underdrain pipe installed below the pavement layer or even the surface of the pavement layer. The excess water after filling up the storage capacity of the system and satisfying the requirement for percolation into native soils will either be drained away through the underdrain pipe as drain outflow or flow away from the pavement surface as surface outflow. When a rainfall event ceases, the rainwater retained in the entire permeable pavement system is depleted through both percolation and evapotranspiration (ET).

The infiltration, percolation, and runoff generation processes during winter seasons are more complicated than those during non-winter seasons. Detailed descriptions about the hydrological processes during winter seasons can be found in Drake et al. (2012). In this note, we concentrate on the non-winter season operation of permeable pavement systems.

### A.2.2 Modeling Permeable Pavements Using the SWMM LID Module

In the LID module of SWMM, a permeable pavement system is

represented by a combination of three vertical layers (i.e., the surface, pavement and storage layers) and an optional underdrain (Rossman 2010). As shown in Table 1, there are altogether 16 parameters used in the LID module to describe a permeable pavement system with an underdrain. In addition to these 16 parameters, the area, width and ET rates of the permeable pavement system and the infiltration parameters of the underlying native soils are also required in the simulations.

Using long periods (e.g., several years or decades) of rainfall records as input to an LID-SWMM model, the total volumes of rainfall ($V_{rain}$, in mm), surface outflow ($V_{sr}$, in mm) and drain outflow ($V_{dr}$, in mm) from a permeable pavement system can be obtained from a continuous simulation run. The long-term average runoff volume reduction rate of the permeable pavement system, $R_{rLID-SWMM}$, determined by LID-SWMM simulations can then be calculated as

$$R_{rLID-SWMM} = \frac{V_{rain} - V_{sr} - V_{dr}}{V_{rain}} \quad \text{(A.1)}$$

### A.2.3 Modeling Permeable Pavements as Equivalent Subcatchments

A permeable pavement system may be represented as a regular pervious subcatchment (or the pervious subarea of a subcatchment) if the subcatchment's parameters are properly related to the parameters of the

permeable pavement system. The basic SWMM which is capable of modeling the rainfall-runoff processes occurring on regular subcatchments can also be used to evaluate the runoff reduction performance of permeable pavement systems.

The depression storage on the pervious subareas of a subcatchment is the maximum surface storage provided by ponding, surface wetting, and interception. In a basic SWMM model, water held in the depression storage due to the force of gravity is treated as water contained in a nonlinear reservoir (Rossman 2010). Rainwater comes into the "reservoir" as inflow; the outflows include infiltration, ET, and runoff. The rate of runoff is controlled by the rate of inflow and the area, width, slope, and roughness of the pervious subarea. This is very similar to a permeable pavement system which also receives rainwater as inflow and releases it through infiltration, ET, and runoff. The only difference is that, when an underdrain is installed, runoff from it includes surface outflow and drain outflow, and drain outflow comes from water that has infiltrated through the surface of the pavement already. Modeling a permeable pavement as a regular pervious subcatchment with its depression storage representing the stormwater retention capacity of the permeable pavement system, the distinction between surface outflow and drain outflow cannot be made, excess water from the stone reservoir is added to water held in the depression storage and drain outflow is treated as a part of

surface runoff.

To ensure that a permeable pavement system is equivalent to the pervious subarea of the subcatchment in a basic SWMM model, the depth of depression storage on the pervious subareas (denoted as $S_d$, in mm) should be set to equal the maximum stormwater retention capacity of the permeable pavement system. The maximum stormwater retention capacity of a permeable pavement system (denoted as $R_{c\max}$, in mm) without underdrains can be calculated as

$$R_{c\max} = S_{ds} + \frac{h_p e_p}{1+e_p} + \frac{h_s e_s}{1+e_s} \quad \text{(A.2)}$$

where $S_{ds}$ is the surface depression storage of the permeable pavement system, in mm; $h_p$ (in mm) and $e_p$ (dimensionless) are the depth and void ratio of the pavement layer, respectively; $h_s$ (in mm) and $e_s$ (dimensionless) are the depth and void ratio of the stone reservoir, respectively. The parameters on the right-hand-side of Equation (A.2) are all required in the LID module of SWMM. All other parameters required in the equivalent subcatchment (i.e., area, width, slope, roughness, and soil infiltration parameters) are the same as those required in the LID module. A unique equivalent subcatchment can therefore be constructed with the definition and calculation of $R_{c\max}$ and the treatment of it as $S_d$, the depth of depression storage on the pervious subareas of the equivalent subcatchment.

Similarly, the maximum stormwater retention capacity of a permeable pavement system with an underdrain installed in the stone reservoir can be calculated as

$$R_{max} = S_{ds} + h_p \theta_{fp} + \frac{h_d e_s}{1 + e_s} \quad \text{(A.3)}$$

where $h_d$ (in mm) is the offset height of the underdrain measured from the bottom of the stone reservoir to the bottom of the underdrain; $\theta_{fp}$ (dimensionless) is the field capacity of the pavement layer. The current LID module of SWMM does not take into account the small storage provided by the field capacity of the pavement layer, therefore, it does not require the input of $\theta_{fp}$. For comparison purposes, the small storage provided by $\theta_{fp}$ is also ignored in this study. However, it is worth noting that a more accurate estimate of the runoff reduction performance of a permeable pavement system can be obtained using Equation (A.3) when the value of $\theta_{fp}$ is available and used.

Using Equations (A.2) or (A.3) to calculate the depression storage depth of the equivalent subcatchments, permeable pavement systems with or without underdrains can be modeled as regular subcatchments in a basic SWMM model. Long-term rainfall records may be used as input to a basic SWMM model, the total volumes of rainfall ($V_{rain}$, in mm) and surface runoff ($V_r$, in mm) from an equivalent subcatchment representing a permeable

pavement system can be obtained from continuous simulations. The long-term average runoff volume reduction rate, $R_{rbasic-SWMM}$, determined by basic SWMM simulations can then be calculated as

$$R_{rbasic-SWMM} = \frac{V_{rain} - V_r}{V_{rain}} \quad \text{(A.4)}$$

Results from Equation (A.4) should be very accurate for cases without underdrains because drain outflow calculations are not required and all the other calculations involved in basic SWMM and LID-SWMM simulations are very similar. For cases with underdrains, since the drain outflow cannot be explicitly calculated using an equivalent subcatchment, the surface runoff rates obtained from the equivalent subcatchment may be less accurate as compared to the LID module results. However, the total volume of surface runoff over a long period of time calculated using the equivalent subcatchment should still be fairly close to the sum of the total volumes of surface outflow and drain outflow calculated using the LID module since the inaccuracies associated with small, medium and large rainfall events tend to be different and would likely cancel each other out. As the total volume of runoff is the main concern, Equation (A.4) should still provide reasonably accurate results.

### A.2.4 Simulation Runs

The values of parameters required in the LID-SWMM simulations are all

listed in Table A.1. The values of parameters used in the basic SWMM simulations are all the same as the values of the corresponding parameters required in the LID-SWMM simulations except $S_d$ which can be determined using Equation (A.2) or (A.3). Permeable pavement systems without vegetative covers are studied in the simulations. Therefore, the vegetative cover coefficient and the imperviousness are both set to be 0. The void ratios of the pavement and the storage layers are set to be their averages based on the recommended values (Rossman 2010). The pavement and the storage layers are usually designed to be highly permeable, and 254 mm/h can be a reasonable value within the possible ranges (Bean et al. 2007; Rossman 2010). Loam soil is assumed to be the native soil in the simulations to represent an average site.

Permeable pavement systems have a tendency to become clogged if they are improperly installed or maintained (USEPA 1999). Numerous studies have shown that the clogging problems can be well improved through proper maintenance practices (e.g., Blades et al. 1995; Bean et al. 2007; Sansalone et al. 2012). Studies conducted by Henderson and Tighe (2011) and Drake et al. (2012) in Canada indicate that different maintenance approaches may produce highly variable results with regards to the recovery of the permeability of permeable pavement systems. However, due to the extremely high initial permeability of the pavement layers, most of the pavements can continue to

maintain sufficient capacity to rapidly infiltrate all rainwater even at reduced permeability levels (Drake et al. 2012). Therefore, the clogging effect is not considered in this study.

**Table A.1 Parameters of permeable pavement systems used in the LID-SWMM simulations**

| | Parameter | Value |
|---|---|---|
| surface layer | storage depth | 1.5 mm |
| | vegetative cover fraction | 0 |
| | surface roughness | 0.015 |
| | surface slope | 1% |
| pavement layer | thickness | 1-200 mm |
| | void ratio | 0.16 |
| | impervious surface fraction | 0 |
| | permeability | 254 mm/h |
| | clogging factor | 0 |
| storage layer | height | 450 mm |
| | void ratio | 0.63 |
| | filtration rate | 3.3 mm/h |
| | clogging factor | 0 |
| underdrain system | drain coefficient | 1000 |
| | drain exponent | 0.5 |
| | drain offset height | 0-400 mm |
| native soil | suction head | 88.9 mm |
| | conductivity | 3.3 mm/h |
| | initial deficit | 0 |
| other parameters | area | 1000 $m^2$ |
| | width | 30 m |
| | ET rate | 0.13 mm/h |

**Note:** Values of suction head and conductivity of native soils are from Rawls et al. (1983)

The 61-year (1945-2005) historical rainfall record from the Hartsfield Airport Station in Atlanta, Georgia was used in both the LID-SWMM and the basic SWMM simulations. The annual precipitation in Atlanta is about 1299.7 mm, and the highest rainfall intensity in the dataset is 90.9 mm/h. The lowest temperature in winter is above 1℃, snowfall seldom occurs in Atlanta. The average ET rate is estimated to be 0.13 mm/h based on the annual pan evaporation data from NOAA (1982). A set of SWMM simulation models are constructed following the two modeling approaches to model the operation of different permeable pavement systems with underdrains. The long-term average runoff reduction rates of these permeable pavement systems are then calculated based on the simulation outputs using Equations (A.1) and (A.4). For illustration purposes, only the effects of the two main design parameters (i.e., $h_p$ and $h_d$) on the hydrologic performance of permeable pavement systems are evaluated using the two SWMM simulation approaches.

## A.3 Results and Analysis

In Figure A.2, the runoff reduction rates determined by the two SWMM simulation approaches are plotted as a function of $h_d$ with $h_p$ fixed at 50 mm. The LID-SWMM determined runoff reduction rate changes significantly with the lengths of simulation time steps (Figure A.2a). When a relatively

short simulation time step (e.g., 5-minute) is used, the LID-SWMM determined runoff reduction rate increases and finally approaches 1.00 when $h_d$ increases from 0 to 400 mm. When a relatively long time, e.g., 1 hour, is used as the simulation time step, the runoff reduction rate increases sharply from 0.31 to 0.78 as $h_d$ increases from 0 to 20 mm; further increases in $h_d$ beyond 20 mm do not result in any increases in runoff reduction rates. This is physically unexplainable since increases in $h_d$ translate directly into increases in the maximum retention capacity of the system [as expressed in Equation (A.3)] which should definitely result in some increases in runoff reduction rates.

Further investigation of the LID-SWMM simulation results showed that when 1-hour is used as the simulation time step, surface outflow $V_{sr}$ stays at about 16880 mm and drain outflow $V_{dr}$ remains at 0 mm with $h_d$ increases beyond 20 mm. This is physically incorrect because (1) the highest input rainfall intensity is 90.9 mm/h, which is far below the permeability of the pavement layers (254 mm/h), surface outflow should therefore never occur as a result of infiltration excess at the surface of the pavement layer; and (2) surface outflow as a result of saturation of the maximum retention capacity of the pavement system is unexpected when there is no drain outflow from the system. The basic SWMM determined runoff reduction rate does not change much with simulation time steps (Figure A.2b). Regardless of the different

time steps used, results determined from basic SWMM simulations are close to those determined from the LID-SWMM simulations with 5-minute time step.

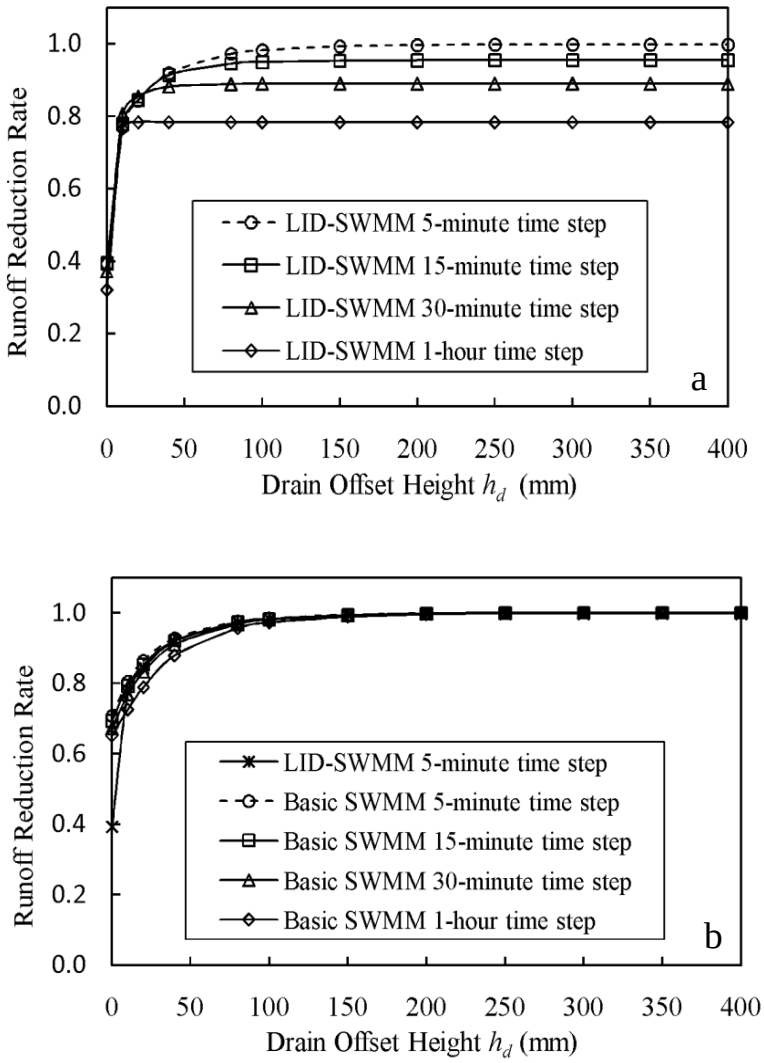


**Figure A.2 Comparison of LID-SWMM and Basic SWMM simulation results ($h_p$ =50 mm)**

Figure A.3 shows the comparison of results for permeable pavement systems with $h_d$ fixed at 50 mm and $h_p$ changing from 1 mm to 200 mm.

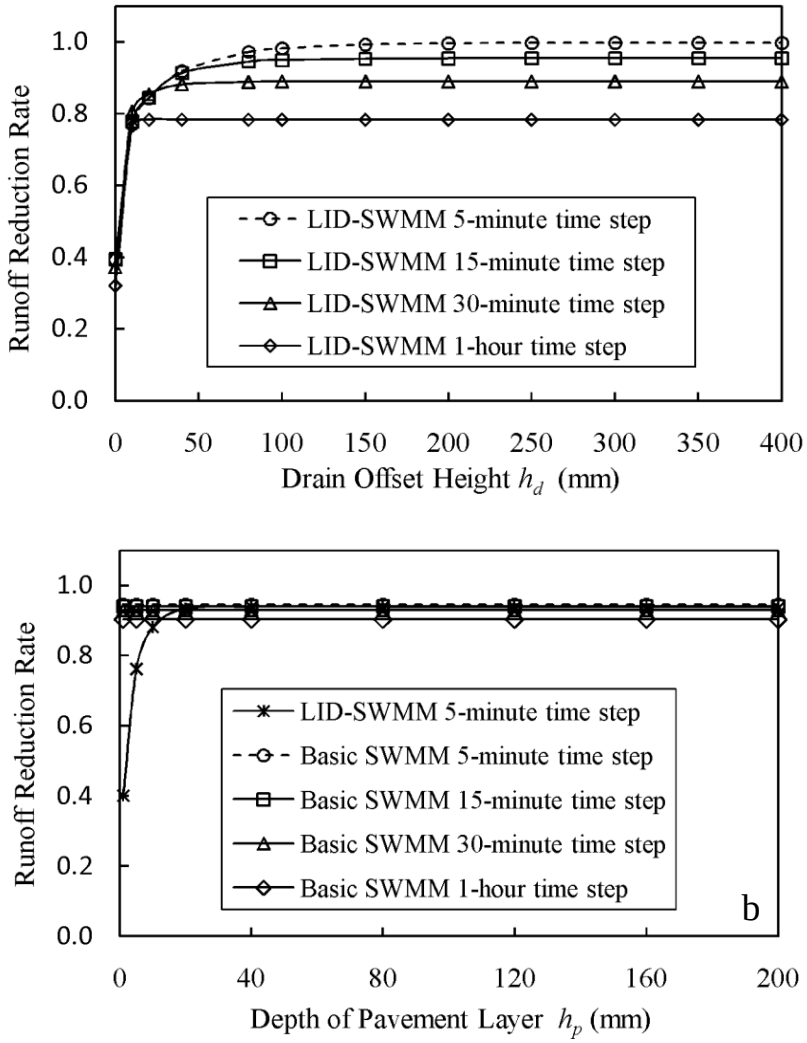


**Figure A.3 Comparison of LID-SWMM and Basic SWMM simulation results ($h_d$ =50 mm)**

Since the storage provided by the field capacity of the pavement layer is ignored (i.e., $\theta_{fp} = 0$) in both the LID-SWMM and basic SWMM simulations, the change of $h_p$ is not expected to result in any variations in the stormwater retention capacity of permeable pavement systems with underdrains. Therefore, the runoff reduction rates determined from the LID-SWMM and

basic SWMM simulations should remain unchanged when $h_p$ changes from 0 mm to 200 mm. The basic SWMM-determined runoff reduction rate does remain at a constant level when different simulation time steps are used and when $h_p$ changes from 0 mm to 200 mm (Figure A.3b). However, the LID-SWMM-determined runoff reduction rate is highly affected by simulation time steps and increases significantly from about 0.30 to about 0.90 when $h_p$ increases from 0 to 120 mm (Figure A.3a). The LID-SWMM results are again physically incorrect or unexplainable.

a

The findings that LID-SWMM can provide reasonable results for some cases with short enough time steps but cannot provide reasonable results for some other cases even with short enough time steps seem to suggest that the problem is perhaps not a simple bug in programming. A preliminary examination of the source code of the LID-SWMM indicates that the actual infiltration rate through the surface of the pavement layer is controlled by the following four factors: 1) the available rainwater on the surface of the pavement layer, 2) the permeability of the pavement layer, 3) the available void space of the pavement layer, and 4) the simulation time step (http://www.epa.gov/nrmrl/wswrd/wq/models/swmm/#Downloads). The storage capacity of the stone reservoir and the drainage capacity of the underdrain (if there is an underdrain) are not considered in the determination of the actual infiltration rate through the pavement layer. This infiltration

calculation method is not complete because, in reality, both the storage capacity of the stone reservoir and the drainage capacity of the underdrain affect the actual infiltration rate as they affect the possibility and extent of system saturation and the associated generation of saturation-excess runoff. This incomplete infiltration calculation method may be one of the causes of the above-reported problems.

Cases without underdrains were also modeled. Similar unreasonable results from LID-SWMM simulations were observed. Without the separate calculation of drain outflow, the possible causes of the unreasonable LID-SWMM results could not be as clearly identified as for cases with underdrains. The basic SWMM model, however, can provide more accurate representation of permeable pavements without underdrains using regular subcatchments. That is why results from cases without underdrains are not presented here.

## A.4 Recommendations

The infiltration calculation algorithm of the LID module of SWMM needs to be improved so that the effect of the storage capacity of the stone reservoir and the drainage capacity of the underdrain on the infiltration process can be considered. The erroneous impact of the depth of pavement layer on runoff generation should also be verified and corrected for cases with

underdrains. Before these improvements are made, the proposed method of representing permeable pavement systems as regular subcatchments can be applied as an alternative method for SWMM users. This method can also be applied by the users of other models (e.g., HEC-HMS) which do not have special LID algorithms to simulate the hydrologic performance of permeable pavement systems. If the current version of the LID module of SWMM is still need to be used, special attention should be paid to the computational time steps in order to minimize inaccuracies, and as much as possible modeling results should be verified with field observations.

**ACKNOWLEDGEMENTS:** This work has been supported by the Natural Sciences and Engineering Research Council of Canada and the China Scholarship Council.

## References

Ball, J. E., and Rankin, K. (2010). The hydrological performance of a permeable pavement. *Urban Water Journal*, 7(2), 79–90.

Bean, E. Z., Hunt, W. F., and Bidelspach, D. A. (2007). Field survey of permeable pavement surface infiltration rates. *Journal Irrigation and Drainage Engineering*, 133 (3), 247–255.

Booth, D. B., and Leavitt, J. (1999). Field evaluation of permeable pavement systems for improved stormwater management. *Journal of American Planning Association*, 65(3), 314–325.

Brattebo, B. O., and Booth, D. B. (2003). Long-term stormwater quantity and quality performance of permeable pavement systems. *Water Research*, 37(18), 4369–4376.

Collins, K. A., Hunt, W. F., and Hathaway, J. M. (2008). Hydrologic comparison of four types of permeable pavement and standard asphalt in eastern North Carolina. *Journal of Hydrological Engineering*, 13(12), 1146–1157.

Credit Valley Conservation Authority and Toronto and Region Conservation Authority (CVC and TRCA). (2010). *Low impact development stormwater management planning and design guide*. CVC and TRCA, Mississauga and Downsview, ON, Canada.

Drake, J., Bradford, A., and Van Seters, T. (2012). Evaluation of permeable pavements in cold climates – Kortright Centre, Vaughan. Toronto and Region Conservation Authority.

Dreelin, E., Fowler, L., and Carroll, R. (2006). A test of porous pavement effectiveness on clay soils during natural storm events. *Water Research*,

40(4), 799–805.

Gilbert, J., and Clausen, J. (2006). Stormwater runoff quality and quantity from asphalt, paver and crushed stone driveways in Connecticut. *Water Research*, 40(4), 826–832.

Henderson, V., and Tighe, S. (2011). Evaluation of pervious concrete pavement permeability renewal maintenance methods at field sites in Canada. *Canadian Journal of Civil Engineering*, 38(12), 1404-1413.

Kuang, X., Sansalone, J., Ying, G., and Ranieri, V. (2011). Pore-structure models of hydraulic conductivity for porous pavement. *Journal of Hydrology*, 399(3–4), 148–157.

National Oceanic and Atmospheric Administration (NOAA). (1982). *Mean Monthly, Seasonal, and Annual Pan Evaporation for the United States.* Washington, D.C. (http://www.nws.noaa.gov/oh/hdsc/PMP_related_studies/TR34.pdf)

North Carolina Division of Water Quality (NCDWQ). (2007). *Stormwater best management practices manual*. North Carolina Department of Environment and Natural Resources, Raleigh, NC, USA.

Pennsylvania Department of Environmental Protection (PDEP). (2006). *Pennsylvania stormwater best management practices manual*. PA DEP Rep. No. 363-0300-002, Harrisburg, PA, USA.

Pratt, C. J., Mantle, J. D. G., and Schofield, P. A. (1989). Urban stormwater reduction and quality improvement through the use of permeable pavements. *Water Science and Technology*, 21(8), 769–778.

Rawls, W. J., Brakensiek, D. L., and Miller, N. (1983). Green-Ampt infiltration parameters from soils data. *Journal of Hydraulic Engineering*, 109(1), 62–70.

Rossman, L. A. (2010). *Storm Water Management Model User's Manual, Version 5.0*, EPA/600/R-05/040, U.S. Environmental Protection Agency, Cincinnati, OH, USA.

Sansalone, J., Kuang, X., Ying, G., and Ranieri, G. (2012). Filtration and clogging of permeable pavement loaded by urban drainage. *Water Research*, 46 (20), 6763–6774.

U. S. Environmental Protection Agency (USEPA). (1999). *Storm Water Technology Fact Sheet: Porous Pavement*. EPA 832-F-99-023.